11

Manganese in Monoclinic Members of the Epidote Group: Piemontite and Related Minerals

Paola Bonazzi and Silvio Menchetti

Dipartimento di Scienze della Terra
Università di Firenze
50121 Firenze, Italia

INTRODUCTION

According to Mayo (1932), who provided a brief historical review of the names used for piemontite, the first researcher who described this mineral has been Cronstedt in 1758 who named it "röd Magnesia." In 1790 Chevalier Napione analyzed the sample described by Cronstedt and termed it "Manganèse rouge." On the basis of his chemical data Haüy designated the substance as "Manganèse oxidé violet silicifère" in 1801. Later, in his Traité de Mineralogie, Haüy (1822) adopted the name proposed by Cordier (1803) who first recognized the mineral as an "Èpidote manganésifere." The name piedmontite was proposed in 1853 by Kenngott the basis of the type locality and more recently transformed into piemontite.

According to the standard guidelines for mineral nomenclature, the name piemontite should be reserved to members of the ternary solid solution $Ca_2Al_2(Mn,Fe,Al)(Si_2O_7)(SiO_4)O(OH)$ that basically contains Mn^{3+} dominant at one site. Nonetheless, the use of this name for any monoclinic manganiferous epidote-group members showing the characteristic strong red-yellow-violet pleochroism is very common and probably convenient with special regard to petrographic purposes. Indeed, the color of manganian (i.e., Mn^{3+} bearing) epidote or clinozoisite ranges to red to pinkish, while manganoan (i.e., Mn^{2+} bearing) members do not exhibit the characteristic reddish hue.

The discredited name "withamite" was used to describe poorly manganiferous piemontite (Hutton 1938; Yoshimura and Momoi 1964) but corresponds, on the basis of the current nomenclature, to a manganian clinozoisite. The name "thulite," sometimes erroneously used for pinkish clinozoisite, should be reserved to Mn^{3+} bearing orthorhombic members.

In this chapter we focus on piemontite *sensu stricto* with the ideal formula $Ca_2Al_2Mn^{3+}(Si_2O_7)(SiO_4)O(OH)$, but also include for the reasons explained above those members of the clinozoisite-epidote-piemontite solid solution series which have been described as piemontite for their peculiar optical properties in many petrological papers. Furthermore, other Mn^{3+}-rich members of the epidote group that differ from piemontite for the occupancy of one or more sites will be taken into account. In particular, strontiopiemontite with the ideal formula $CaSrAl_2Mn^{3+}(Si_2O_7)(SiO_4)O(OH)$ is related to piemontite by the homovalent exchange $^{A1}Ca \leftrightarrow {}^{A1}Sr$. A further substitution $^{M1}Al \leftrightarrow {}^{M1}Mn^{3+}$ relates strontiopiemontite to tweddillite with the ideal formula $CaSrAlMn^{3+}{}_2(Si_2O_7)(SiO_4)O(OH)$. On the other hand, androsite-(La), ideal formula $Mn^{2+}REE^{3+} Mn^{3+}Al Mn^{2+}(Si_2O_7)(SiO_4)O(OH)$, is related to piemontite by the heterovalent exchange $^{A2}Ca \leftrightarrow {}^{A2}REE$ coupled to $^{M3}Mn^{3+} \leftrightarrow {}^{M3}Mn^{2+}$ besides the substitutions $^{A1}Ca \leftrightarrow {}^{A1}Mn^{2+}$ and $^{M1}Al \leftrightarrow {}^{M1}Mn^{3+}$. Furthermore, the exchange mechanism

$^{M3}(Mn^{2+},Fe^{2+}) + {}^{O10}OH^- \leftrightarrow {}^{M3}(Mn^{3+},Fe^{3+}) + {}^{O10}O^{2-}$ describes the oxidation of octahedral divalent cations and the corresponding deprotonation when REE-bearing piemontites are heated in air.

STRUCTURE AND CRYSTAL CHEMISTRY

The crystal structure of piemontite is topologically identical to that of the other monoclinic members of the epidote group (space group $P2_1/m$). It consists of Si_2O_7 and SiO_4 units linked to two independent edge-sharing octahedral chains, both extending parallel to the *b*-axis (Fig. 1). One chain consists of M2 octahedra while the other chain is formed by M1 octahedra with M3 octahedra attached on alternate sides along its length. This arrangement gives rise to two additional types of cavities, the smaller nine-fold coordinated A1 and the larger ten-fold coordinated A2 sites. For an ideal piemontite endmember the site occupancy can be schematically described as A1 and A2 = Ca, M1 and M2 = Al, and M3 = Mn^{3+}.
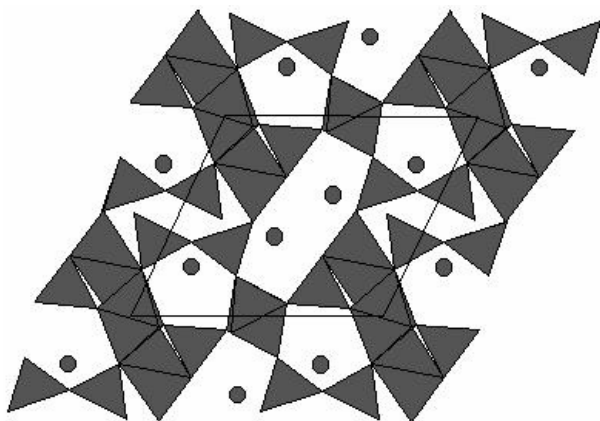

Figure 1. Piemontite structure projected onto (010); dots = Ca.

M sites

Since the first structural and spectroscopic studies on members of the epidote group (Ito et al. 1954; Strens 1966; Burns and Strens 1967) it is generally assumed that Fe^{3+} and Mn^{3+} mainly substitute Al in M3, which is significantly larger and more distorted (axially compressed) than the other octahedral sites, even in the unsubstituted clinozoisite endmember. In particular, the tetragonal distortion of M3 makes this site very suitable to house the $3d^4$-configurated Mn^{3+} ion, in agreement with the requirements of the Jahn-Teller effect. However, for appropriate compositions, a significant M^{3+} ($M^{3+} = Mn^{3+} + Fe^{3+}$) substitution in at least one of the other two octahedral sites was assumed. Based on the structural model of Ito et al. (1954) who had erroneously determined decreasing octahedral distortion in the order M3 > M2 > M1, Burns and Strens (1967) in their spectroscopic study assigned the additional Mn^{3+} to the M2 site. The first structural approach to the question of cation ordering in piemontite stems from Dollase (1969) who refined the structure of a piemontite with $M^{3+} = 1.03$ per formula unit (pfu) and analyzed the geometrical features distinctive of piemontite. It is evident from Dollase's study that the transition metals occupy preferentially the M3 site ($M^{3+} = 0.83$ pfu) and to a lesser extent the M1 site ($M^{3+} = 0.20$ pfu). This result does not contradict the spectroscopic interpretation of Burns and Strens (1967) as the M1 octahedron was found to be more distorted than M2, which is always the smallest and most regular octahedron of the

structure throughout the compositional field of the epidote minerals (see Franz and Liebscher 2004). Because of the comparable X-ray scattering power of Mn^{3+} and Fe^{3+}, however, any possible ordering of Fe^{3+} and Mn^{3+} between M3 and M1 remained undetermined. To determine the site assignment of Fe^{3+} and Fe^{2+} and to explore possible variations in the degree of ordering, Dollase (1973) investigated several synthetic and natural samples of the epidote group including three piemontite crystals by means of ^{57}Fe Mössbauer spectroscopy. Fe^{3+} was found to occupy both M3 and M1 site with a marked preference for M3 site. In particular, the three piemontite samples analyzed showed Fe^{3+} (M3) = 0.287, 0.097, and 0.106 pfu and Fe^{3+} (M1) = 0.043, 0.013, and 0.014 pfu, respectively. If it is arbitrarily assumed that Mn^{3+} fractionates between M3 and M1 exactly like Fe^{3+}, the distribution coefficient K_D (M^{3+} - Al) for the intracrystalline exchange reaction

$$^{M3}\left(Fe^{3+} + Mn^{3+}\right) + {}^{M1}Al = {}^{M1}\left(Fe^{3+} + Mn^{3+}\right) + {}^{M3}Al \tag{1}$$
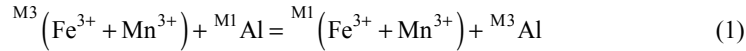
is

$$K_D\left(M^{3+} - Al\right) = \frac{^{M1}\left(Fe^{3+} + Mn^{3+}\right){}^{M3}Al}{^{M3}\left(Fe^{3+} + Mn^{3+}\right){}^{M1}Al} \tag{2}$$

For these piemontite samples the distribution coefficients K_D (= 0.015, 0.024, and 0.021, respectively) are similar to those estimated for synthetic epidote on the basis of Mössbauer spectroscopy (Dollase 1973). However, they are significantly lower than those determined by a single crystal diffraction study (Giuli et al. 1999) in synthetic epidote. For a sample of piemontite from the type locality (St. Marcel, Piemonte, Italy) the spectroscopic results (Dollase 1973) were tentatively combined with the structural data previously obtained (Dollase 1969). On this basis, the following site occupancies were derived: M3 = 0.54 Mn^{3+} + 0.29 Fe^{3+} + 0.17 Al and M1 = 0.16 Mn^{3+} + 0.04 Fe^{3+} + 0.80 Al. For the intracrystalline partitioning of Fe^{3+} and Mn^{3+} between M1 and M3

$$^{M3}\left(Fe^{3+}\right) + {}^{M1}\left(Mn^{3+}\right) = {}^{M1}\left(Fe^{3+}\right) + {}^{M3}\left(Mn^{3+}\right) \tag{3}$$
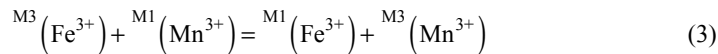
these values correspond to

$$K_D\left(Mn - Fe\right) = \frac{^{M1}\left(Fe^{3+}\right) + {}^{M3}\left(Mn^{3+}\right)}{^{M3}\left(Fe^{3+}\right) + {}^{M1}\left(Mn^{3+}\right)} = 0.47 \tag{4}$$

and indicate a stronger preference of Fe^{3+} for the more distorted M3 site compared to Mn^{3+}. According to Dollase (1973) such a conclusion "must be considered suspect" being in contrast with the known preference of Mn^{3+} for tetragonally distorted sites. In fact, the axial compression of the M3 octahedron, involving the electron hole of $3d^4$ in d_{z^2} orbital, yields a rather small crystal field stabilization energy (CFSE) compared with those typical of Mn^{3+} in other crystal structures (e.g., Mn^{3+} substituting Al in the axially elongated octahedra of the andalusite structure type; Langer et al. 2002). Ferraris et al. (1989) determined the Mn^{3+}-Fe^{3+} distribution in a strontian piemontite by single-crystal neutron-diffraction. Their site occupancy refinement led to M3 = 0.61 Mn^{3+} + 0.33 Fe^{3+} + 0.06 Al and M1 = 0.17 Mn^{3+} + 0.02 Fe^{3+} + 0.81 Al. The corresponding K_D (Mn-Fe) of 0.23 seems to confirm the above-mentioned odd behavior of preferential incorporation of Fe^{3+} in M3. On the other hand Ferraris et al. (1989) pointed out that a look at the absolute quantities of Mn^{3+} in the respective sites would eliminate the apparent oddity. Catti et al. (1989) refined the structure of additional five strontian piemontite crystals and confirmed the previous findings that M^{3+} (= Mn^{3+} + Fe^{3+}) has a stronger preference for M3 than for M1. Furthermore, Catti et al. (1989) observed a departure from linearity in

the function $^{M1}M^{3+} = f\,(^{M3}M^{3+})$ indicating a saturation effect with increasing total M^{3+}content. No correlation was found between the site occupancy at M3 and M1 and the total Mn content determined by microprobe analysis. This may suggest that the crystal chemical behavior of Mn^{3+} and Fe^{3+} in piemontite is not so different despite their different electronic configurations ($3d^4$ and $3d^5$, respectively).

Recently, Langer et al. (2002) discussed the structural and geometrical changes in the structure of piemontite induced by increased Mn^{3+} or M^{3+} incorporation in synthetic and natural crystals, respectively. There is no significant difference in the distribution behavior of Mn^{3+} or other M^{3+} ions between M1 and M3 if the intracrystalline distribution is plotted as a function of the total Mn^{3+} or M^{3+} content. However, when $^{M1}M^{3+}$ is plotted as a function of $^{M3}M^{3+}$ it becomes evident that synthetic piemontite in which $M^{3+} = Mn^{3+}$ exhibits a quite different order-disorder behavior from that of natural piemontite in which $M^{3+} = Mn^{3+} + Fe^{3+}$. In Figure 2 the available data for the partitioning of M^{3+} between M1 and M3 are plotted together with curves of constant K_D (= 0.005, 0.010, 0.020, 0.050, and 0.10, respectively). Most of the natural piemontites have a K_D between 0.005 and 0.020, higher K_D values close to 0.050 being found only for the piemontite crystal refined by Dollase (1969) and for a manganian epidote from Lom, Norway. By contrast, all synthetic piemontites exhibit K_D values between 0.064 and 0.080 (Fig. 2). Two reasons might explain the higher disorder observed in pure synthetic piemontites. The first one is that the entry of Mn^{3+} in M1 stabilizes the structure more than Fe^{3+} does, possibly due to the axial compression, which also affects the M1 octahedron, although to a lesser extent than M3. A second cause of the higher disorder observed is the crystallization temperature used for the synthetic crystals (700°C), rather high compared to the natural one. Nevertheless, Langer et al. (2002) claimed that "an effect of a temperature difference of about 200°C between natural and synthetic crystals will not greatly change the general distribution pattern". By analogy with the results obtained for the intracrystalline Fe^{3+} distribution in epidote (e.g., Bird and Helgeson 1980; Giuli et al. 1999; see Franz and Liebscher 2004), the
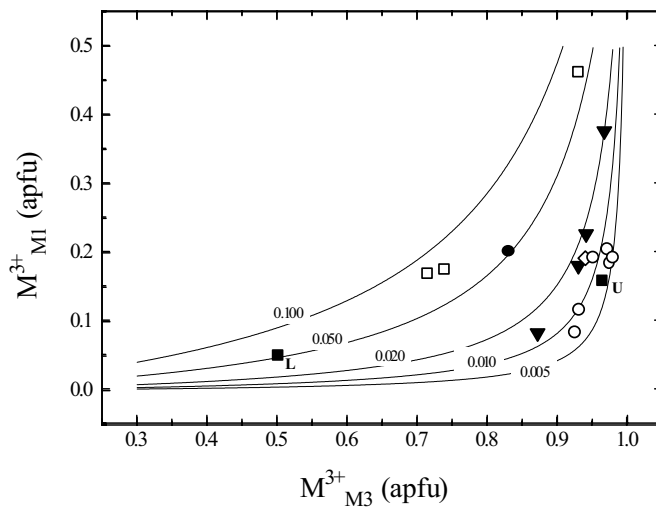
Figure 2. Relationship between M^{3+} (= Mn^{3+} + Fe^{3+}) content in the octahedral sites M1 and M3 in piemontite. Lines refer to constant fractionation values (K_D = 0.005, 0.010, 0.020, 0.050 and 0.10, respectively; see text). Symbols refer to data from literature as follows: solid circle = type locality (Dollase 1969); solid downward triangles = type locality (Catti et al. 1989); open diamond = type locality (Ferraris et al. 1989); open circles = different localities (Bonazzi 1990); solid squares = different localities (Langer et al. 2002); L = Lom, Norway; open squares = synthetic piemontite (Langer et al. 2002).

higher disorder in synthetic piemontite may be caused by the high crystallization temperature and/or a possible metastable rapid growth.

The mean M3-O and M1-O bond distances increase as a function of their M^{3+} content (Fig. 3a,b). However, because most data for M3 cluster at $M^{3+} > 0.90$ pfu, the regression line is not reliable to predict the <M3-O> behavior. Thus, the extrapolation towards $M^{3+} = 0$ does not match the <M3-O> value of clinozoisite (1.977 Å; Dollase 1968). On the contrary, the data for <M1-O> cover a wide range of M^{3+} values and the linear model obtained

$$<M1\text{-}O> (\text{Å}) = 1.910(1) + 0.101(3)\ M^{3+}\ (pfu)\ (r = 0.989)$$
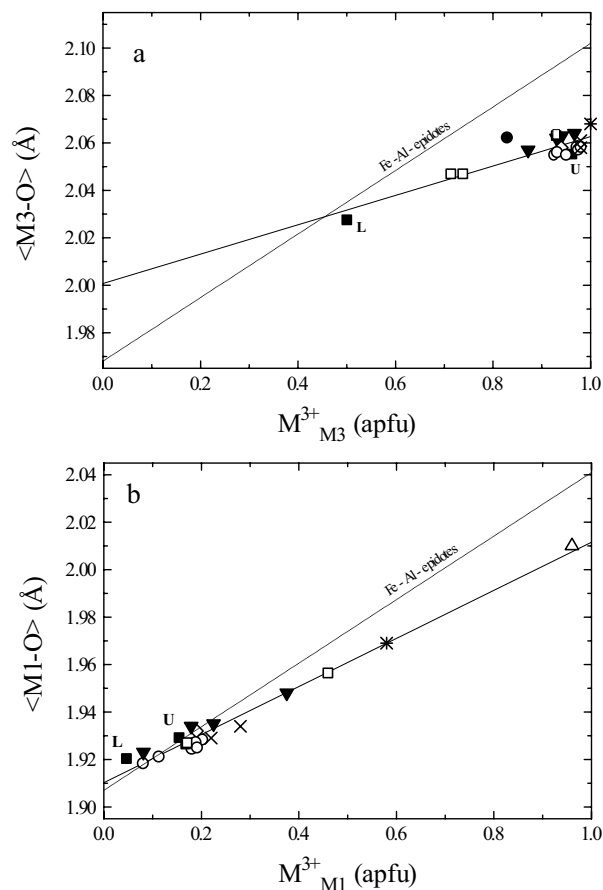
Figure 3. a) Mean octahedral M3-O distance plotted vs. the M^{3+} (= Mn^{3+} + Fe^{3+}) content in the M3 site: Data fit the equation (solid regression line) <M3-O> = 2.001(7) + 0.062(8) M^{3+}_{M3} ($r = 0.874$). b) Mean octahedral M1-O distance (Å) plotted *vs.* the M^{3+} (= Mn^{3+} + Fe^{3+}) content in the M1 site (pfu): Data fit the equation (solid regression line) <M1-O> = 1.910(1) + 0.101(3) M^{3+}_{M1} ($r = 0.989$). Symbols: solid circle = piemontite, type locality (Dollase 1969); solid downward triangles = piemontite, type locality (Catti et al. 1989); open diamond = piemontite, type locality (Ferraris et al. 1989); open circles = piemontite, different localities (Bonazzi 1990); crosses = strontiopiemontites, type locality (Bonazzi et al. 1990); star = tweddillite, type locality (Armbruster et al. 2002); solid squares = piemontite, different localities (Langer et al. 2002); open squares = synthetic piemontite (Langer et al. 2002); open upward triangle = androsite-(La), type locality (Bonazzi et al. 1996). Dashed lines refer to natural Fe-Al epidotes (Bonazzi and Menchetti 1995).

describes well the increase of the mean bond distance as a function of the M^{3+} content. For $M^{3+}(M1) = 0$ the regression line obtained for piemontite, including data for strontiopiemontite, tweddillite, and androsite-(La), matches closely both the value found in clinozoisite (1.906 Å; Dollase 1968) and the value extrapolated from the regression line obtained for the clinozoisite-epidote solid-solution series (1.907 Å; Bonazzi and Menchetti 1995). With the increase of M^{3+} content the regression lines for piemontite and clinozoisite-epidote solid solution diverge. For M^{3+} (M1) = 1, the distance <M1-O> is 2.011 Å in piemontite and 2.041 Å in clinozoisite-epidote (Fig. 3b). Although this different behavior is reasonably due to the different structural influence of Mn^{3+} and Fe^{3+}, it is difficult to quantify the proportion of Mn^{3+} in M1 only on the basis of the shift of data points from the regression lines. This shift is indeed also affected by differences in the instruments and/or refining methods such as the use of scattering curves for neutral rather than ionized atomic species.

Some ideas of the different structural effects of Mn^{3+} and Fe^{3+} can be obtained from the individual M3-O and M1-O bond distances (Langer et al. 2002). Because the M3 octahedron is compressed along the O4-M3-O8 axis (Fig. 4) a distinct Jahn-Teller effect of Mn^{3+} occurs in piemontite with the electron hole of the d^4 cation occurring in the d_z2 orbital along this direction. Therefore, any increase of Mn^{3+} in this site will cause an increase of the octahedral volume but at the same time will enhance the relative compression along the O4-M3-O8 octahedral axis. This effect is more pronounced for pure Mn^{3+} substitution in synthetic piemontite than in natural Fe^{3+} bearing piemontite, since the spherical d^5-configurated Fe^{3+} obviously does not cause any compression. Accordingly, in the minerals of the clinozoisite-epidote series ($0.24 < Fe^{3+} < 1.14$ pfu) studied by Bonazzi and Menchetti (1995), the individual M3-O bond distances continuously increase from clinozoisite to Fe-rich epidote as a function of Fe^{3+} substitution (see also Franz and Liebscher 2004), except for a red-colored manganian epidote which exhibits a relative shortening of the M3-O4 and M3-O8 distances due to the entry of 0.20 Mn^{3+} pfu.

The effect of Mn^{3+} on the distortion of the M3 octahedron is also evident from the comparative study on Mn free allanite and REE bearing piemontite (Bonazzi and Menchetti 1994). In both minerals, the presence of REE^{3+} substituting for Ca requires the entry of divalent cations (Fe^{2+}, Mn^{2+}, Mg) in the octahedral sites. Upon heating in air, oxidation of Fe^{2+} (or Mn^{2+}) to Fe^{3+} (or Mn^{3+}) mainly results in a shortening of the mean <M3-O> distance and, to a lesser extent, of the mean <M1-O> distance. With the increase of trivalent cations at M3, the octahedral axial distances decrease accordingly. In Mn-free allanite oxidation implies an increase of Fe^{3+} and, therefore, both the equatorial O1-O2 (×2) and the apical O4-O8 distances decrease with the same slope suggesting no additional tetragonal distortion. By contrast, the
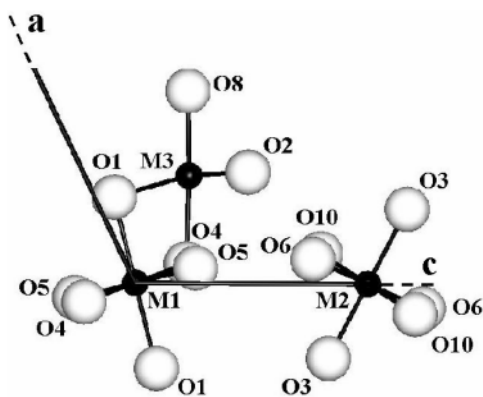

Figure 4. The M1, M2 and M3 independent octahedra in the piemontite structure projected along the [010] axis, atoms are labeled according to Dollase (1969).

increase of Mn^{3+} in the case of REE bearing piemontite results in a strong contraction of O4-O8, in accordance with the Jahn-Teller effect, while the equatorial O1-O2 distance does not change significantly, indicating a pronounced additional tetragonal distortion (for a detailed discussion of REE-bearing monoclinic epidote minerals see Gieré and Sorensen 2004).

Langer et al. (2002) also noted a significant distortion of the M1 octahedron with the octahedral axis of compression being O4-M1-O4 (Fig. 4). As in the case of M3, the relative octahedral compression of the M1 octahedron increases with increasing Mn^{3+} content in the site. Therefore it is not surprising that Mössbauer spectroscopy (Dollase 1973) and neutron diffraction (Ferraris et al. 1989) data indicate that not all Mn^{3+} is ordered in M3 at the expense of Fe^{3+}. It is worth noting that in tweddillite (Armbruster et al. 2002) where $Mn^{3+} + Fe^{3+} > 1.5$ (with $Mn^{3+} > Fe^{3+}$) the content of trivalent transition metals in M1 is 0.58 pfu and the <M1-O> distance reaches 1.969 Å (Fig. 3b). This value seems to be the highest one for M1 at least in epidote group members having M3 occupied only by trivalent cations. As M3 and M1 share a common O1-O4 edge (Fig. 4), the partitioning of M^{3+} between M3 and M1 also depends on geometrical constraints. Thus, M1 can house even higher amounts of M^{3+} cations when the entry of divalent cations in M3 further increases the M3 volume. If the volume of M3 reaches a value of about 11 $Å^3$ the local strain is lowered by a significant incorporation of M^{3+} in M1 (Bonazzi and Menchetti 1995). In REE bearing piemontite (Bonazzi et al. 1992) the $^{M1}(Mn+Fe)/^{M3}(Mn+Fe)$ ratio therefore correlates positively with the REE content. In androsite–(La) the exceptionally high M3 volume of 12.60 $Å^3$ that is due to the entry of divalent cations, allows a corresponding expansion of the edge-sharing M1 octahedron and results in occupancy of M^{3+} in M1 close to 1 pfu (Bonazzi et al. 1996).

As already mentioned the substitution of REE^{3+} for Ca in REE bearing piemontite requires the entry of divalent cations (Mn^{2+}, Fe^{2+}, Mg) in the octahedral sites. In Pb and REE rich piemontite from Nezilovo, Macedonia, the observed <M3-O> distance (2.082 Å) is significantly longer than expected for site occupancy by trivalent cations only (Bermanec et al. 1994). The authors therefore assumed that M^{2+} mainly orders in the M3 site. Bonazzi et al. (1992) have drawn a similar conclusion for REE bearing piemontite from the Apuan Alps. In these samples, however, they also found a slight discrepancy between observed and expected <M1-O> values and tentatively attributed it to the entry of the small quantities of Mg in M1 that were detected by electron microprobe analyses (Bonazzi et al. 1992).

A sites

The A1 and A2 sites in piemontite (Fig. 5) have been described as seven- and eight-fold coordinated, respectively (Dollase 1969), thus including distances ranging from 2.2 to 2.9 Å. As the charge balance appears more satisfactory if two more neighboring oxygen atoms are included in the first coordination shell, A1 and A2 are better described as nine- and ten-fold coordinated, respectively. The A1 site is generally occupied exclusively by Ca although few samples exhibit a significant substitution by Mn^{2+}. Bonazzi et al. (1996) studied the structural effect of this substitution and considered the changes in the arrangement of the O atoms linked to A1. Increasing Mn^{2+} in A1, the distance of the seventh neighbor (O6) increases so that A1 should be more appropriately described as six-fold coordinated (r_{Mn2+} in six-fold coordination = 0.83 Å; Shannon 1976). The distance difference between the sixth and seventh neighbor (δ_{6-7}) increases linearly from 0.316 Å in piemontite (Dollase 1968) to 0.419 Å in REE bearing piemontite from the Varenche mine (Bonazzi et al. 1996). In androsite-(La) in which Mn^{2+} is the prevailing cation in A1, δ_{7-6} reaches even 0.490 Å (Fig. 6a). The presence of Mn^{2+} also affects the mean <A1-O> distance for six-fold coordination, which linearly decreases with increasing Mn^{2+} content (Fig. 6b). In the sample from Nezilovo (Bermanec et al. 1994) an Mn^{2+} content close to 0.30 pfu in A1 can be assumed on the basis of the average chemical composition (Ca + REE + Pb + Na = 1.70 pfu; Al + Fe + Mn + Mg + Zn = 3.27 pfu). Calculating δ_{6-7} and <A1-O> in six-fold coordination for the Nezilovo sample the value of 0.30
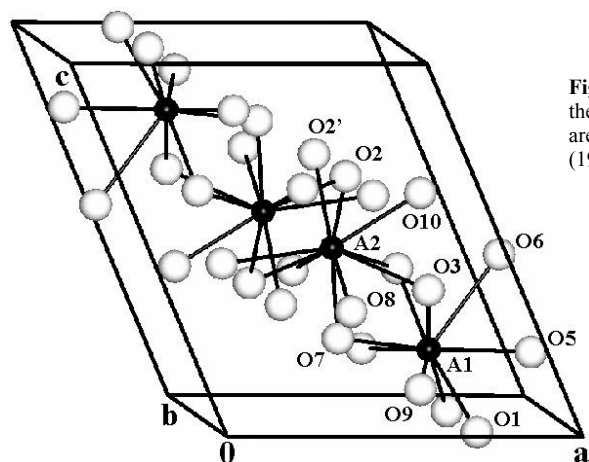
Figure 5. A1 and A2 polyhedra in the unit cell of piemontite; atoms are labeled according to Dollase (1969).
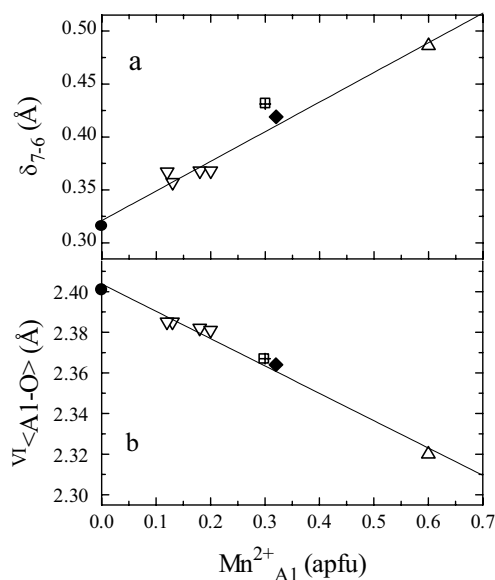
Figure 6. Parameters of the A1 polyhedron as a function of the Mn^{2+} content in A1 along the piemontite-androsite-(La) solid solution. a) The difference between the seventh (A1-O6) and the sixth longest (A1-O5) distances is designed δ_{7-6}; the equation of the regression line is $\delta_{7-6} = 0.321(5) + 0.28(2)\ Mn^{2+}_{A1}$ ($r = 0.991$). b) The average of the six shortest A1-O distances is designed $^{VI}<A1-O>$; the equation of the regression line is $^{VI}<A1-O> = 2.404(2) - 0.135(7)\ Mn^{2+}_{A1}$ ($r = -0.993$). Symbols: solid circle = piemontite, type locality (Dollase 1969); open downward triangles = REE bearing piemontites, Apuan Alps (Bonazzi et al. 1992); solid diamond = REE bearing piemontite, Varenche mine (Bonazzi et al. 1996); open upward triangle = androsite-(La), type locality (Bonazzi et al. 1996); crossed open square (not used in the fitting) = piemontite, Nezilovo (Bermanec et al. 1994).

Mn^{2+} pfu in A1 perfectly fits the linear equations modeling the oxygen environment around A1 (see crossed squares in Fig. 6).

Apart from the entry of Mn^{2+}, the geometrical changes concerning the A1 polyhedron are minor and related to the chemical substitutions occurring in the adjacent, face-sharing A2 polyhedron (Fig. 5). When heterovalent substitutions take place (i.e., in REE bearing piemontite), variations of individual A1-O distances occur to compensate the local charge imbalance associated with the entry of REE^{3+} in A2 and divalent cations in M3. The homovalent Ca ↔ Sr substitution also causes adjustments within the A1 polyhedron although Sr is completely ordered in the A2 site. Increasing Sr in A2 shortens the A1-O7 distance to compensate the bond strength imbalance on O7 due to the marked lengthening of the A2-O7 distance. A2-O7 is the shortest A2-O distance and correlates linearly ($r = 0.993$) with

the Sr content in A2 (Fig. 7). The regression obtained works equally along the piemontite-strontiopiemontite and the piemontite-tweddillite join. The other short distances (i.e., A2-O10 and A2-O2; see Fig. 5) correlate as well with the Sr content although with a flatter slope of the regression lines. On the other hand, the values for the longer distances (i.e., A2-O2′, A2-O3, A2-O8; see Fig. 5) are randomly distributed with respect to the Sr content. A similar although more pronounced effect will reasonably occur with the entry of Pb^{2+} that has an ionic radius greater than Sr (r_{Sr} in ten-fold coordination = 1.36 Å, r_{Pb} in ten-fold coordination = 1.40 Å; Shannon 1976). Indeed, the value for A2-O7 (2.273 Å) observed in the Pb- and REE-rich piemontite crystal from Nezilovo (Bermanec et al. 1994) is significantly greater than that predicted for A2-O7 with A2 = Ca (2.249 Å). Unfortunately, the effect of the Ca $\leftrightarrow$ Pb substitution is difficult to quantify in this sample due to the simultaneous presence of REE^{3+} in A2.

In piemontite REE^{3+} as well as Th^{4+} and U^{4+} appear to be always completely ordered in A2, in spite of the fact that the ionic radii of $LREE^{3+}$ (r_{La-Ce} in ten-fold coordination = 1.27 to 1.25 Å; Shannon 1976) exceed only slightly the ionic radius of Ca (r_{Ca} in ten-fold coordination = 1.23 Å; Shannon 1976). This is mainly due to the bond strength imbalance occurring on O2 when divalent cations occupy the M3 site. Similar to allanite (Bonazzi and Menchetti 1995), the <A2-O> distance is not substantially modified by the Ca $\leftrightarrow$ REE^{3+} substitution but variations are observed in the individual A2-O distances. In particular, the A2-O2 distance correlates negatively with the REE content (Fig. 8). This relationship is related to a charge compensation mechanism rather than to geometrical constraints as shown by the lengthening of the A2-O2 distance with the increase of oxidation in a heated REE bearing piemontite (see Fig. 8). Due to the opposite effect caused by the entry of larger divalent cations, the crystals from Varenche (^{A2}Sr = 0.19 pfu) and Nezilovo (^{A2}Pb = 0.19 pfu) do not fit the model and have been neglected in the calculation of the regression line (Fig. 8) Sr in the other samples does not exceed 0.04 pfu.
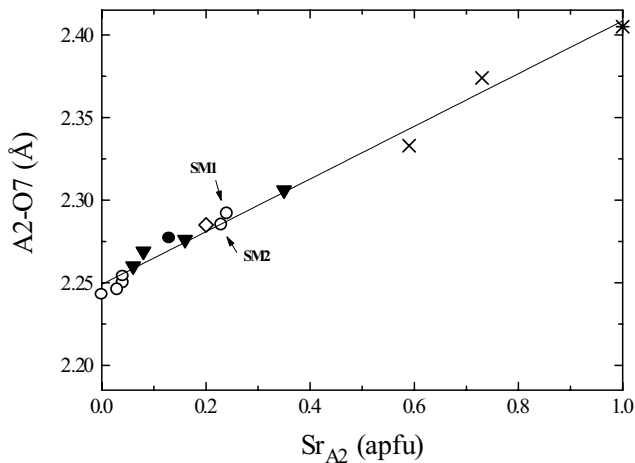
Figure 7. The A2-O7 bond distance vs. the Sr content in the A2 site in members of the piemontite-strontiopiemontite and piemontite-tweddillite series. The equation of the regression line is A2-O7 = 2.249(2) + 0.160(5) Sr_{A2} (r = 0.993). Symbols: solid circle = piemontite, type locality (Dollase 1969); solid downward triangles = piemontite, type locality (Catti et al. 1989); open diamond = piemontite, type locality (Ferraris et al. 1989); open circles = piemontite, different localities (Bonazzi 1990); crosses = strontiopiemontite, type locality (Bonazzi et al. 1990); star = tweddillite, type locality (Armbruster et al. 2002).
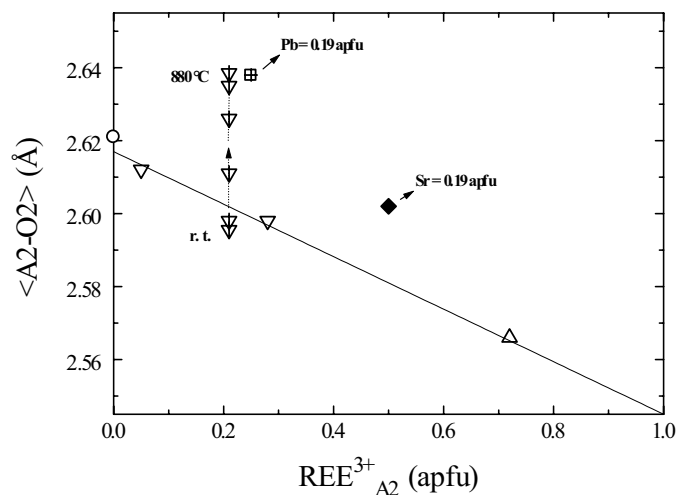
Figure 8. The <A2-O2> bond distance (average of four values) plotted vs. the REE content in the A2 site. The equation of the regression line is <A2-O2> = 2.617(3) − 0.072(8) REE$^{3+}_{A2}$ ($r = -0.983$). Symbols: open circle = piemontite, Mt. Corchia, Apuan Alps (Bonazzi 1990); open downward triangles = REE bearing piemontite, Apuan Alps (Bonazzi et al. 1992); solid diamond (not used in the fitting) = REE bearing piemontite, Varenche mine (Bonazzi et al. 1996); open upward triangle = androsite-(La), type locality (Bonazzi et al. 1996); crossed open square (not used in the fitting) = piemontite, Nezilovo (Bermanec et al. 1994). Lined open downward triangles (not used in the fitting) refer to natural (r.t. = room temperature) and heated REE bearing piemontite; heating temperatures 380 to 880°C (Bonazzi and Menchetti 1994).

T sites

Looking at the tetrahedral bond distances in piemontite as reported in the literature it is evident that the mean distances can be considered as a constant value for every tetrahedron, while individual bond distances and angles fairly change as a consequence of substitutions in the other sites of the structure. Therefore, in close agreement with the results of a neutron diffraction refinement (Ferraris et al. 1989), no significant substitution of Si by other cations affects these sites.

The most significant variation concerning the tetrahedra is the change of the mutual orientation of the Si1 and Si2 tetrahedra, linked together to form a cis-oriented Si_2O_7 group. As reported by several authors (Dollase 1971; Gabe et al. 1973; Carbonin and Molin 1980; Bonazzi and Menchetti 1995; see also Franz and Liebscher 2004), the bending angle Si1-O9-Si2 in the epidote group minerals decreases with the increase of substitution of larger cations for Al in the M3 octahedron. Bermanec et al. (1994) also found a strong negative linear relationship between the bending angle and the octahedral M3-O8 distance. In piemontite the decrement of the Si1-O9-Si2 value is even greater when $M^{3+} = Mn^{3+}$ (Langer et al. 2002).

Hydrogen bonding

Like in the other epidote group minerals, the proton in piemontite is bonded to O10 that links two M2 and one A2 cations. Hydrogen bonding between O10 (donor) and O4 (acceptor) constitutes an additional link between the M1 and the M2 octahedral chains. By analogy with dollaseite-(Ce) (Peacor and Dunn 1988), incorporation of F⁻, if any, occurs at the O4 site.

Using the atomic coordinates from the neutron diffraction refinement of Ferraris et al. (1989), the hydrogen bonding environment in piemontite is H-O10 = 0.966 Å, H-O4 = 2.003 Å, O10-O4 (donor–acceptor) distance = 2.955 Å, and O10-H-O4 bending angle = 168°. The

shortest hydrogen-cation distance is H-M2 = 2.475 Å. By heating REE free piemontite in air, in which oxidation of octahedral cations (already in their high valence state) is excluded, no deprotonation occurs below the breakdown temperature of the structure at 880°C (Catti et al. 1988). In contrast, the heating in air of REE bearing piemontite results in a loss of H to compensate the oxidation of M^{2+} to M^{3+}. This is evident from the lengthening of the donor acceptor distance that increases almost gradually from 2.959 Å (550°C) to 3.053 Å (880°C) (Bonazzi and Menchetti 1994). With ongoing deprotonation also the amount of M^{3+} in M2 becomes significant (up to 0.18 M^{3+} pfu after the 880°C heat treatment) as the presence of H inhibits the incorporation of M^{3+} in M2 due to the very short M2-H distance.

High-temperature behavior

The thermal behavior of Sr bearing piemontite was studied by Catti et al. (1988) by *in-situ* high temperature X-ray diffraction. As expected, the octahedra exhibit positive thermal expansion coefficients and the expansion of M3 is the most pronounced and very anisotropic. With increasing temperature the two shortest distances shrink while the longest ones expand causing a further flattening of the octahedron along O4-M3-O8, in close agreement with the fact that the direction of the least thermal expansion of the lattice is close to the O4-M3-O8 alignment. The thermal expansion of the A1 and A2 polyhedra is less than expected and affects mainly the shortest distances. As a consequence, the regularity of these polyhedra increases as a function of temperature. Both T1 and T2 tetrahedra exhibit negative thermal expansion coefficients. To compensate for the imbalance of bond strength due to the lengthening of weaker bonds some of the Si-O distances (e.g., Si1-O1, Si1-O7, Si2-O3) decrease with the increase of temperature.

Unit-cell parameters

The unit-cell volume of piemontite is known to vary as a function of the substitutional degree in both the octahedral (Anastasiou and Langer 1977; Langer et al. 2002) and the A sites (Bonazzi et al. 1990; 1996; Akasaka et al. 2000). Like in Fe-Al epidote (see Franz and Liebscher 2004), *b* increases markedly with the M^{3+} content whereas *a* and *c* increase only slightly. The monoclinic β angle exhibits minor variation also depending on the A site population. Nevertheless, these correlations are not as close as in Fe-Al-epidote, mainly as a consequence of the peculiar crystal chemical behavior of the Jahn-Teller active Mn^{3+} cation. As discussed above an increase of Mn^{3+} causes a further compression of the M3 octahedron along the O4-M3-O8 alignment which is approximately parallel to the *a* axis (Fig. 4). For this reason, the Mn/Fe ratio in piemontite affects both the *a/b* and *a/c* axial ratios resulting in a rather wide spread of values for the unit-cell parameters as a function of the octahedral substitutional degree. The relationships are further complicated by the substitutions at the A sites.

In Figure 9, the individual parameters (*a*, *b*, *c*, and β, respectively) of piemontite and other manganiferous members of the epidote group are plotted against the unit-cell volume. For comparison the corresponding variations in members of the clinozoisite-epidote series are reported. From an overall comparison of the plots it appears that the $Mn^{3+} \leftrightarrow Fe^{3+}$ substitution affects *a* and *b* more sensibly than *c* and β. As expected, Fe free synthetic piemontite (open and dotted squares) exhibits values of the *a* parameter lower than those of Fe-bearing natural piemontite (Fig. 9a). In particular, the "piemontite" from Lom, Norway, studied by Langer et al. (2002) closely approaches the regression line of the Fe-Al-epidotes due to its extremely low Mn/Fe ratio (= 0.33). The *b* parameter shows an opposite behavior (Fig. 9b), with a more pronounced increment as a function of the M^{3+} content in pure synthetic piemontite where $M^{3+} = Mn^{3+}$. Natural piemontite with variable Mn/Fe ratios displays *b* values between synthetic piemontite and Fe-Al epidote. An exception is Sr rich piemontite in which the strong expansion of the unit cell due to the $Sr \leftrightarrow Ca$ substitution mainly occurs along the *c*sinβ axis. The variation of *c* as a function of the unit cell volume (Fig. 9c) differentiates only slightly
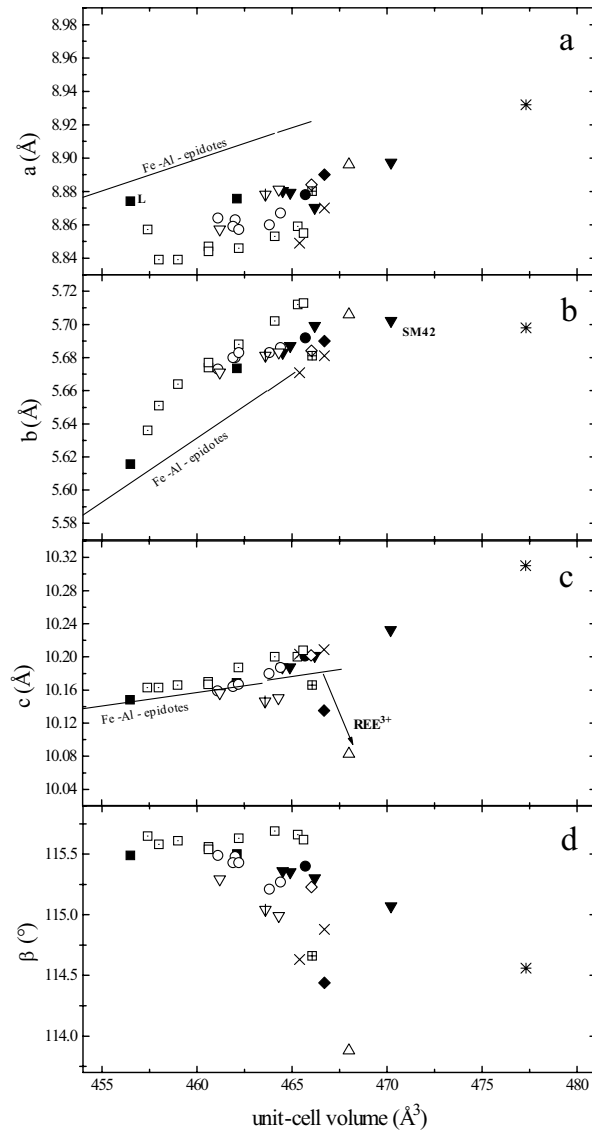
Figure 9. Unit cell parameters, *a* (a), *b* (b), *c* (c), and the monoclinic β angle (d) plotted *vs.* the unit cell volume for monoclinic manganiferous epidote-group members. Solid lines refer to natural Fe-Al epidotes (Bonazzi and Menchetti 1995). Symbols: solid circle = piemontite, type locality (Dollase 1969); dotted open squares = synthetic piemontite (Anastasiou and Langer 1977); solid downward triangles = piemontite, type locality (Catti et al. 1989); open diamond = piemontite, type locality (Ferraris et al. 1989); open circles = piemontite, different localities (Bonazzi 1990); crosses = strontiopiemontite, type locality (Bonazzi et al. 1990); open downward triangles = REE bearing piemontites, Apuan Alps (Bonazzi et al. 1992); lined open downward triangle = REE bearing piemontite from Apuan Alps (Bonazzi and Menchetti 1994); crossed open square = piemontite from Nezilovo (Bermanec et al. 1994); solid diamond = REE-bearing piemontite, Varenche mine (Bonazzi et al. 1996); open upward triangle = androsite-(La), type locality (Bonazzi et al. 1996); star = tweddillite, type locality (Armbruster et al. 2002); solid squares = piemontite, different localities (Langer et al. 2002); open squares = synthetic piemontite (Langer et al. 2002).

between the Al-Fe and the Al-Mn members; this parameter, however, is an accurate measure of the androsite-(La) component in members of the piemontite-androsite-(La) series (Bonazzi et al. 1996) as the incorporation of REE^{3+} in A2 and Mn^{2+} in A1 causes a strong contraction along c (solid arrow in Fig. 9c). Furthermore, along the piemontite-androsite-(La) join the β angle decreases linearly down to 113.88° in androsite-(La) as a function of the REE content according to the equation

$$\beta(°) = 115.49 - 2.09 \, ^{A2}REE^{3+} \, (pfu) \, (r = -0.979)$$

As apparent from Figure 9d, β is also strongly affected by the Sr ↔ Ca substitution, which causes a decrement of this value (down to 114.56° in tweddillite; Armbruster et al. 2002). Thus very low values of the monoclinic angle are distinctive of high contents of either REE^{3+} or Sr. In the latter case, however, c will be much greater. In the absence of substitutions in the A sites, variations of β are almost negligible (Fig. 9d), although synthetic Mn-Al piemontite exhibits slightly higher β values (115.54 – 115.69°) than Al-Fe epidote (115.46 - 115.35°).

OPTICAL AND SPECTROSCOPIC PROPERTIES

Looking at the data widely reported in the literature, it appears that densities (3.30 to 3.61 g/cm³) and refractive indices (α = 1.730 to 1.794, β = 1.740 to 1.807, and γ = 1.762 to 1.829; Deer et al. 1986) of piemontite are generally higher than those of the members of the clinozoisite-epidote join. This is a consequence of the generally greater substitution of M^{3+} for Al in piemontite. Indeed, the Gladstone-Dale constant of Fe_2O_3 is slightly higher than that of Mn_2O_3, while both values are higher than that of Al_2O_3 (Mandarino 1981). Accordingly, epidote minerals with only small amounts of Mn^{3+} exhibit refractive indices at the lower limits of the above range (e.g., 'withamite' from Glen Coe; Hutton 1938) or even lower indices similar to those of clinozoisite (e.g., α = 1.714, β = 1.724, and γ = 1.730; Yoshimura and Momoi 1964). Some values reported in the literature lie outside the ranges given above. For instance, γ = 1.843 was determined for a piemontite from Goldongri, India (Nayak and Neuvonen 1966) and α = 1.772, β = 1.813, and γ =1.860 were determined by Strens (1966) on a piemontite from Chikla, India.

Several attempts to correlate the variation of refractive indices (as well as other optical features) of natural samples with their composition were carried out (Short 1933; Guild 1935; Strens 1966; Tanaka et al. 1972). The results obtained were sometimes inconsistent even internally. Strens (1966) considered the variation of the optical properties in relation to site symmetry and occupancy. According to his data, indices and composition correlate linearly in the range 0.8 < (Mn + Fe) < 1.5 pfu although some samples show a wide scatter which cannot be attributed to the Mn/(Mn + Fe) ratio.

To separate the influence of the Fe^{3+} and Mn^{3+} content on the physical properties of natural piemontite, Anastasiou and Langer (1977) measured the refractive indices of a series of synthetic Al-Mn^{3+} piemontites with Mn^{3+} up to 1.75 pfu. They found the refractive indices of the synthetic samples to be generally lower than those of the natural ones and explained this result partly with the lower refractive power of Mn^{3+} compared to Fe^{3+} and partly with the influence of possible replacement of Ca in natural piemontite. Later, Langer et al. (2002) performed a new study on synthetic Al-Mn^{3+} piemontite with Mn^{3+} up to 1.50 pfu. This study shows that all three refractive indices increase as a function of Mn content although with slightly different slopes, the increase of n being in the order $n_\gamma > n_\beta > n_\alpha$. Moreover, no discontinuities at Mn^{3+} ca. 1 pfu as previously observed by Anastasiou and Langer (1977) were found.

As noted by Wieser (1973) "piemontite presents a rare example of a mineral which was distinguished basing on chemical composition (Mn content) but in practice is the

pleochroism which is now decisive feature in distinction between piemontite and epidote". The pleochroic scheme of Al-Mn-Fe epidote is basically X = lemon yellow or orange yellow, Y = amethyst, violet or pink, and Z = bright red. Burns and Strens (1967; see also Burns 1993) measured polarized absorption spectra of Al-Fe and Al-Fe-Mn epidotes and provided interesting structural interpretations thus demonstrating the origin of the pleochroic scheme and absorption colors. They examined the polarized absorption spectra of a piemontite that contains 0.625 Mn^{3+} pfu (Fig. 10); as shown in the corresponding energy level diagram (Fig. 11), the number and energy position of the observed bands are well in accord with the presence of Mn^{3+} in the tetragonally compressed (D_{4h} point symmetry) M3 octahedron. Although the splitting between d_{xz} and d_{yz} is not resolved in the spectra, an orthorhombic pseudosymmetry (C_{2v}), which basically describes the M3 site in piemontite, is best in accord with the number of the observed bands and their polarization (Langer et al. 2002). When the intensities of the absorption bands are taken into account, the different vividness of color is also easily explained. Thus, piemontite displays vivid colors correlating with high values of the molar extinction coefficients (ε) and originating from the spin-allowed transitions within Mn^{3+} ions
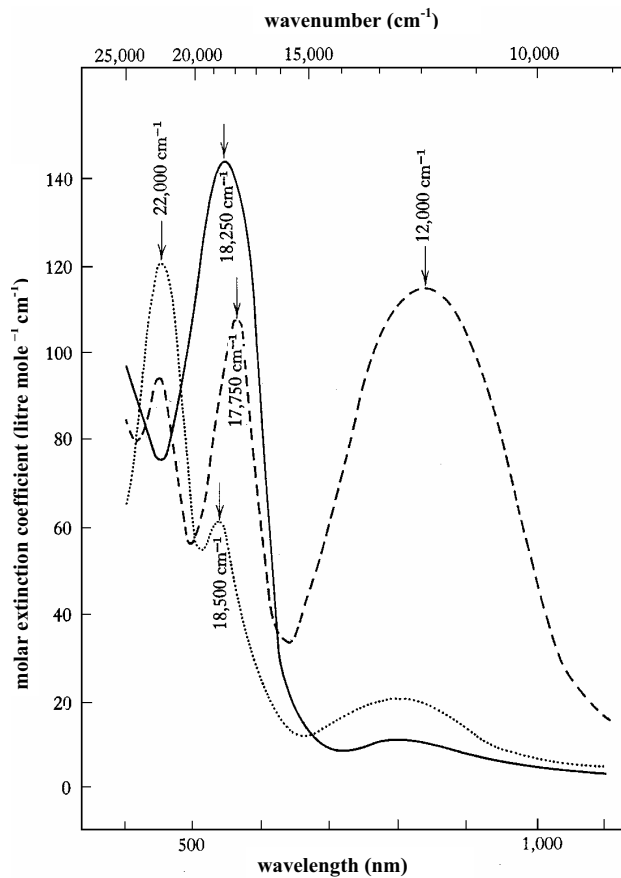
Figure 10. Polarized absorption spectra of piemontite from the type locality containing 0.625 Mn^{3+} pfu; .... = α (X) spectrum; ---- = β (Y) spectrum; —— = γ (Z) spectrum. Reproduced with permission of Cambridge University Press, from Burns (1993).
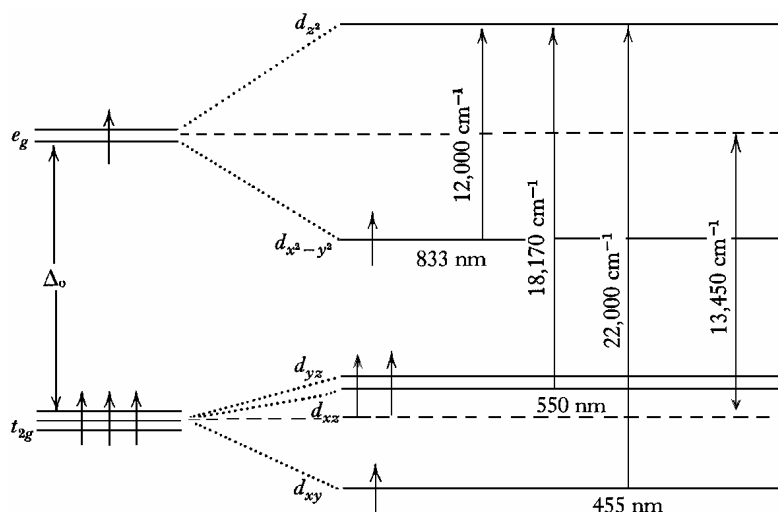
Figure 11. Schematic energy level diagram for Mn^{3+} in axially compressed octahedral coordination (M3 site). Observed transitions refer to the polarized absorption spectra given in Figure 10. Reproduced with permission of Cambridge University Press, from Burns (1993).

located in the non-centrosymmetric and very distorted M3 octahedron. On the other hand the Al-Fe epidotes display pastel shades that are characterized by relatively low molar extinction coefficients typical of spin-forbidden transitions within Fe^{3+} ions.

Much spectroscopic work (Wood and Strens 1972; Langer et al. 1976; Langer and Abu-Eid 1977; Smith et al. 1982; see also Liebscher 2004) has been done on this subject. In particular, Wood and Strens (1972) developed a method for calculating the *d*-orbital energy levels of transition-metal ions within coordination polyhedra and applied the derived equations to Mn^{3+} in the M3 site of piemontite. Smith et al. (1982) measured the polarized absorption spectrum of natural piemontite at 295 K and 100 K. Lowering the temperature resulted in a sharpening of broad bands in the 10,000 to 25,000 cm^{-1} regions, supporting their assignment to single Mn^{3+} in the non-centrosymmetric M3 site. Langer et al. (2002) reported single crystal polarized electronic spectra of natural (0.57 < M^{3+} < 1.17 pfu) and synthetic (0.83 < M^{3+} < 1.47 pfu) piemontites, respectively. Spectra were measured in the range 35,000 to 5,000 cm^{-1} at room temperature with E parallel to all three axes of the optical indicatrix. Spectra are dominated by a slightly polarized absorption edge in the UV region and also by three intense and strongly polarized absorption bands (v_I, v_{II}, v_{III}) that are typically spin-allowed *dd* transitions of Mn^{3+} in the distorted (compressed) M3 octahedron of the piemontite structure. The energy and linear absorption coefficients of these three bands shift as a function of the Mn^{3+} content in M3, so that information about the Mn^{3+}–Fe^{3+} ordering between M3 and M1 in natural piemontite can be obtained. Although in the most Mn^{3+}-rich synthetic piemontite appreciable amounts of Mn^{3+} enter the M1 site, no clear conclusion could be drawn with respect to the spin-allowed *dd* bands of Mn^{3+} in the compressed M1 octahedron. The reasons are the strong overlapping of the band in the complex spectrum and the low intensities of the Mn^{3+}(M1) bands due to the centrosymmetry of the M1 site (Langer et al. 2002).

Infrared (IR) spectroscopic studies of piemontite were preformed by Tanaka et al. (1972), Langer et al. (1976), and Perseil (1987, 1990). By means of FTIR spectroscopy in the OH region, Della Ventura et al. (1996) studied several Sr bearing piemontites (SrO from 0.78 to 5.93 wt%) and some Al-Fe epidotes with low contents of Mn^{3+} and little or no substitution

of Sr for Ca. The spectra of the Sr bearing piemontites (Fig. 12) exhibit a well resolvable doublet at almost constant wavenumber (3417 to 3454 cm^{-1}) and differ from those of Al-Fe epidotes which show a single OH band, the position of which is a linear function of the Fe^{3+} content (Langer and Raith 1974). Della Ventura et al. (1996) explained this IR feature as a consequence of two simultaneous effects: *i*) the entry of Mn^{3+} in the non OH-coordinated M3 octahedron and its consequent strong anisotropic deformation and *ii*) the entry of Sr substituting for Ca in the adjacent A2 polyhedron (for a more detailed review of spectroscopic studies on epidote minerals see Liebscher 2004).

COMPOSITIONAL VARIABILTY OF PIEMONTITE

This section deals with the compositional variability of piemontite and its related minerals as derived from a number of natural occurrences of piemontite. Chemical variations of this mineral are shown mainly by graphic representations to facilitate the readability of numerical data. 225 chemical analyses were selected from the literature and evaluated by the following criteria.

Chemical formulae were calculated on the basis of 8 cations. Fe was always considered as Fe^{3+} and the content of Mn^{2+} was estimated with respect to Mn^{3+} on the basis of a total number of positive charges equal to 25 (in the absence of F$^-$). In some cases, the sum of positive charges was < 25 even if all Mn (and Fe) was considered in the trivalent state. In these cases, the amount of Mn^{2+} was fixed to 0 pfu. Analyses showing a sum of positive charges lower than 24.90 were disregarded. If the estimated Mn^{2+} content exceeds Mn$_{tot}$ (only few analyses) Mn^{3+} was fixed to 0 pfu. Moreover, analyses were only taken into account if they satisfied the criterion 2.90 < Si^{4+} < 3.10 pfu as the T sites in epidote minerals are generally considered to be fully occupied by Si (see above). As a result, all the graphic representations are based on 198 accepted chemical analyses; complete data are given in Tables A and B of the Appendix. In the case of REE bearing piemontite (19 analyses), Mg was added to the octahedral cations (Cat$_{oct}$), as well as Ti, Cu, and Zn if present. The content of Mn^{2+} entering the M sites (Mn$^{2+}_{oct}$) was estimated on the basis of 3 − Cat$_{oct}$. Therefore, Mn$_{oct}$ = Mn^{3+} for all REE free piemontites and Mn$_{oct}$ = Mn^{3+} + Mn$^{2+}_{oct}$ for the REE bearing piemontites. The octahedral cation population in terms of Al, Mn$_{oct}$, and Fe^{3+} is illustrated in Figure 13, whereas Figure 14 reports the frequency distribution plots of Al, Fe^{3+}, Mn$_{oct}$, and Ca, respectively.
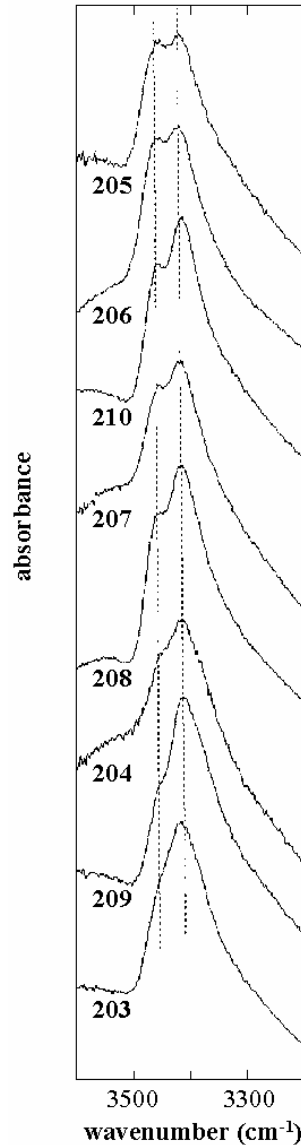
Figure 12. FTIR spectra for Sr bearing piemontites. Labeling refers to chemical analyses as reported in Table A of the Appendix. Modified from Della Ventura et al. (1996).
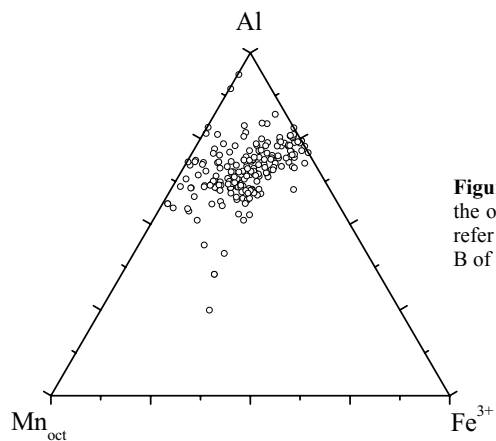
Figure 13. Ternary (Al-Fe^{3+}-Mn$_{oct}$) diagram showing the octahedral cation population of piemontite. Data refer to the analyses (n = 198) given in Tables A and B of the Appendix.
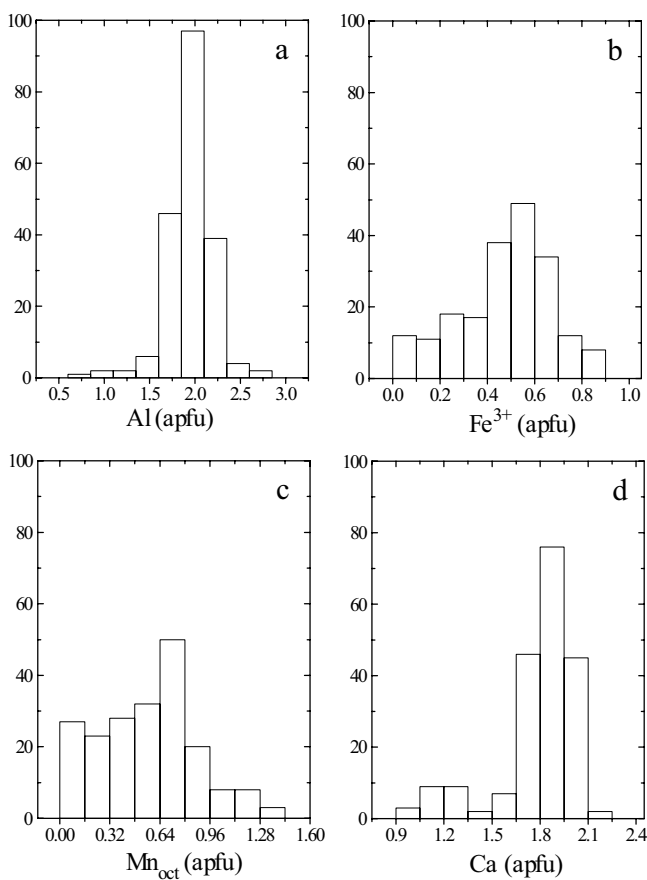
Figure 14. Frequency distribution (n = 198) of Al (a), Fe^{3+}(b), Mn$_{oct}$ (c), and Ca (d) of piemontite. Class interval was chosen according to the formula: interval= range/k, with k = 1+3.322 (log$_{10}$ n) (Carlson and Thorne 1977).

Al_2O_3 ranges from 6.25 (Enami and Banno 2001) to 31.50 wt% (Reinecke 1986b) corresponding to 0.74 and 2.80 Al pfu, respectively. The histogram for Al (Fig. 14a) shows a unimodal frequency distribution with a maximum at about 2.0 Al pfu. The minimum value observed (0.74 pfu) in the sample described by Enami and Banno (2001) is too low to fill the M2 site. It is coupled with a high content of the other trivalent cations, Mn^{3+} in particular. This composition (with some differences in the Sr, Pb, and Ba content) is very similar to that of tweddillite, $CaSr(Mn^{3+},Fe^{3+})_2Al(SiO_4)(Si_2O_7)O(OH)$, the new mineral recently described by Armbruster et al. (2002). High Al_2O_3 (up to 29.77 wt%, corresponding to 2.73 Al pfu) and low Mn_2O_3 contents are typical of the so called *withamite*. Fe_2O_3 ranges from 0.10 (= 0.01 Fe pfu) to 14.97 wt% (= 0.89 Fe pfu). The histogram for Fe^{3+} (Fig. 14b) shows an almost unimodal frequency distribution with a maximum in the range 0.50 to 0.60 pfu. However, low values (< 0.20 pfu) are not uncommon. Fe^{3+} (pfu) shows a fairly good negative correlation with Mn_{oct} (Fig. 15).
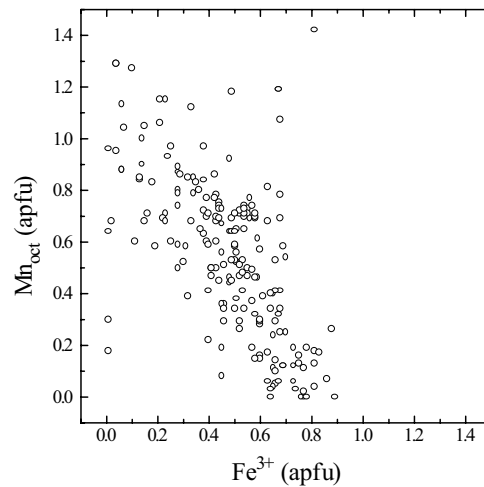
Figure 15. Mn_{oct} plotted *vs.* Fe^{3+}; data as in Figure 13. For explanation see text.

Mn_2O_3 ranges from very low values in manganian clinozoisite to about 20 wt%. Actually, an analysis of piemontite from Langban, Sweden, made by Jakob and quoted by Malmqvist (1929) gives Mn_2O_3 = 22.00 wt% which is to our knowledge the maximum content reported for a natural piemontite. This analysis, however, should be disregarded because the sum of positive charges (24.67) is far from the expected value of 25, due to a suspiciously high content of univalent cations (Na = 0.42, K = 0.06 pfu). Strens (1966) and Anastasiou and Langer (1977) have already doubted the accuracy of this analysis. Mn_{oct} shows a negative correlation with Al (Fig. 16). Due to the presence of several analyses of manganian clinozoisite, the histogram of Mn_{oct} (Fig. 14c) exhibits an irregular frequency distribution in its left side. The highest frequency values are between 0.65 and 0.80) with a spread of values for Mn_{oct} extending towards 1.40 pfu. The maximum value, 1.42 pfu, is found in the sample from Sanbagawa belt (Enami and Banno 2001) fulfilling the definition of tweddillite (Armbruster et al. 2002). The expansion of the compositional field to low or very low values of Mn is based on petrological rather than crystal chemical definition of piemontite (see above). In some instances, where strong and complex zoning in Al, Mn^{3+}, and Fe^{3+} are observed, Mn-poor compositions may correspond to fluctuations in the f_{O_2} conditions.

Small amounts of CuO (up to 1.85 wt% = 0.13 Cu pfu) and ZnO (up to 0.75 wt% = Zn 0.05 pfu) were found in piemontite from the Varenche mine (Bonazzi et al. 1996) and Nezilovo (Bermanec et al. 1994), respectively.

MgO may be present in piemontite reaching a maximum of 3.7 wt% (= 0.44 Mg pfu) in a sample from a garnet bearing muscovite-piemontite-quartz schist, Nagatoro district, Saitama Prefecture, Japan (Tanaka et al. 1972). The charge balance of the chemical formula requires in this sample, as in any REE free piemontite, Mg in the A sites together with Ca and Mn^{2+}. A high MgO content (0.35 pfu) was also found in a piemontite from schist at Chikla, India (Bilgrami 1956). However, the latter analysis was disregarded, due to the low value of Si (2.90 pfu) and the low total positive charge (24.16). MgO contents above the detection limit of the electron
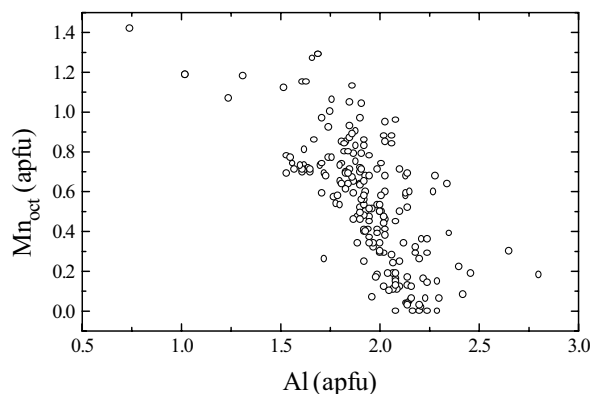
Figure 16. Mn$_{oct}$ plotted *vs*. Al; data as in Figure 13. For explanation see text.

microprobe are present in REE bearing piemontite corresponding to Mg contents (pfu) of 0.06 to 0.09 in the Pb and REE rich piemontite from Nezilovo (Bermanec et al. 1994), 0.02 to 0.08 in REE bearing piemontite from the Apuan Alps, Italy (Bonazzi et al. 1992), 0.019 in the REE bearing piemontite from Venn-Stavelot Massif, Ardennes, Belgium (Kramm 1979), and 0.17 for the REE bearing piemontite from the Varenche mine (Bonazzi et al. 1996). Except for the REE bearing piemontites from the Venn-Stavelot Massif (Kramm 1979; Schreyer et al. 1982) a positive correlation is found between Mg and REE^{3+}, pointing towards a solid solution with dissakisite-(Ce).

Other interesting chemical variations occur in the A sites. CaO ranges from 9.40 wt% (= 0.97 Ca pfu) in piemontite from Varenche mine (Bonazzi et al. 1996) to 24.75 wt% (= 2.10 Ca pfu, an evidently over-estimated value) in piemontite from Tucson Mountains, Arizona, USA (Guild 1935). The histogram of Ca shows a bimodal frequency distribution (Fig. 14d), with a maximum at Ca = 1.95–2.00 and a second distribution peak in the range 0.90–1.50, corresponding to Sr and REE rich piemontites.

SrO from 0.20 (= 0.01 Sr pfu) to about 18 wt% (= 0.92 Sr pfu) is reported in more than 60 analyses, most of them piemontite and strontiopiemontite from Andros, Greece (Reinecke 1986a, b), St.Marcel, Italy (Mottana and Griffin 1982; Mottana 1986; Della Ventura et al. 1996), Val Graveglia, Italy (Bonazzi et al. 1990), Falotta and Parsettens manganese deposits, Switzerland (Perseil 1990), Tokoro, Hokkaido, Japan (Akasaka et al. 1988; Togari and Akasaka 1987), Shiromaru manganese mine, Tokyo, Japan (Kato and Matsubara 1986), Sanbagawa belt, Japan (Enami and Banno 2001; Minagawa 1992), and Nezilovo, Macedonia (Bermanec et al. 1994). According to Mottana and Griffin (1982) Sr in piemontite from St. Marcel is essentially controlled by local bulk composition, rather than pressure or temperature. The same was observed in rocks from Andros, Greece (Reinecke 1986a) and from the Iberian Massif, Spain (Jiménez-Millán and Velilla 1993). However, Mottana (1986) observed that early-formed piemontite is richer in Sr and poorer in Mn^{3+} than late piemontite. A weak chemical zoning with increasing Sr from core to rim was observed by Enami and Banno (2001) in piemontite from the Sanbagawa metamorphic belt, Japan. Reinecke (1986b) also observed a distinct and complex zoning with respect to the Sr ↔ Ca substitution in piemontite occurring at Vitali (Andros, Greece).

High contents of PbO were found in piemontite from Nezilovo described by Bermanec et al. (1994) with up to 10.35 wt% PbO (= 0.28 Pb pfu) and in a sample described by Enami and Banno (2001) with up to 7.55 wt% PbO (= 0.20 Pb pfu). The latter also exhibits an unusually

high BaO content (up to 6.71 wt% BaO, = 0.25 Ba pfu). According to Enami and Banno (2001) such high contents of Pb and Ba in members of the piemontite-strontiopiemontite-tweddillite solid solution points to two theoretical new endmembers for epidote group minerals, "Ba-piemontite" and "Pb-piemontite". BaO up to 0.26 wt% were also observed in piemontite from the type locality, St. Marcel, Italy (Mottana and Griffin 1982).

Na$_2$O ranges from zero (most of the electron microprobe analyses) to a maximum of 2.41 wt% (= 0.37 Na pfu; Bilgrami 1956) and 2.59 wt% (= 0.42 Na pfu; Malmqvist 1929). Likewise, the presence of K$_2$O in piemontite is reported only in a few, often very old, analyses. In principle, a possible heterovalent exchange ^{A}Ca $\leftrightarrow$ ^{A}Na (or K) could be charge balanced, by analogy with dollaseite-(Ce), with a heterovalent anion substitution at the O4 site $^{O4}O^{2-} \leftrightarrow$ $^{O4}(OH^-,F^-)$. However, no recent structure refinement of piemontite supports this hypothesis. Therefore it appears more likely that relatively high amounts of Na and K result from impurities (i.e., intergrown feldspar).

It is well know that variable amounts of REE are common in the Fe rich members (epidote-allanite-ferriallanite series; see Gieré and Sorensen 2004). However, in recent years several analyses revealed the presence of REE also in piemontite. Actually, the first analysis was given by Hillebrand (quoted in Williams 1893 and Clarke 1910) who detected Ce$_2$O$_3$ = 0.89 wt% and other REE = 1.52 wt% (total REE$_2$O$_3$ = 2.41 wt%) in a piemontite from rhyolite of South Mountain, Pennsylvania, USA. As Williams (1893) stated, "this analysis is of especial interest in showing that the South Mountain piemontite is a connecting link between three recognized members of the epidote group" (piemontite, allanite, epidote s.s.). Kramm (1979) and Schreyer et al. (1986) described REE bearing piemontite from Venn-Stavelot Massif. A REE$_2$O$_3$ content close to 8 wt% (with La$_2$O$_3$ = 4.39 wt%) was found in piemontite from the Apuan Alps, Italy (Bonazzi et al. 1992). Several analyses by Bermanec et al. (1994) on piemontite from Nezilovo show REE$_2$O$_3$ varying between 6.09 and 8.56 wt%. The La content prevails on the other REE and exhibits a strong positive correlation with Pb (Bermanec et al. 1994). An REE$_2$O$_3$ content of about 14 wt% (with Ce$_2$O$_3$ largely prevailing on La$_2$O$_3$) was found in piemontite from the Varenche mine (Bonazzi et al. 1996). These occurrences clearly confirm the existence of a solid solution of piemontite towards manganian-allanite and androsite-(La). Data on the chemical composition of allanite and REE bearing epidote (Frondel 1964; Exley 1980; Sakai et al. 1984; Fleischer 1985; Deer et al. 1986) show that Ce is usually the dominant REE and often constitutes over half of the total quantity of lanthanide elements. Dollaseite-(Ce) and dissakisite-(Ce) present a similar trend. On the contrary, the Mn-rich epidotes (e.g., manganian allanite, piemontite and androsite-(La)) exhibit a rather different relative abundance of REE usually with La > Ce. Figure 17 shows the chondrite-normalized REE patterns of piemontite from the Apuan Alps, Nezilovo, and Varenche together with that of androsite-(La). A negative Ce anomaly is evident in all the patterns, with the exception of piemontite from Varenche. All patterns, with this exception, show a strong enrichment in LREE, while the Varenche piemontite exhibits a flatter pattern suggesting a minor depletion of HREE. For the other REE bearing piemontites complete chemical data were not provided, but some considerations can be made. The analysis of piemontite from Pennsylvania provides a Ce$_2$O$_3$ content of 0.89 wt%, while the sum of the other REE is given as 1.52 wt%. Because Ce$_2$O$_3$ is half of the other REE, it is likely that the La$_2$O$_3$/Ce$_2$O$_3$ ratio is about 1, which means that a Ce anomaly is present. In an analysis of piemontite from Venn-Stavelot Massif (Schreyer et al. 1986) only the Ce$_2$O$_3$ content (4.09 wt%) is reported. However, the total wt% of the analysis is very low (93.18), pointing to the possible presence of up to 5 wt% of other REE$_2$O$_3$. In the latter case, the presence of a Ce anomaly is only speculative. Finally, the piemontite from Venn-Stavelot Massif described by Kramm (1979) has a total REE$_2$O$_3$ content of 5.0 wt%, and the author notes that REE oxides are "dominantly La$_2$O$_3$, Pr$_2$O$_3$, and Nd$_2$O$_3$". Therefore, in this case a Ce anomaly is likely. It may also be noted that the La/Ce ratio is often greater than 1 in Mn-rich allanites (Deer et al. 1986).
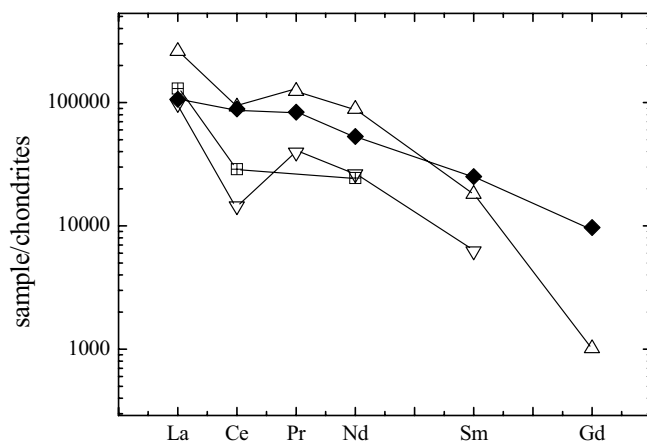
Figure 17. Chondrite-normalized REE patterns of piemontite from Apuan Alps (open downward triangles; Bonazzi et al. 1992), Nezilovo (crossed open squares; Bermanec et al. 1994), Varenche mine (solid diamonds; Bonazzi et al. 1996) and androsite-(La) (open upward triangles; Bonazzi et al. 1996). Values used in normalizing REE were taken from Anders and Ebihara (1982).

These data suggest a general trend in epidote group minerals that a Ce anomaly correlates with a high Mn^{3+} content. This correlation is not surprising because the high oxidation conditions, which favor piemontite formation, also favor a high Ce^{4+}/Ce^{3+} ratio, thereby preventing Ce incorporation in piemontite.

OCCURRENCE AND PARAGENESIS OF PIEMONTITE

Piemontite as a major rock-forming mineral is comparably rare. Nevertheless, as an accessory or minor phase, it occurs in a wide variety of rocks of different bulk compositions that were formed under different physicochemical conditions. Piemontite is a typical metamorphic mineral, while magmatic occurrences are very rare or questionable as truly magmatic. Hydrothermal occurrences are described, but not very frequent.

Guild (1935) determined the Mn concentration in a number of piemontite bearing and piemontite free rock samples and was the first to note that the occurrence of piemontite "must be due to some undetermined peculiarity of the geophysical conditions" rather than to an unusually high Mn content of the host rock. Numerous subsequent occurrences as well as experimental studies have then clarified that these "peculiar conditions" are mainly related to an unusually high oxygen fugacity although high Mn contents enlarge the stability field of piemontite. Thus, piemontite is typically found in highly oxidized manganiferous sedimentary rocks that were affected by low to high-pressure metamorphism in a wide temperature range; the typical protolith for piemontite rocks is Mn-rich chert, former ocean floor sediment. In his review of the alpine occurrences of blueschist facies manganiferous cherts Mottana (1986) pointed out that piemontite occurs in the "oxidized" assemblages associated with Mn rich varieties of sodic clinopyroxene and mica, braunite, and ardennite. The chemistry of piemontite in the metacherts depends on the availability of certain cations rather than on the metamorphic *P-T* conditions and is critically controlled by f_{O_2}. In particular, piemontite is richest in Mn^{3+} when it coexists with the other Mn^{3+} bearing phases braunite and ardennite but is significantly depleted in Mn^{3+} when it coexists with spessartine. In the latter case it may contain Mn^{2+} which substitutes for Ca. Furthermore, piemontite from high pressure manganiferous assemblages coexists with vein piemontite, which was formed later at low pressure and usually shows

lower Sr contents (Mottana and Griffin 1982). Possible mechanisms which may determine a so high f_{O_2} in the rock to stabilize piemontite range from external buffering by hydrothermal solutions to internally controlled factors like premetamorphic minerals capable of buffering f_{O_2} to a high level (Keskinen and Liou 1987). Although the composition and parageneses of piemontite bearing assemblages indicate that piemontite predominantly forms as a product of low to moderate temperature metamorphism, very high f_{O_2} and low partial pressure of CO_2 in the fluid phase together with high Mn contents in the host rock may enhance the stability field of piemontite to higher temperature (Keskinen and Liou 1987, Abs-Wurmbach and Peters 1999).

In this section we review the different occurrences of piemontite reported in the literature with emphasis given to the parageneses and, if available, the physicochemical conditions that favor piemontite formation. Due to for their relative scarcity and often incomplete *P-T* determination we organize piemontites in terms of their regional distribution rather than petrologic characteristics and subdivide them roughly into three sections only: i) metamorphic; ii) contact metamorphic and metasomatic; and iii) magmatic, pegmatitic, and hydrothermal.

Metamorphic occurrences

Europe and Russian Federation. At the type locality (Praborna mine, St. Marcel Valley, Piemonte, Italy) piemontite occurs in the upper parts of a Mn ore deposit composed of micaschist that include bands of Mn silicates (spessartine, piemontite, Mn phengite) with lenses of Mn oxides intercalated with bands rich in Fe silicates (epidote, clinopyroxene) and hematite (Martin and Kienast 1987). The Praborna deposit records different stages of the Alpine metamorphic cycle. A cretaceous high pressure event at 450–500°C and 0.8–1.0 GPa was followed by a meso-Alpine lower amphibolite to greenschist facies stage that overprinted much of the metapelitic rocks related to the Mn ore bodies and its metabasic cover rocks (Martin and Kienast 1987). Brown et al. (1978) determined the *P-T* conditions for this meso-Alpine overprint to about 300°C and 0.8 GPa and pointed to the unusual suite of minerals accompanying piemontite at St. Marcel including manganoan omphacite ('violan'), albite, quartz, braunite, microcline, hollandite, and strontian calcite. Piemontite at Praborna generally contains significant amounts of Sr substituting for Ca (Mottana and Griffin 1982). A high Sr content in the piemontite bearing horizons at St.Marcel is also confirmed by Sr rich Mn oxides of the cryptomelane-hollandite-coronadite series (Perseil 1988). Piemontite occurrences are also reported from several localities within the metasedimentary cover series (the so called "schistes lustrès") of the ophiolitic sequence of the Zermatt-Saas zone (Switzerland). In the Valsesia-Valtournanche area (Italy) piemontite occurs in manganiferous quartzite and schist and displays a wide compositional variation that reflects the pre-metamorphic heterogeneous Mn distribution and oxidation state within the protoliths rather than different metamorphic conditions (Dal Piaz et al. 1979). A detailed petrologic study of the manganiferous quartzite at Cignana Lake in Valtournanche is provided by Reinecke (1991). At this locality piemontite records two different stages of metamorphism. Piemontite from the high to ultrahigh-pressure assemblage has high Mg content substituting for Ca and coexists with pyrope rich garnet, magnesian braunite, unusually Mg–rich ardennite, kyanite, phengite, talc, paragonite, zoned tourmaline with dravite rich cores, hematite, and rutile. Coesite or quartz pseuodomorphs after coesite are found as inclusions in dravite and pyrope rich garnet. Contrary, piemontite from the low-pressure assemblage is Mg poor and coexists with braunite, tourmaline, garnet, and ardennite that are also characterized by a lower content of Mg. Other Alpine occurrences of piemontite in the "schistes lustrés" are reported from Haute Maurienne (France) where piemontite is restricted to oxidized assemblages in paragenesis with quartz, garnet, braunite, talc, phlogopite, phengite, chlorite, and hematite (Chopin 1978), from Steinen Valley (Switzerland) where it coexists with quartz, spessartine, braunite, and cryptomelan in calcareous schist and siliceous dolomites that were progressively metamorphosed from lower greenschist to higher amphibolite facies conditions (Frank 1983), and from quartzitic marble cropping out in the area of Sant'Andrea di Cotone (Eastern Corsica, France; Caron et al.

1981). The latter occurrence represents metamorphic conditions of about 0.8 GPa and 300°C as derived from the phase assemblage with clinopyroxene, garnet, blue amphibole, phengite, chlorite, stilpnomelane, lawsonite, pumpellyite, and deerite (Caron et al. 1981). Piemontite with a composition intermediate between common piemontite and androsite-(La) is described from a fine grained, reddish-brown gneiss from the dump of the abandoned Mn mine at Varenche, St. Barthélemy Valley (Western Alps, Italy; Bonazzi et al. 1996). The metasedimentary rocks at the Varenche mine probably form part of the Tsatè nappe (Dal Piaz 1988; Marthaler and Stampfli 1989) and were metamorphosed at greenschist facies conditions but locally, like in the gneiss containing the described REE bearing piemontite, show relics of a low grade, high pressure metamorphism. At Piz Cam (Bergell Alps, Switzerland) bladed crystals of piemontite up to 1 cm long occur together with spessartine, rhodonite, rhodochrosite, and kutnahorite in quartzite layers, which are intercalated in a massive sequence of chlorite-muscovite-clinozoisite-albite schist and marble metamorphosed under greenschist facies conditions (Wenk and Maurizio 1978).

Several occurrences of piemontite are reported from the Apennine, Italy. In Val Graveglia, Northern Apennine, piemontite occurs in manganese ore deposits within the metacherts on top of an ophiolite sequence. Here, a prehnite-pumpellyite facies metamorphism produced complex unusual Mn rich mineral assemblages including a wide variety of rare mineral species (Cortesogno and Venturelli 1978; Cortesogno et al. 1979). At the Cerchiara mine piemontite occurs with sodic-clinopyroxenes (aegirine, aegirine-augite, and namansilite), alkali and sodic-calcic amphibole, andraditic garnet, pectolite, ganophyllite, calcite, manganoan calcite, calcian rhodochrosite, and rhodochrosite (Lucchetti et al. 1988). At the Molinello and Cassagna mines strontiopiemontite was found in veins containing calcite, rhodonite, rhodochrosite, and ganophyllite (Bonazzi et al. 1990). Within Mn rich beds of the "Brecce di Seravezza" formation of the Apuan Alps piemontite is associated either with braunite and rare hausmannite or with braunite, hollandite, and minor amounts of rhodochrosite and kutnahorite. Both assemblages formed during alpine metamorphism at 0.4–0.6 GPa, 350–380°C and f_{O_2} values higher than those of the hematite-magnetite buffer (Franceschelli et al. 1996). Bonazzi et al. (1992) described REE bearing piemontite from braunite mineralizations in calcschist horizons within marble of the Apuan Alps at the slope of Mt. Brugiana - La Rocchetta. The piemontite occurs as minute prismatic crystals in bent veinlets associated with quartz and minor amounts of braunite, Mn-oxides, titanite, apatite, mica, and manganoan calcite.

In glaucophane schist and associated rocks from the Ile de Groix (Brittany, France) piemontite coexists with ottrelite and is only found in rocks that lack garnet and possibly reequilibrated at lowest greenschist facies conditions. In these rocks the Mn content of piemontite directly reflects that of its precursor mineral (Makanjuola and Howie 1972).

In Spain piemontite is described from the Ossa-Morena central belt (Iberian Massif) and provides an example of the interplay between f_{O_2}, rock composition, mineral assemblage, and piemontite composition. Here, successive greenschist facies metamorphic events progressively reduced initial, highly oxidized braunite nodules and produced minute euhedral crystals of piemontite in paragenesis with Ti rich braunite, hematite, and spessartine (Velilla and Jiménez-Millán 2003). Depending on the physicochemical conditions piemontite from Ossa-Morena displays a wide chemical variation ranging from manganian epidote to piemontite (Jiménez-Millán and Velilla 1993). The Mn^{2+} content of piemontite correlates inversely with f_{O_2}. The control of the mineral assemblage on piemontite composition is evident from braunite vs. hematite bearing assemblages. The strong fractionation of Mn^{3+} into braunite prevents high Mn^{3+} contents in coexisting piemontite. On the other hand, a high modal amount of hematite leads to Mn^{3+}/Fe^{3+} ratios in coexisting piemontite up to three times higher than in piemontite coexisting with braunite. Finally, a comparison between the bulk composition of piemontite bearing and piemontite free lithologies from Ossa-Morena suggests that high Ca contents enhance the stability of piemontite (Jiménez-Millán and Velilla 1993).

In the highly oxidized Mn and Al rich layers of the low-grade metamorphic metasediments of Salmchâteau, Venn-Stavelot Massif, Ardennes (Belgium), a Mg and REE rich piemontite occurs as a rare phase forming a peculiar assemblage with viridine (solid solution between andalusite and kanonaite), muscovite, paragonite, Mg chlorite, braunite, hematite, quartz, rutile, and apatite (Kramm 1979). A similar REE rich but Mg free piemontite occurs together with spessartine, quartz, and kutnahorite in the low-temperature chlorite veinlets that crosscut the low-grade manganiferous deposit of the Lienne Valley in the southwestern part of the Venn-Stavelot Massif (Schreyer et al. 1986).

Two extensively studied piemontite occurrences are from the Islands of Andros and Evvia (Greece) that both belong to the Attic-Cycladic blueschist belt. These occurrences provide one of the few opportunities to study the low to medium grade evolution of piemontite bearing silicate assemblages in response to changes in temperature and pressure (Reinecke 1986a) and will be discussed in detail below. Besides the more common piemontite studied by Reinecke (1986a) extremely Mn^{2+} and Mn^{3+} rich but Fe^{3+} poor REE bearing piemontite with composition extending to androsite-(La) occurs as minor or accessory constituent in Ca poor assemblages (e.g., spessartine quartzite, rhodonite rhodochrosite braunite fels) at Petalon Mountain, central Andros (Bonazzi et al. 1996).

In Mn rich metasediments from the Lower Paleozoic formation of the Inner West Carpathians (Slovakia) zoned piemontite occurs together with Fe-oxides in the rim of spessartine nodules that were formed by greenschist facies metamorphism of sedimentary Mn concretions (Spisiak et al. 1989).

An unusually REE and Pb rich piemontite was found at Nezilovo, Macedonia, in the upper part of Babuna River, within a greenschist facies mica schist containing red mica, quartz, ardennite, gahnite, and franklinite (Bermanec et al. 1994).

Piemontite in paragenesis with manganoan muscovite and quartz is reported from the manganiferous mica schists at Dealul Negru (Lotru Mountains, Romania) that also contain manganoan biotite, sericite, chlorite, orthoclase, microcline, albite, spessartite-calderite, ferrian braunite, bixbyite, hematite, rutile, apatite, and zircon (Balan and David 1978).

An extraordinary piemontite occurrence is reported from the Vestpolltind iron manganese deposit (Lofoten-Vesterålen province, Norway). In the jasper banded hematite ore of this deposit piemontite is found in layers closely associated with tremolite-actinolite, diopside, quartz, and minor amounts of manganophyllite, garnet, and sillimanite (Krogh 1977). The observed mineral assemblage, suggesting textural equilibrium, was formed under granulite facies conditions of 0.9–1.1 GPa and 770°C with a local temperature peak of 940 ± 50°C (Krogh 1977). It thus represents, at least to the authors' knowledge, the highest-grade occurrence of piemontite so far reported.

Several piemontite occurrences are reported from the Ural Mountains. In the lowest grade metamorphic jasper deposits of the southern Urals piemontite occurs as an accessory mineral together with minor amounts of chlorite, actinolite, magnetite, pumpellyite, stilpnomelane, calcite, and albite (Krizhevskikh 1995). At the Uchaly deposit (Southern Urals) piemontite coexists with high aluminum and high fluorine titanite in Mn-rich quartzites (the so called "gondites"; see Roy and Purkait 1968 for nomenclature) associated to metavolcanics that probably experienced a high-pressure metamorphism that was followed by a prehnite-pumpellyite facies metamorphism (Pletnev et al. 1999). In metamorphic rocks of the Maldynyrd Range (Subpolar Urals) piemontite and Mn rich varieties of allanite occur in nodule shaped segregations (Yudovich et al. 2000). The host rocks of these nodules are different types of metarhyolite characterized by various degrees of alteration (Yudovich et al. 2001). In the aporhyolite schist complex of the Al'kesvozh Sequence piemontite forms small prismatic crystals and is dispersed together with spessartine in nodules that are made up of alternating

layers of fine grained sericite and coarse grained muscovite and quartz. In the sericite quartz schists of the Lake Grubependity cirque nodules mainly consist of piemontite, braunite, and quartz, with minor amounts of hematite, ilmenite, zircon, ardennite, and xenotime. Lenses containing the rare minerals skorodite and arsenosiderite are also enclosed in these nodules. The peculiar mineral chemistry of these nodules, mirrored by anomalously high concentrations of Sr, Ba, As, and Zr in piemontite, is probably due to an internal mobilization of schist derived elements as well as an infiltration of external material (Kozyreva et al. 2001). In the valley of the Alda-Ishkin River and the Khar-Taiga Mountains piemontite occurs in albite-sericite-chlorite-quartz schists (Voznesenskii 1961).

Africa.

Tanzania. At Mautia Hill at the western margin of the Monzambique Orogenic belt small subhedral piemontite occurs in talc phlogopite and in talc edenitic hornblende rich layers with subordinate amounts of viridine and yoderite (Basu and Mruma 1985).

Several occurrences of amphibolite facies piemontite in a variety of parageneses have been reported from the Mn rich metasedimentary rocks of the Konse Series in central Tanzania (Meinhold and Frish 1970). In particular, piemontite is a major constituent of amphibolites and quartz schists whereas it is a minor constituent in marble, calc-silicate rocks, quartz-chlorite-mica schist, and quartz-viridine-mica schist.

Asia.

China. In the braunite ore deposits widely distributed along the western margin of the Yangtze Platform, piemontite commonly occurs together with rhodonite, spessartine and other metamorphic silicate minerals in layers, which rhythmically alternate to primary Mn oxide and carbonate layers (Liu and Xue 1999). In the felsic metavolcanic layers from Mulan Mountain (Hubei Province) fine-grained piemontite is rimmed by epidote and records metamorphic conditions transitional between blueschist and greenschist facies (Zhou et al. 1993). On Hainan Island, Guangdong province, a high f_{O_2} under alkaline conditions favored the formation and stability of piemontite (Peng and Zheng 1984). One of the few high to ultrahigh pressure occurrences of piemontite is reported from gneisses that are associated with the eclogites at Sulu-Dabie Mountains (southern Henan). Here, piemontite besides quartz, apatite, phengite, albite, epidote, titanite, and omphacite occurs as inclusion in zircon and is interpreted as a relic of the regional ultrahigh pressure metamorphism (Liu et al. 1998; for a detailed review of epidote minerals in high to ultrahigh pressure rocks see Enami et al. 2004).

India. Piemontite that formed during a lower amphibolite facies metamorphism occurs in manganiferous metasediments of the Manbazar area (Purulia District, West Bengal) coexisting with quartz, spessartine, manganophyllite, braunite, hematite, and oligoclase (Acharyya et al. 1990). A later contact metamorphism overprinted this assemblage and formed manganian andalusite at the expense of piemontite spessartine, and braunite. Amphibolite facies piemontite is also described from the manganiferous silicate rocks of Gowari Wadhona in the manganese belt of the Sausar Group (Roy and Purkait 1968). In these rocks, first named "gondites" by Fermor (1909), amphibolite facies metamorphism on the original manganiferous sediments produced piemontite-bearing assemblages with unusual manganese rich spessartine, rhodonite, clinopyroxenes, amphibole, manganophillite, alurgite, braunite, and hollandite besides quartz and minor amounts of apatite, plagioclase, calcite, dolomite, and microcline. In the calc-silicate rocks from the Sausar Group piemontite coexists with garnet in braunite bearing and braunite free assemblages

(Fukuoka et al. 1990). Piemontite and garnet are both Mn enriched in the braunite bearing compared to the braunite free assemblages in contradiction to the findings of Jiménez-Millán and Velilla (1993) from Ossa-Morena, Spain (see above).

Pakistan. The only piemontite occurrence from Pakistan so far reported is close to the contact between the Lower Swat-Buner schistose group and the epidote amphibolites of the Kohistan basic complex (North-Western Pakistan). Here, piemontite occurs in schists together with quartz, albite, margarite, tourmaline, muscovite, rare spessartine, Mn rich chlorite, rutile, and magnetite, as euhedral, elongated crystals that form laminae within the plane of schistosity (Jan and Symes 1977).

Thailand. Piemontite occurs in quartz schists from the Nam Suture Zone in Northen Thailand that were derived from hemipelagic to pelagic Mn rich sediments and metamorphosed under the blueschist facies conditions (Singharajwarapan and Berry 2000).

Japan. Within the different metamorphic areas of Japan piemontite occurs in a variety of lithologies and records diverse physicochemical conditions. In veins from the manganiferous iron ore deposits of the Tokoro Belt, Hokkaido, Sr rich piemontite coexists with Mn bearing pumpellyite and/or okhotskite, hematite, and bixbyite (Togari et al. 1988, Akasaka et al. 1988). These veins occur in the ore bodies themselves and in the associated radiolarian cherts. Except for the Fukuyama mine, piemontite from veins in the ore bodies tends to contain more Mn^{3+} and Fe^{3+} than that from veins in the cherts, whereas its Sr content is higher in the latter, therefore suggesting a chemical control by the host rock (Akasaka et al. 1987). Based on the metamorphic conditions of about 250°C and 0.4–0.5 GPa at very high f_{O_2}, Akasaka et al. (1988) interpreted the assemblage piemontite + Mn pumpellyite as the low *P*, low *T* equivalent of the piemontite sursassite assemblages discussed by Reinecke (1986a). Metamorphic conditions of the prehnite-pumpellyite facies were also estimated for fine disseminated piemontite that coexists with manganoan grossular in the Dainichi manganese ore deposit (Kanagawa Prefecture; Hirata et al. 1995). Most piemontite occurrences of Japan, however, record greenschist, blueschist to epidote amphibolite facies conditions and belong to the different high *P/T* metamorphic belts of Japan. In the Yamagami metamorphic rocks of the northeastern Abukuma Plateau piemontite coexists with phengitic muscovite, albite, chlorite, tourmaline, rutile, and manganian hematite (Akasaka et al. 1993) and is often microboudinaged defining a stretching lineation (Masuda et al. 1995). Comparable microboudinaged piemontite is also found in quartzites from Nuporomaporo (northern part of Kamuikotan belt) with muscovite and apatite, from Asemi (Sanbagawa belt) with albite, chlorite, muscovite, and apatite, and from Matsunosako (Nagasaki belt) with muscovite, albite, and tourmaline (Masuda et al. 1990).

A detailed description of blueschist to epidote amphibolite facies piemontite from two localities of the Sanbagawa belt stems from Izadyar (2000) and Izadyar et al. (2000, 2003) who studied the relationship between chemical variation in piemontite, host rock bulk chemistry, parageneses, and metamorphic conditions at Asemi-gawa and Besshi. Their results will be presented and discussed below in comparison to piemontite from Evvia and Andros Islands (Greece). In the Shirataki and Oboke areas of the Sanbagawa belt piemontite occurs in siliceous schists that show increasing metamorphic conditions from greenschist to blueschist up to epidote amphibolite facies (Ernst and Seki 1967). These schists are characterized by the ubiquitous coexistence of piemontite, quartz, and stilpnomelane and show an increasing piemontite/stilpnomelane ratio with increasing metamorphic grade. A

very peculiar piemontite occurrence of the Sanbagawa belt is described from epidote amphibolite facies rocks of central Shikoku (Enami and Banno 2001). Here, common piemontite as well as barian plumboan strontiopiemontite occur in Mn rich lenses within a layer of quartz schist that was metamorphosed at 480–580°C and 0.7–1.0 GPa (Enami et al. 1994). The Mn rich lenses are mainly composed of piemontite, quartz, hematite, dolomite, and calcite with minor amounts of muscovite, chlorite, talc, and apatite. Small nodules within these lenses consist of an abswurmbachite rich inner zone with minute inclusions of noélbensonite and a hollandite rich outer zone with subordinate amounts of calcite, muscovite, quartz, and piemontite. The barian plumboan strontiopiemontite occurs in clusters of piemontite in occasional mutual grain contact with the latter and gives no textural evidence for chemical disequilibrium between both phases (Enami and Banno 2001). In schists of the Kotu-Bizan district (Eastern Shikoku) piemontite is associated with the typical blueschist facies paragenesis glaucophane, rare lawsonite, and sodic pyroxene (Ernst 1964). Lower amphibolite facies (>0.3 GPa and 530–560°C) piemontite with Mn white mica, viridine, spessartine, Mn tourmaline, and Ti-Mn hematite is reported from a highly oxidized manganiferous layer within the quartz mica schists of the Hidaka Mountains, Hokkaido (Grapes and Hashimoto 1978). It is typically restricted to areas where most viridine has been altered to sericite and occurs disseminated in the matrix as well as in monomineralic veins. These veins do not extend outside the manganiferous layer and crosscut its foliation. Comparable *P-T* conditions (~0.5 GPa and 550°C) were derived for the highly oxidized siliceous schist of the Mineoka tectonic zone (Boso Peninsula) where piemontite coexists with cuprian phlogopite, aegirine-augite, riebeckitic tirodite, quartz, albite, K-feldspar, apatite and hematite (Ogo and Hiroi 1991; Hiroi et al. 1992).

Piemontite associated with braunite (and hematite) ores occurs coexisting with ardennite and/or sursassite in several manganese deposits of the Sanbagawa belt (Enami 1986; Minakawa and Momoi 1987) and in the Tone mine, Nagasaki Prefecture (Sasaki et al. 2002), and as subordinate phase together with aegirine, rhodonite, spessartine, and jacobsite in veinlets within the ore at the Kamisugai mine, Ehime Prefecture (Kato et al. 1982).

America.

U.S.A. In the Shadow Lake tuffs (eastern Sierra Nevada, California) piemontite bearing assemblages, first described by Short (1933), are the product of an upper greenschist to lower amphibolite facies overprint of dacitic to rhyodacitic pyroclastic deposits (Keskinen 1981). Besides its occurrence in shaly and schistose layers, piemontite is found as well in late hydrothermal veins at this locality. The piemontite bearing assemblage consists mainly of quartz, albite, phengitic muscovite, phlogopite, and tremolite and is characterized by sporadic piemontite, absence of other epidote group minerals, and a relatively high concentration of finely grained disseminated hematite. Although this mineral assemblage is normally indicative of the greenschist facies, Keskinen (1981) speculated that it might have persisted to temperatures higher than those usually attributed to greenschist facies rocks due to the high f_{O_2} conditions. The Shadow Lake occurrence also provides further evidence for the overwhelming importance of the f_{O_2} in stabilizing piemontite compared to the bulk composition, as the metavolcanic rocks, although characterized by a variety of Mn rich minerals, do not exhibit unusually high Mn contents.

Studying the amphibolite facies occurrences from San Gorgonio Pass (southern California) and Las Tablas and Picuris Range (northern New Mexico), respectively, Smith and Albee (1967) and then Stensrud (1973) showed that the occurrence of

piemontite under amphibolite facies conditions is not as unusual as stated by different authors (e.g., Makanjuola and Howie 1972). The microcline-plagioclase-quartz gneiss cropping out near San Gorgonio Pass locally contains piemontite bearing layers that were formed under highly oxidizing conditions and are characterized by hematite, ferrian spessartine, ferrian muscovite, and ferromagnesian silicates (phlogopite, pyroxene, and amphibole) that exhibit high Mg/Fe ratios and unusually high Fe^{3+} contents (Smith and Albee 1967). The piemontite bearing schists from Las Tablas and Picuris Range rarely contain garnet and consists of piemontite, hematite, ferrian muscovite, phlogopite, and microcline. Assuming amphibolite facies temperatures they indicate an f_{O_2} of probably higher than 10–15 bars (Stensrud 1973).

Amphibolite facies piemontite with spessartine, manganian andalusite, braunite, abundant tourmaline, and rare manganiferous zincian staurolite is also reported from a manganiferous layer that crops out along the contact between the Vadito and Ortega Groups (northern New Mexico) was metamorphosed at 500–540°C and 0.38–0.46 GPa (Grambling and Williams 1985).

Argentina. Descriptions of piemontite from South America are rare. Piemontite has been mentioned by Gelos et al. (1988) as an important mineral in sediments of the continental platform in Argentina, and is known from skarn deposits of Alta Gracia, Sierras de Gordoba and from hydrothermal alteration zones in the Jujuy province (Viramonte and Sureda, pers. comm.)

Oceania.

New Zealand. In a quartz-albite-ardennite-spessartine-phengite-hematite-chlorite-rutile-tourmaline schist of the Haast Schist Group near Arrow Junction, western Otago, piemontite with about 0.7 wt% SrO and 0.06 wt% PbO occurs in crack-seal quartz veins (Coombs et al. 1993). These veins formed shortly after peak metamorphism in the chlorite zone of the greenschist facies at about 0.45 GPa and 390°C. The protolith of the schist has been a highly oxidized (Fe, Mn)–oxide and –hydroxide bearing siliceous pelagic sediment (Coombs et al. 1993). The manganiferous members of the epidote group in the rocks of the Haast Schist Group display a continuous compositional range in terms of total Mn content from Mn^{3+}-rich piemontite through manganian epidote to manganoan epidote in which Mn^{2+} substitutes for Ca (Kawachi et al. 1983). As usually, Mn^{3+} richer piemontite tends to occur in rocks with a higher oxidation ratio, confirming that the critical factor to form piemontite is a high oxidation state rather than a very high Mn content. Geochemical investigations show that the formation of piemontite in the schists from Arrow Junction is also closely related to the excess oxygen inherited from the original Mn oxides (Coombs et al. 1985). Contrary to the schists, piemontite from the metacherts of the Haast River Area coexists with quartz, albite, muscovite, phlogopite, actinolitic-tremolitic amphibole, spessartine, tourmaline, hematite, apatite, and titanite and corresponds to a higher metamorphic grade than in the other occurrences of the Haast Schist Group (Hutton 1940; Kawachi et al. 1983; Cooper 1971, Coombs et al. 1993).

Australia. In the Wilyama Orogenic Domain (South Australia) piemontite occurs in a manganiferous unit within the albite rich metavolcanic sedimentary sequence of the Olary Block and ranges in composition from manganian epidote ($Mn^{3+} = 0.14$ pfu) to extreme Mn rich specimen (Mn^{3+} up to 1.05 pfu) (Ashley 1984). Geothermometry leads to metamorphic temperatures of 400 to 500°C. The assemblage includes spessartine rich garnet, albite, phengite, manganoan tremolite, phlogopite, quartz, and Mn bearing hematite, and indicates a f_{O_2} above the hematite-magnetite buffer.

Contact metamorphic and metasomatic occurrences

To the authors' knowledge, no piemontite occurrence that could be unequivocally attributed to a classical contact metamorphism has so far been described. In the Odenwald (near Darmstadt/Germany) piemontite occurs in a viridine hornfels but was probably formed during a retrograde alteration (Abraham and Schreyer 1975). In the medium grade schists of the contact aureole of the Brezovica peridotite (Serbia) piemontite occurs in a talc phengite assemblage (Abraham and Schreyer 1976). But contrary to classical contact metamorphism this occurrence indicates very high pH$_2$O and is attributed to a subduction zone emplacement of the ultramafic mass at 25 to 35 km depth (Schreyer and Abraham 1977).

Metasomatic piemontite is described from rare Mn bearing skarn deposits associated with gabbro to dioritic plutons of northwestern Iran (Tikmeh Dash pluton and Bostan Abad area). Here, piemontite is primarily found in epidote exoskarns with bixbyite and hematite as the main ore minerals (Somarin and Moayyed 2002). In the Upper Proterozoic Nyarovoisk suite near the Kharbei molybdenite ore deposit (Polar Urals, Russia) piemontite occurs in metasomatized zones of quartz feldspar sericite chlorite schists (Litoshko and Nikitina 1984). In the metasomatic gold pyrite deposits of the Baimak area (Southern Urals, Russia) piemontite occurs with pumpellyite and clinozoisite-epidote (Ismagilov 1976). In (meta)rodingites that are associated with the Bou Azzer ophiolite (Anti-Atlas Mountains, Morocco) piemontite coexists with grossular, salite, and prehnite and formed during an Mg-Ca-Mn metasomatism. This metasomatic event can be related to the serpentinization process that occurred in the associated ophiolite at 200–350°C and 0.2 GPa (Leblanc and Lbouabi 1988).

Magmatic, pegmatitic, and hydrothermal occurrences

Piemontite in intermediate and acid volcanic rocks has been only rarely reported (see Deer et al. 1986; e.g., Lausen 1927; Guild 1935, Lyashkevich 1958). Nonetheless, it was most probably formed during postmagmatic hydrothermal activity rather than as a primary magmatic phase. In the volcanic sequence at Sulphur Spring Valley (Arizona, USA) piemontite occurs in narrow veinlets and fractures in andesite with considerable amounts of quartz and some kaolinite and was probably deposited by postmagmatic hydrothermal solutions (Lausen 1927). The manganian clinozoisite ('withamite') described by Hutton (1938) from veinlets and vesicles within andesite at Glen Coe, Scotland, also points to a hydrothermal origin. In the Tucson Mountains (Arizona, USA) described by Guild (1935) piemontite is restricted to cavities and fissures that are primarily filled by calcite and quartz and clearly indicates a hydrothermal origin. Likewise, piemontite from the nepheline syenite of Alain Range described by Lyashkevich (1958) generally occurs as replacement of biotite and thus implies postmagmatic alteration. In the fine-grained groundmass of the "Imperial Porphyry" that belongs to the Dokhan volcanic sequence, Eastern Desert, Egypt, piemontite is associated with basaltic hornblende (Basta et al. 1980, 1981).

Piemontite from pegmatites is only rarely reported as a late phase in the crystallization sequence (Deer et al. 1986). It was first described by Bilgrami (1956) from the Sitasaongi mine in the Bhandara district (India) where it coexists with other accessory Mn minerals like bixbyite, braunite, hollandite, manganite, pyrolusite, and cryptomelane in a calc-alkaline pegmatite vein crosscutting the manganese ore horizons (Mitra 1964). Similar occurrences from India are reported from the manganese ore deposits at Kajlidori mine in the Jhabua district (Nayak 1969) and Goldongri mine in the Panchmahal district (Nayak and Neuvonen 1966). In the latter, piemontite occurs at the contact between pegmatite and ore body. In Notodden and Tinnsjo (Norway) manganian clinozoisite (described as withamite) occurs as a late stage crystallization or replacement product in pegmatites and quartz veins that crosscut higher-grade metamorphic rocks (Morton and Carter 1963). Piemontite bearing "pegmatoidal" feldspar segregations are described from gneisses of the Sudeten Mountains (Poland) that are

associated with amphibolites (Wieser 1973). Despite their association with amphibolite facies rocks these segregations are probably due to a lower grade hydrothermal activity as testified by the presence of microcline and low temperature albite and therefore let Wieser (1973) to question the stability of piemontite at amphibolite facies conditions.

At Rémigny, Quebec (Canada), fractured, prehnitized, and epidotized dioritic rocks are cut by a series of small veins that were probably precipitated during the terminal stage of the Lac-Rémigny intrusive complex from low temperature (< 300°C) hydrothermal solutions. The veins consist of albite, armenite, Mn zoisite ('thulite'), and piemontite with minor amounts of natrolite, kaolinite, calcite, quartz, and hematite as accessory phases (Pouliot et al. 1984). The primary epidote group mineral in the veins is manganiferous zoisite that locally contains a core of iron rich zoisite. Piemontite formed latest in the sequence of epidote group minerals and typically replaces manganiferous zoisite in irregular patches and along the grain boundaries (Pouliot et al. 1984).

At the Kalahari manganese field of the Transvaal Supergroup (South Africa) fluid rock interaction during high-grade diagenesis and lower greenschist facies metamorphism was followed by up to three hydrothermal events and superficial weathering and led to a complex mineral assemblage. Earliest minerals include sedimentary and diagenetic kutnahorite, Mn rich calcite, braunite, and hematite. Piemontite and Sr-rich piemontite occur in calc-silicate bodies and formed during the oldest of the three hydrothermal events at about T = 450°C together with albite, orthoclase, banalsite, andradite, henritermierite, tephroite, minerals of the pectolite-serandite series, pyroxenes (acmite, Mn bearing diopside), rhodonite, and ruizite (Gutzmer and Beukes 1996). More recently tweddillite was described in the hydrothermally altered calc-silicate rocks of this locality associated with serandite-pectolite and braunite (Armbruster et al. 2002). In the sedimentary to hydrothermal lead manganese ore deposit of Ushkatyn III (Central Kazakhstan) piemontite occurs in an unusual mineral assemblage including braunite, coronadite, kentrolite, garnet, tephroite, barite, and calcite (Dzhaksybaev et al. 1991).

Hydrothermal piemontite partially to completely replaces biotite in the quartz sericite biotite schist and quartzite of the metamorphic series at Sierra Pelona (California, USA; Simonson 1935). Here, the hydrothermal activity is related to the intrusion of a quartz dioritic dike. Extensive development of hydrothermal Mn poor piemontite, epidote, and chlorite characterizes a quartzitic explosion breccia in the Archean migmatites of Labrador, Canada (Taylor and Baer 1973).

PIEMONTITE COMPOSITION
AS A FUNCTION OF *P, T* AND HOST ROCK COMPOSITION

Compared to the Al-Fe epidotes (see e.g., Grapes and Hoskin 2004), systematic studies of the interplay between mineral composition, host rock composition, and metamorphic conditions are rather rare for piemontite. This is mostly due to the spot character of the occurrence of piemontite bearing lithologies that normally does not allow tracing and studying the evolution of these assemblages along metamorphic arrays in individual metamorphic terrains. The following discussion therefore relies only on the two well-studied examples from the Sanbagawa belt (Japan) and the Attic-Cycladic belt (Greece).

Sanbagawa belt

Izadyar (2000) and Izadyar et al. (2000, 2003) studied the relationship between chemical variations in piemontite, host rock bulk chemistry, parageneses, and metamorphic conditions at the Asemi-gawa and Besshi areas of the Sanbagawa belt. Samples from Asemi-gawa come from the garnet zone (~0.8–0.9 GPa and 400°C) whereas samples from Besshi come from the

slightly higher grade-albite biotite zone (~1.0 GPa and 500°C). At both localities piemontite coexists with quartz, albite, phengite, chlorite, braunite, apatite, hematite, ± garnet, ± talc, and ± crossitic or barrositic amphibole. Based on the presence or absence of talc, the piemontite schists can be subdivided into talc bearing and talc free assemblages at Asemi-gawa as well as at Besshi. The two assemblages are also distinguished by different compositions of the coexisting minerals in both areas. As the bulk chemistry and f_{O_2} of each of the two assemblages are similar at both localities, differences in the composition of piemontite from talc bearing and talc free assemblages, respectively, between Asemi-gawa and Besshi may be attributed to the different metamorphic conditions. Within both assemblages piemontite from Asemi-gawa tends to have higher Mn contents than that from Besshi (Fig.18) and suggests a decreasing Mn content in piemontite with increasing grade (Izadyar 2000). Although the zonation patterns of individual piemontite crystals are generally not very clear and distinct at both localities, two zonation trends may be observed at Asemi-gawa: In the talc bearing assemblage piemontite displays a large inner zone (core) and a narrow outer zone (rim). This rim is enriched in Fe^{3+} and slightly depleted in Mn^{3+} compared to the core (Fig. 18). Piemontite from the talc free assemblage displays a somewhat more complex zonation with a core, an inner rim (mantle), and an outer rim. From core to mantle Mn^{3+} significantly decreases whereas from mantle to outer rim it increases again (Fig.18). With respect to the relationship between Mn content in piemontite and metamorphic grade outlined above, Izadyar (2000) interpreted these zonation trends as reflecting the prograde (core to rim/core to mantle) or the retrograde (mantle to outer rim) path, respectively.

Attic-Cycladic belt

Reinecke (1986a,b) provides detailed descriptions of the low to medium grade evolution of piemontite bearing silicate parageneses from highly oxidized Mn rich rocks in response to variable metamorphic grade and physicochemical conditions from Evvia and Andros Islands (Greece). Both areas belong to the Attic-Cycladic blueschist belt and indicate an early (Eocene)
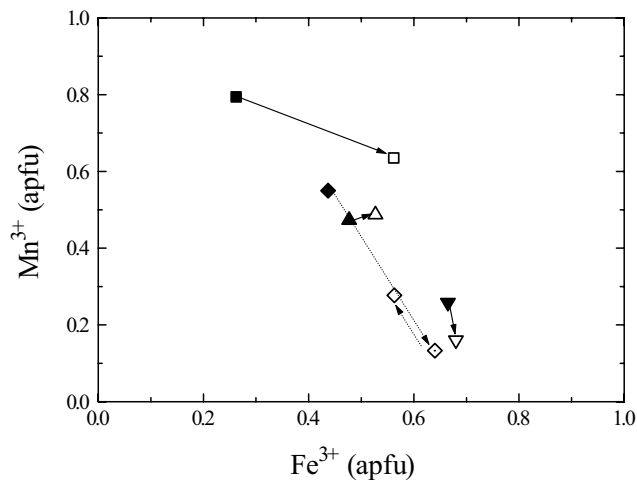
Figure 18. Mn^{3+} *vs*. Fe^{3+} contents in piemontite from Sanbagawa quartz schists (central Shikoku, Japan; Izadyar (2000). Solid arrows indicate zonation trend from inner (= core = solid symbols) to outer zone (= rim = empty symbols). Dashed arrows indicate zonation trend from core to intermediate zone (= mantle = dotted symbol) and from mantle to rim, respectively (see text). Symbols refer to different assemblages and localities: squares = talc bearing assemblage, Asemi-gawa; diamonds = talc free assemblage, Asemi-gawa; upward triangles = talc bearing assemblage, Besshi; downward triangles = talc free assemblage, Besshi.

high P/low T blueschist facies metamorphism that was followed and variably overprinted by a later (Oligocene/Miocene) greenschist facies metamorphism. The corresponding metamorphic conditions were ~400°C and >0.8–0.9 GPa and 400–500°C and >1.0 GPa for the blueschist and <400°C and <0.5–0.8 GPa and 400–500°C and 0.5–0.6 GPa for the greenschist stage on Evvia and Andros, respectively. Thus, Andros reports slightly higher metamorphic conditions. Piemontite occurs in quartzite (Evvia and Andros) and in metapelitic and metacalcareous schists (Andros).

The characteristic assemblages in piemontite bearing quartzite are piemontite, quartz, sursassite, braunite and/or hematite, and Mg chlorite on Evvia and piemontite, quartz, spessartine, braunite and/or hematite, chlorite, and rutile with minor amounts of phengite, crossite, ardennite, albite, tourmaline, apatite, and rare titanite and phlogopite on Andros. The main mineralogical difference between both areas is the ubiquitous occurrence of sursassite on Evvia and of spessartine on Andros. On Evvia spessartine is very rare and replaces sursassite whereas on Andros sursassite only occurs as a relic phase in some of the samples. Compositional zoning is generally absent. In both areas, piemontite in braunite bearing, hematite free assemblages show higher Mn^{3+}/Fe^{3+} ratios (from 2.1–8.3) than in hematite bearing assemblages (from 0.7–2.2). This is the opposite trend to that observed by Jiménez-Millán and Velilla (1993) in rocks from Ossa-Morena but is in accordance with the finding of Fukuoka et al. (1990) in the calc-silicate rocks from the Sausar Group, India (see above). Significant amounts of Sr (up to 0.17 pfu) and Mn^{2+} (up to 0.28 pfu) can substitute for Ca in piemontite from both localities. Nevertheless, Mn^{2+} is systematically higher in the spessartine bearing assemblages of Andros. The higher Mn^{2+} content on Andros is probably governed by a $Ca–Mn^{2+}$ exchange reaction between piemontite and spessartine as it corresponds to Ca enriched rims in spessartine.

Contrary to piemontite in quartzite, piemontite in metapelitic and metacalcareous schist from Andros may show complex compositional zoning. Based on textural and chemical criteria piemontite generations I and II can be distinguished. Piemontite I, formed during the blueschist facies metamorphism, coexists with braunite, manganian phengite (alurgite), Mn^{3+}- Mn^{2+} bearing Na pyroxene ('violan'), carbonate, quartz, hollandite, and hematite, and often shows a continuous zonation trend. On the contrary, piemontite II grew during the greenschist facies overprint as narrow, chemically discontinuous rims on piemontite I or as small separate grains and may coexist with Mn^{3+} bearing zoisite ('thulite') in braunite and hematite free assemblages. Like in piemontite from the quartzite on Evvia and Andros, the Fe^{3+} and Mn^{3+} contents of piemontite I largely depend on the presence or absence of hematite and/or braunite and reflect slightly different bulk compositions. Piemontite I from assemblages with hematite but without braunite has ~ 0.63 Fe^{3+} pfu and ~ 0.26 Mn^{3+} pfu, that from braunite bearing assemblages without hematite ~ 0.05 Fe^{3+} pfu and ~ 0.78 Mn^{3+} pfu, and piemontite I from assemblages with hematite and braunite has ~ 0.30 Fe^{3+} pfu and ~ 0.61 Mn^{3+} pfu. Independent of assemblage and absolute element concentrations, the continuous zonation trend of piemontite I, when observed, generally shows an enrichment of Fe^{3+} and Al over Mn^{3+} towards the rims. Reinecke (1986b) interpreted this trend as reflecting continuous equilibration between piemontite I and coexisting minerals on the prograde path of the blueschist facies event. Such a decrease of Mn^{3+} with increasing metamorphic grade is in good accordance with the results of Izadyar (2000) from the Sanbagawa belt (see above). Piemontite II, formed during the greenschist facies overprint, normally occurs as discontinuous rims on piemontite I but also as small discrete grains. In 'thulite' free, hematite and/or braunite bearing assemblages piemontite II is generally Al poorer but Mn^{3+} and Fe^{3+} richer compared to the outer parts of piemontite I on which it grows; furthermore, its Fe^{3+}/Mn^{3+} ratio does not show any correlation with the Fe^{3+}/Mn^{3+} ratio of piemontite I and may vary considerably. Additionally, piemontite II often shows high Sr contents (~ 0.21 pfu) compared to the corresponding piemontite I (~ 0.08 pfu), which can be explained by the transformation of

strontian aragonite to strontian poor or free calcite during decompression. Contrary, in 'thulite' bearing, hematite and braunite free assemblages piemontite II is significantly enriched in Al ($\sim$ 2.57 pfu) and depleted in Mn^{3+} ($\sim$ 0.27 pfu) compared to the corresponding piemontite I ($\sim$ 2.28 Al and 0.73 Mn^{3+} pfu). The difference in Sr content between piemontite II and I is not so distinct as in the 'thulite' free assemblages but follows the same trend. In both assemblages piemontite II formed during the decompression from blueschist to greenschist facies conditions due to the breakdown of manganian omphacite. This breakdown reaction may also involve braunite and/ or hematite as educt and tremolite, chlorite, albite, calcite, and quartz as product phases. Some of the piemontite bearing metapelitic and metacalcareous rocks from Andros show additional spessartine. In these cases coexisting piemontite may contain considerable amounts of Mn^{2+} (0.05 to 0.25 pfu) substituting for Ca. Textural relations indicate that spessartine formed at a late stage of the greenschist facies event at the expense of piemontite and probably braunite and other minor phases. Possible spessartine forming and piemontite consuming reactions include

piemontite (I,II) + braunite + CO_2 =
$$\text{spessartine + calcite + quartz} \pm \text{hematite} + H_2O + O_2$$
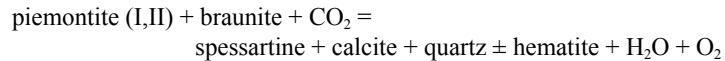
in calcite bearing assemblages and

piemontite (I,II) + braunite + rutile + quartz =
$$\text{spessartine + titanite + hematite} + H_2O + O_2$$
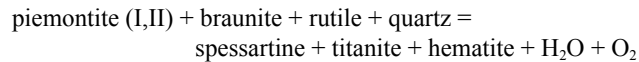
in calcite free assemblages. As the textures of coexisting piemontite and braunite do not suggest any instability between these two phases and spessartine occurs only in some samples, the breakdown of piemontite and formation of spessartine was most probably triggered by the infiltration of localized, non-pervasive CO_2-rich fluids rather than by changes in *P/T* conditions.

MONOCLINIC – ORTHORHOMBIC RELATIONS IN MANGANIAN EPIDOTE GROUP MINERALS

Although this chapter is primarily concerned with the monoclinic Mn members of the epidote group, we will shortly address the problem of the monoclinic to orthorhombic transition in Mn bearing systems. Natural coexisting orthorhombic ('thulite') and monoclinic Mn bearing epidote minerals are only rarely reported. This might be partly due to the fact that especially in older studies pink to purplish colored epidote minerals were generally referred to as 'thulite' without further specification of symmetry. Abrecht (1981) showed by means of X-ray powder diffraction that 'thulites' from six out of nine localities reported in the literature are actually monoclinic. It is therefore reasonable to assume that a careful inspection of the different 'thulite' occurrences might show that coexisting orthorhombic and monoclinic Mn bearing epidote minerals are much more widespread than recently known. Assemblages with coexisting Mn zoisite and piemontite are reported from e.g. different localities in Norway like Lom and Lexviken and from Andros Island (Greece). Reinecke (1986b) studied in detail the textural and chemical relationships between coexisting Mn zoisite and piemontite from Andros Island, so that we will mostly refer to his data in the following text. Mn zoisite on Andros Island most probably grew synchronously with piemontite II during the greenschist facies event (see above). It is generally Fe^{3+} poor (< 0.04 Fe^{3+} pfu) and contains less Mn^{3+} (0.09 to 0.22 pfu) than the coexisting piemontite (0.18 to 0.31 pfu) although the absolute Mn^{3+} contents vary from sample to sample. The data therefore prove a compositional gap or transition loop between Mn zoisite and piemontite comparable to the Al – Fe^{3+} system. The width of this gap however is variable in the different samples from Andros Island and range from Δ (Mn^{3+}+ Fe^{3+}) = 0.07 to 0.15 pfu. As the metamorphic history and phase assemblages of the different samples are almost identical, parameters other than *P* and *T* must account for this

different width of the transition loop. Reinecke (1986b) proposed the continuous Mn zoisite forming reaction

piemontite + CO_2 = Mn zoisite + calcite + quartz + $Mn^{2+}Ca_{-1}$ [calcite] + H_2O + O_2
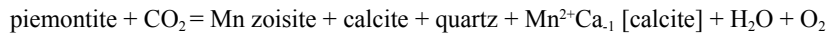
to explain his results. According to this reaction, piemontite and coexisting Mn zoisite should become enriched in Al with increasing f_{CO_2} and decreasing f_{O_2} whereas calcite should become enriched in Mn^{2+}. In good agreement calcite that coexists with Mn zoisite and piemontite displays increasing Mn^{2+} content with decreasing Mn^{3+} contents in coexisting Mn zoisite and piemontite.

Systematic experimental studies on the crystal chemical relationships between orthorhombic and monoclinic Mn bearing epidote minerals are lacking. Langer et al. (2002) synthezised coexisting Mn zoisite and piemontite at 800°C, 1.5 GPa and f_{O_2} buffered to Mn_2O_3/MnO_2 in the Fe free system in a run with a bulk composition of $X_{Mn} = 0.6$ ($X_{Mn} = Mn/(Mn+Al)$). Unfortunately, they only provided the composition of the Mn zoisite. With ~ 0.51 Mn^{3+} pfu this zoisite is significantly richer in Mn^{3+} than the natural samples from Andros Island. If this difference in Mn^{3+} reflects the higher *P* and *T* conditions of the experimental study or different f_{O_2} is not clear. Nevertheless, this discrepancy clearly shows that further studies are necessary to establish the relationships between orthorhombic and monoclinic Mn bearing epidote minerals.

EXPERIMENTAL STUDIES

The first attempts to synthesize piemontite are from Strens (1964) who used a glass as starting material that was seeded with epidote crystals. He performed synthesis runs at 550 to 650°C and 0.21 to 0.4 GPa with the f_{O_2} internally buffered to Mn_2O_3/MnO_2. He obtained piemontite crystals that contain up to 1.2 (Mn^{3+}+ Fe^{3+}) pfu and found piemontite to be the stable phase throughout the *P-T* region investigated. For this reason, he argued that the progressive disappearance of piemontite towards higher-temperature metamorphic conditions normally found in natural rocks most probably reflects a decrease of f_{O_2} with the increase of temperature, rather than temperature conditions outside the stability field of piemontite.

To study the relationships between chemical composition, stability, and physical properties of piemontite Anastasiou and Langer (1976, 1977) performed experiments in the pure $CaO-Al_2O_3-Mn_2O_3-SiO_2-H_2O$ system. Synthesis runs were carried out at 800°C and 1.5 GPa with f_{O_2} buffered to Mn_2O_3/MnO_2 in order to prevent an incorporation of Mn^{2+} to replace for Ca. Starting material consisted of calcium-silicate glass, Mn_2O_3, and $\gamma-Al_2O_3$ powdered and mixed in stoichiometric amounts according to the piemontite formula $Ca_2(Al_{3-x}Mn^{3+}_x)Si_3O_{11}O(OH)$. Bulk compositions ranged from x = 0.25 to x = 3.0. Mn^{3+} bearing zoisite formed at x = 0.25 whereas piemontite was the main phase in runs with starting compositions x = 0.50 to 1.75. In runs with x ≥ 2.00 piemontite was found to coexist with braunite and minor amounts of pyrolusite, wollastonite, quartz, and a phase with the formula $Ca_3 Mn^{3+}_2(Si_2O_7)_2$ that probably formed during quenching (Anastasiou and Langer 1976). On the basis of discontinuities observed in the lattice parameters of piemontite from runs with x = 1.75 and 2.00 Anastasiou and Langer (1977) supposed an upper limit for the piemontite solid solution series of about 1.9 Mn^{3+} pfu at the *P-T-*f_{O_2} conditions of their experiments. According to them the high temperature and pressure as well as the very high f_{O_2} were probably responsible for such a high Mn^{3+} content in synthetic piemontite, noticeably higher than that of natural piemontite. Unfortunately, the Mn content in run products was not determined directly, but inferred indirectly from the variations of physical and optical properties as well as the relative amounts of run products. Thus, with respect to the inferred chemical compositions, their results are at least questionable.

More recently, Langer et al. (2002) carried out a new set of synthesis experiments under the same physical conditions of 1.5 GPa, 800°C, f_{O_2} = Mn_2O_3/MnO_2 buffer). The synthesized crystals reached a size that allowed a complete characterization of the run products by microchemical, structural, and spectroscopic methods. For bulk compositions with x_{Mn}^{3+} from 0.60 to 2.00, the Mn^{3+} content in piemontite ranges from 0.83 to 1.47 pfu, thus lowering the upper substitutional limit of the piemontite solid solution series to ~ 1.5 Mn^{3+} pfu which is more realistic when compared to natural samples.

Keskinen and Liou (1979) studied the upper thermal stability of piemontite with the composition $Ca_2Al_2Mn^{3+}Si_3O_{11}O(OH)$. The breakdown reaction of piemontite can be represented by the redox dehydration reaction

$$Ca_2Al_2 Mn^{3+}Si_3O_{11}O(OH) = Ca_2Mn^{2+}Al_2Si_3O_{12} + 0.5\ H_2O + 0.25\ O_2$$

It is evident that this reaction is strongly affected by f_{O_2} and that a high f_{O_2} should enhance the stability field of piemontite. To keep the experimental conditions as close as possible to those existing in natural metamorphic environments and to study the influence of different f_{O_2}, Keskinen and Liou (1979) carried out synthesis as well as reversal experiments at 0.1 to 0.82 GPa, 212 to 764°C and f_{O_2} defined by the hematite-magnetite (HM), cuprite-tenorite (CT), and copper-cuprite (CC) buffers, respectively. The starting material for the synthesis runs was an oxide-carbonate mixture in the stoichiometric proportions of piemontite composition $Ca_2Al_2Mn^{3+}Si_3O_{11}O(OH)$, tempered at 900°C to break down the carbonates. The starting material for the reversal runs was a mixture of synthetic piemontite and its high temperature equivalents in sub equal proportions. At an f_{O_2} defined by the HM buffer, garnet rather than piemontite was the stable phase under any experimental conditions indicating an upper limit of piemontite thermal stability at 250°C under these conditions. This is in accordance with evidence from natural assemblages in which piemontite rarely, if ever, occurs with magnetite. On the contrary, in the reversal experiments under higher f_{O_2} defined by the CC or CT buffers piemontite was found to be stable up to 402 ± 10°C and 0.1 GPa and 404 ± 10°C and 0.2 GPa under CC buffer conditions and up to 591 ± 10°C and 0.1 GPa and 617 ± 10°C and 0.2 GPa under CT buffer conditions. The data indicate that pressure has only a minor effect on the thermal stability of piemontite compared to f_{O_2}. This is in accordance with the natural parageneses that generally indicate that the f_{O_2} is the most important factor to control piemontite stability.

From a comparison with the stability field of Mn free epidotes (Liou 1973) Keskinen and Liou (1979) predicted that incorporation of Fe in piemontite would expand its stability field to lower f_{O_2} and/or higher temperature. Later, Keskinen and Liou (1987) performed additional experiments starting from a bulk composition that corresponds to the intermediate member $Ca_2Al_2Mn^{3+}_{0.5}Fe^{3+}_{0.5}Si_3O_{11}O(OH)$ of the epidote-piemontite solid solution series. As expected by the authors the incorporation of Fe expands the stability field of piemontite to higher temperatures. At 0.2 GPa the upper thermal stability limit of the investigated piemontite (477 ± 10°C for the f_{O_2} of the CC buffer and 645 ± 10°C for the f_{O_2} of the CT buffer) is slightly higher compared to the upper thermal stability limit of pure piemontite determined in their previous study (404 ± 10°C and 617 ± 10°C, respectively). At the conditions of the hematite-magnetite buffer the data indicate a breakdown of piemontite at 365 ± 10°C compared to < 250°C in the Fe free system (Fig.19). In keeping with field observations, the growth of piemontite at the expense of garnet + anorthite is favored by decreasing temperature and/or increasing f_{O_2}. The addition of iron to the system makes the breakdown reaction for the intermediate piemontite more complex than that of pure piemontite. Keskinen and Liou (1987) derived a balanced breakdown reaction of the general form

$$1.6\ Ca_2Al_2Mn^{3+}_{0.5}Fe^{3+}_{0.5}Si_3O_{11}O(OH) + 0.2\ SiO_2 =$$
$$Ca_{2.2}Mn^{2+}_{0.8}Al_{1.2}Fe^{3+}_{0.8}Si_3O_{12} + CaAl_2Si_2O_8 + 0.8\ H_2O + 0.2\ O_2$$
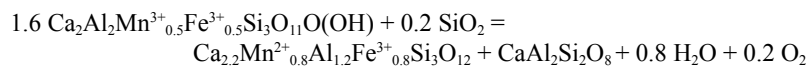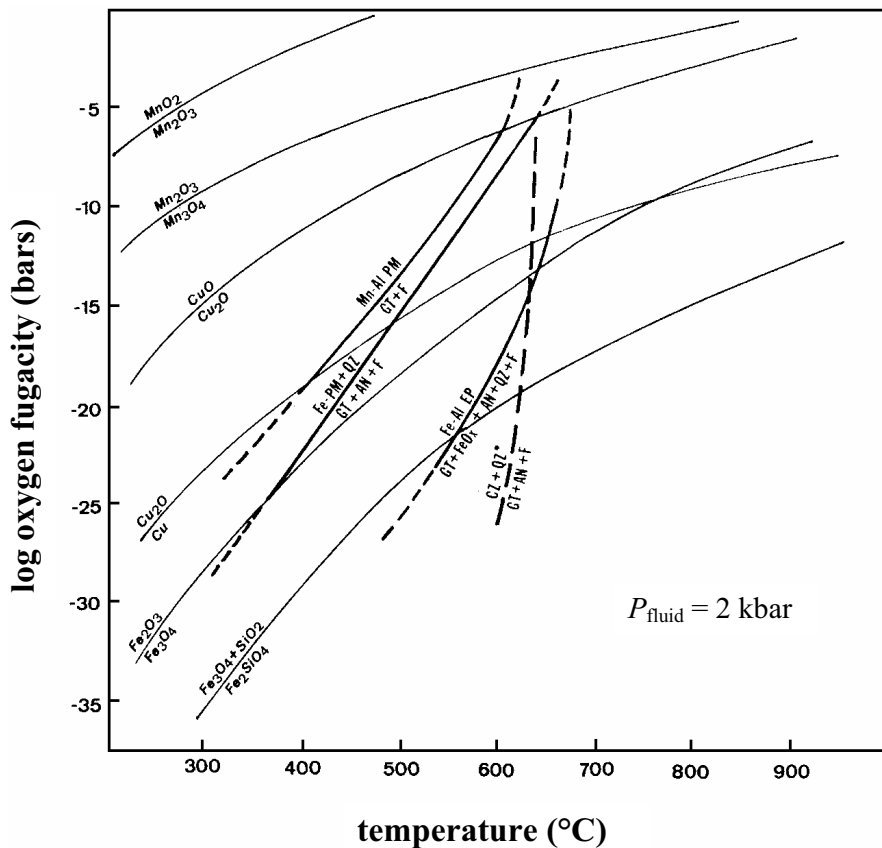
Figure 19. Isobaric (P_{fluid} = 2 kbar) log f_{O_2} – T relationships for Mn-Al piemontite (Keskinen and Liou 1979), Fe bearing piemontite (Keskinen and Liou 1987), and Al-Fe epidote (solid line: Liou 1973; dashed line: Holdaway 1966). Modified from Keskinen and Liou (1987).

Their data indicate that this reaction is discontinuous. Unfortunately, due to the very small crystal sizes Keskinen and Liou (1987) were unable to determine the compositions of the participating phases but inferred them from their modal abundances and X-ray data. As piemontite and garnet can show extensive solid solution in terms of their Mn/Fe and (Mn+Fe)/Al ratios, the breakdown of Mn-Fe piemontite might also represent a continuous equilibrium between coexisting piemontite and garnet. As the Mn/Fe and (Mn+Fe)/Al ratios in piemontite and garnet are sensitive to temperature and/or f_{O_2} such a potential continuous breakdown reaction would take place over a narrow f_{O_2}-T region wherein the proportion and composition of the reacting phases would show a continuous change. Such a continuous change of piemontite composition would be in good accordance with the continuous or sliding reactions typical for epidote minerals of the Al-Fe solid solution series. Independent of the actual nature of the breakdown reaction the data clearly show that the piemontite breakdown reactions generally have a positive slope in f_{O_2}-T space and that the stability field of piemontite is enlarged in the Fe bearing system to higher temperature and lower f_{O_2} (Fig. 19). However, the stability curves of pure piemontite and Mn free epidote converge with the increase of f_{O_2}, indicating that at extremely high f_{O_2} the two curves may cross, so that pure Mn^{3+} piemontite

might have a higher temperature stability than Mn poor epidote minerals (Fig. 19). Additional studies, both experimental and on natural systems, are necessary to determine the exact breakdown reactions of piemontite as a function of P, T, f_{O_2}, and bulk composition.

Piemontite also formed during hydrothermal experiments carried out by Akasaka et al. (2003) in order to synthesize minerals of the pumpellyite-okhotskite series and to investigate their stability relationships. Using a $Ca_4MgMn^{3+}_3Al_2Si_6O_{24.5}$ oxide mixture + excess H_2O as starting material piemontite was synthesized together with Mn pumpellyite in runs at 0.2 GPa and 400°C, 0.3 GPa and 300–400°C and f_{O_2} buffered to Mn_2O_3/MnO_2 and Cu/Cu_2O. Runs at 0.2 GPa and 300°C (f_{O_2} = Mn_2O_3/MnO_2 and Cu/Cu_2O) and at 0.3 and 0.4 GPa and 300°C (f_{O_2} = Cu/Cu_2O) did not yield any piemontite. In the runs at 0.3 GPa and 300 and 400°C and f_{O_2} buffered to Mn_2O_3/MnO_2 and Cu/Cu_2O the modal amount of piemontite increases from 300–400°C whereas the amount of Mn pumpellyite decreases. The data suggest a continuous reaction between Mn pumpellyite and piemontite with a negative slope in P-T space and an increased stability field of piemontite with increasing f_{O_2}. Piemontite in the different runs has a composition ranging from $Ca_2Mn^{3+}Al_2Si_3O_{11}O(OH)$ to $Ca_2Mn^{3+}_{1.5}Al_{1.5}Si_3O_{11}O(OH)$, very similar to that found in natural piemontite coexisting with Mn-pumpellyite (Akasaka et al. 1988). To further study the stability relations between piemontite and Mn pumpellyite Akasaka et al. (2003) conducted additional experiments at 0.3 GPa and 250, 300, 400, and 500°C and f_{O_2} buffered to Mn_2O_3/MnO_2, Cu_2O/CuO, and Cu/Cu_2O using synthetic pure piemontite + excess H_2O as starting material. At 500°C and f_{O_2}= Mn_2O_3/MnO_2 and Cu_2O/CuO no reaction was observed and piemontite was the only phase stable whereas at T < 500°C piemontite always reacted to form Mn pumpellyite + other phases for all f_{O_2}-conditions. The lower T stability at 0.3 GPa of pure Mn piemontite is therefore located between 400 and 500°C. On the basis of the results obtained by Akasaka et al. (2003), the natural assemblages including piemontite and Mn pumpellyite or okhotskite, such as those occurring in the Tokoro manganiferous iron ores (e.g., Togari and Akasaka 1987; Akasaka et al. 1988), can be interpreted as the result of decreasing temperature from above the upper limit of the Mn pumpellyite stability field (crystallization of piemontite alone) through the field of coexistence of piemontite and Mn pumpellyite down to below the lower limit of piemontite stability field (okhotskite).

Sr bearing piemontite was investigated by Akasaka et al. (2000) who performed hydrothermal synthesis experiments at 0.2–0.3 GPa, 500–600°C and f_{O_2} at the Mn_2O_3/MnO_2 and CuO/Cu_2O buffer conditions. Following the method of Keskinen and Liou (1979) the starting material was prepared from $CaCO_3$, $SrCO_3$, Al_2O_3, MnO_2, and SiO_2 mixed in appropriate amounts to yield $Ca_{2-x}Sr_xAl_2Mn^{3+}Si_3O_{11}O(OH)$ with x = 0.0, 0.4, 0.8, 1.0, 1.2, and 2.0. In the Sr free system, run products were almost single-phase piemontite. Starting materials with $0 < x \leq 1.2$ yielded Sr bearing piemontite with variable amounts of lawsonite, bixbyte, garnet, and other minor phases depending on the different physical run conditions. The highest Sr content found in piemontite was close to 1.0 pfu even in the runs with $x = 1.2$ suggesting that the upper limit of the Ca-Sr substitution was reached. From the Ca free oxide mixture ($x = 2$) piemontite did not form under any synthesis conditions. By comparing their experimental results with those obtained by Keskinen and Liou (1979) on pure piemontite Akasaka et al. (2000) concluded that the stability of piemontite is not influenced significantly by Sr incorporation.

CONCLUDING REMARKS

Although piemontite rarely occurs as major rock forming mineral, it is found as a minor phase in a wide variety of rocks formed under different *T, P* and *X* conditions. In accordance with the natural parageneses that generally indicate that f_{O_2} is the most important factor to control the piemontite stability, experimental data indicate that pressure has only a minor

effect on the thermal stability of piemontite. Both experimental and field evidence clearly indicates that piemontite, although predominantly occurring as a product of low to moderate temperature metamorphism, may persist to temperatures higher than those usually attributed to greenschist facies rocks due to the high f_{O_2} conditions. At f_{O_2} defined by the hematite-magnetite buffer, garnet rather than piemontite is the stable phase at temperatures >250°C. Accordingly, piemontite rarely, if ever, occurs with magnetite in natural assemblages. Mechanisms, which may induce a so high f_{O_2} to stabilize piemontite in the rock, range from external buffering by hydrothermal solutions to internally controlled factors as premetamorphic minerals capable of buffering f_{O_2} to a high level (Keskinen and Liou 1987). Low partial pressure of CO_2 in the fluid phase together with high Mn contents in the host rock may extend the stability field of piemontite to higher temperature. In accordance with the wide variability of forming conditions, a wide range of chemical compositions of piemontite has been observed.

The presence of Fe^{3+} substituting Mn^{3+} at the octahedral sites is very common, mainly depending on temperature, bulk-rock Fe^{3+} and Mn^{3+} contents, and f_{O_2}. In particular, incorporation of iron in piemontite expands its stability field to lower f_{O_2} and/or higher temperature. Additionally, the presence of Fe in the system makes the breakdown reaction of the intermediate piemontite more complex than that of pure piemontite. Nevertheless, both additional experimental studies and further observation of natural systems are necessary to determine the exact breakdown reactions of piemontite as a function of *P, T,* f_{O_2}, and bulk composition (Keskinen and Liou, 1987).

In recent years, the presence of trivalent REE substituting for Ca in piemontite has been detected more commonly than expected, thus indicating solid solutions of piemontite towards allanite (Fe^{2+}), dissakisite (Mg), and manganoan allanites (Fe^{2+}, Mn^{2+}) or androsite-(La) (Mn^{2+}), the latter case implying also a partial replacement of Ca by Mn^{2+} in the A-sites. The presence of Mn^{2+} replacing Ca is usual in piemontite coexisting with spessartine and significantly depleted in Mn^{3+} (Mottana and Griffin 1982).

In REE free piemontite the presence of detectable amounts of Mg replacing Ca in the A sites seems to be distinctive of high to ultrahigh pressure assemblage (Reinecke 1991).

Appreciable contents of Sr or, to a lesser extent, Pb, indicate solid solution towards strontiopiemontite and tweddillite or hancockite, respectively. So far, no experimental studies of the effect of substitutions of Ca by other cations at the A sites on the stability field of piemontite have been published, except that of Akasaka et al. (2000), who concluded that the stability of piemontite is not influenced significantly by Sr incorporation. The positive correlation between Sr and (Mn^{3+} + Fe^{3+}) often observed in piemontite would indicate that significant Sr incorporation in piemontite is favored by the expansion of the unit cell volume due to incorporation of (Mn^{3+} + Fe^{3+}) at the octahedral sites (Enami and Banno 2001). Therefore, the content of Sr might be only indirectly related to metamorphic conditions.

Structural adjustments as a response of both homovalent and heterovalent substitutions in the epidote group minerals have been studied in great details. Major difficulties arise in determining cation distribution in piemontites and other Mn^{3+} bearing members, because of the simultaneous presence of Fe^{3+}, which exhibits a comparable X-ray scattering power. Few attempts have been made to determine any possible ordering of Mn^{3+} and Fe^{3+} between the M3 and M1 sites in natural piemontites by combining both crystallographic and spectroscopic methods (Dollase 1973; Langer et. al. 2002) or by neutron diffraction techniques (Ferraris et al. 1989). Alternatively, this issue has been approached by studying crystal chemistry and physics of Fe-free synthetic piemontites and clinozoisites (Langer et al. 2002). Nonetheless, the comparable scarcity of data and the high number of variables that can play a role in the degree of ordering (i.e., Fe/Mn ratio, crystallization temperature, additional substitutions in other sites of the structure) show that considerable crystal-chemical research is still necessary

to perform a quantitative model for Mn^{3+}-Fe^{3+} intracrystalline distribution in piemontite. Last but not least, the chemically controlled, monoclinic to orthorhombic phase transition in the Mn^{3+} bearing systems requires further characterization of natural and synthetic systems wherein the two phases coexist.

ACKNOWLEDGMENTS

REFERENCES

Abraham K, Schreyer W (1975) Minerals of the viridine hornfels from Darmstadt, Germany. Contrib Mineral Petrol 49:1-20

Abraham K, Schreyer W (1976) A talc-phengite assemblage in piemontite schist from brezovica, Serbia, Yugoslavia. J Petrol 17:421-439

Abrecht J (1981) Pink zoisite from the Aar Massif, Switzerland. Mineral Mag 44:45-49

Abs-Wurmbach I, Peters Tj (1999) The Mn-Al-Si-O system: an experimental study of phase relations applied to parageneses in manganese-rich ores and rocks. Eur J Mineral 11:45-68

Acharyya KS, Mukherjee S, Basu A (1990) Manganian andalusite from Manbazar, Purulia District, West Bengal, India. Mineral Mag 54:75-80

Akasaka M, Sakakibara M, Togari K (1987) Sr-piemontite from manganiferous hematite ore deposit, Tokoro belt. Mineral Soc of Japan Trans:96 (in Japanese, English abstr.)

Akasaka M, Sakakibara M, Togari K (1988) Piemontite from the manganiferous hematite ore deposits in the Tokoro Belt, Hokkaido, Japan Mineral Petrol 38:105-116

Akasaka M, Suzuki Y, Watanabe H (2003) Hydrothermal synthesis of pumpellyite-okhotskite series minerals. Mineral Petrol 77:25-37

Akasaka M, Watanabe J, Togari K, Kawamura M (1993) Mineralogy of piemontite-bearing schist in the Yamagami metamorphic rocks of northeastern Abukuma Plateau. Ganko 88:141-156 (in Japanese, English abstr.)

Akasaka M, Zheng Y, Suzuki Y (2000) Maximum strontium content of piemontite formed by hydrothermal synthesis. J Mineral Petrol Sci 95:84-94

Anastasiou P, Langer K (1976) Synthese und Stabilität von Piemontit, $Ca_2Al_{3-p}Mn^{3+}_p(Si_2O_7/SiO_4/O/OH)$. Fortschr Mineral 54:3-4

Anastasiou P, Langer K (1977) Synthesis and physical properties of piemontite $Ca_2Al_{3-p}Mn^{3+}_p(Si_2O_7/SiO_4/O/OH)$. Contrib Mineral Petrol 60:225-245

Anders E, Ebihara M (1982) Solar-system abundances of the elements. Geochim Cosmoch Acta 46: 2363-2380

Armbruster T, Gnos E, Dixon R, Gutzmer J, Hejny C, Döbelin N, Medenbach O (2002) Manganvesuvianite and tweddillite, two new Mn^{3+}—silicate minerals from the Kalahari manganese fields, South Africa. Mineral Mag 66:137–150

Ashley PM (1984) Piemontite-bearing rocks from the Olary District, South Australia. Austral J Earth Sci 31: 203-216

Balan M, David M (1978) Mineralogical data on piemontite paragenesis at Dealul Negru (Lotru Mts). Studii si Cercetari de Geologie, Geofizica, Geografie: Geologie 23:229-238 (in Romanian, English abstr.)

Banno S (1964) [Petrologic studies on Sanbagawa crystalline schists in the Bessi-Ino district, Central Sikoku, Japan. J Fac Sci Univ Tokyo, sect II, 15: 203-319]. *Data reported in:* Rock-Forming Minerals. Vol. 1B Disilicates and Ring Silicates.Deer WA, Howie RA, Zussman J (eds) Longman, Harlow, UK 1986

Basta EZ, Kamel OA, Awadallah MF (1981) Petrography of Gabal Dokhan Volcanics, Eastern Desert, Egypt. Egyptian J Geol 22:145-171

Basta EZ, Kotb H, Awadallah MF (1980) Petrochemical and geochemical characteristics of the Dokhan formation at the type locality, Jabal Dokhan, Eastern Desert, Egypt. I.A.G. Bull 3:121-140

Basu N, Mruma AH (1985) Mineral chemistry and stability relations of talc-piemontite-viridine bearing quartzite of Mautia Hill, Mpwapwa district, Tanzania. Indian J Earth Sci 12:223-230

Battaglia S, Nannoni R, Orlandi P (1977) La piemontite del Monte Corchia (Alpi Apuane), Atti Soc Tosc Sci Nat A84:174-178

Bermanec V, Armbruster T, Oberhansli R, Zebec V (1994) Crystal chemistry of Pb- and REE-rich piemontite from Nezilovo, Macedonia. Schweiz Mineral Petrog Mitt 74:321-328

Bilgrami SA (1956) Manganese silicate minerals from Chikla, Bhandara district, India. Mineral Mag 31:236-244

Bird DK, Helgeson HC (1980) Chemical interaction of acqueous solutions with epidote-feldspar mineral assemblages in geological system, I: thermodynamic analysis of phase relations in the system CaO-FeO-Fe_2O_3-Al_2O_3-SiO_2-H_2O-CO_2. Amer J Sciences 280:907-941

Bonazzi P (1990) Nuovi dati chimici e cristallografico-strutturali ricavati da campioni di clinozoisite-epidoto e piemontite: considerazioni inerenti alla cristallochimica del gruppo. Tesi di Dottorato, Dipartimento di Scienze della Terra, Università di Firenze 321 pp

Bonazzi P, Garbarino C, Menchetti S (1992) Crystal chemistry of piemontites: REE-bearing piemontite from Monte Brugiana, Alpi Apuane, Italy. Eur J Mineral 4:23-33

Bonazzi P, Menchetti S (1994) Structural variations induced by heat treatment in allanite and REE-bearing piemontite. Amer Mineral 79:1176-1184

Bonazzi P, Menchetti S (1995) Monoclinic members of the epidote group: effects of the Al $\leftrightarrow$ Fe^{3+} $\leftrightarrow$ Fe^{2+} substitution and of the enty of REE^{3+}. Mineral Petrol 53:133-153

Bonazzi P, Menchetti S, Palenzona A (1990) Strontiopiemontite, a new member of the epidote group, from Val Graveglia, Liguria, Italy. Eur J Mineral 2:519-523

Bonazzi P, Menchetti S, Reinecke T (1996) Solid solution between piemontite and androsite-(La), a new mineral of the epidote group from Andros Island, Greece. Amer Mineral 81:735-742

Brown P, Essene EJ, Peacor DR (1978) The mineralogy and petrology of manganese-rich rocks from St. Marcel, Piedmont, Italy. Contrib Mineral Petrol 67:227-232

Burns RG (1993) Mineralogical Applications of Crystal Field Theory. II edition. University Press, Cambridge, UK

Burns RG, Strens RGJ (1967) Structural interpretation of polarized absorption spectra of the Al-Fe-Mn-Cr epidotes. Mineral Mag 36:204-226

Carbonin S, Molin G (1980) Crystal-chemical considerations on eitgh metamorphic epidotes. N Jb Miner Mh 205-215

Carlson WL, Thorne B (1997) Applied Statistical Methods. Prentice Hall, Upple Saddle River. New Jersey

Caron JM, Kienast JR, Triboulet C (1981) High-pressure-low-teperature metamorphism and polyphase Alpine deformation at Sant'Andrea di Cotone (Eastern Corsica, France). Tectonophysics 78:419-451

Catti M, Ferraris G, Ivaldi G (1988) Thermal behaviour of the crystal structure of strontian piemontite. Amer Mineral 73:1370-1376

Catti M, Ferraris G, Ivaldi G (1989) On the crystal chemistry of strontian piemontite with some remarks on the nomenclature of the epidote group. N Jb Miner Mh 357-366

Chopin C (1978) Les paragenèses réduites ou oxydées de concentrations manganésifères des « schistes lustrés » de Haute-Maurienne (Alpes françaises). Bull Minéral 101:514-531

Clarke FW (1910) Analyses of rocks and minerals from the Laboratory of the U.S. Geolog Sur Bulletin 419:272

Coombs DS, Dowse M, Grapes RH, Kawachi Y, Roser B (1985) Geochemistry and origin of piemontite - bearing and associated manganiferous schists from Arrow Junction, western Otago, New Zealand. Chem Geol 48:57-78

Coombs DS, Kawachi Y, Reay A (1993) An occurrence of ardennite in quartz veins in piemontite schist, western Otago, New Zealand. Mineral Petrol 48:295-308

Cooper AF (1971) Piemontite schists from Haast River, New Zealand. Mineral Mag 38:64-71

Cordier L (1803) Analyse du minéral connu sus le nom de Mine de Manganese violet du Piédmont, faite au Labratoire de l'Ecole de Mines. Jour Min 13:135

Cortesogno L, Lucchetti G, Penco AM (1979) Manganese mineralizations in the "Diaspri di M.Alpe" formation of the Ligurian ophiolites: mineralogy and formation. Rend Soc Ital Mineral Petrol 35:151-197

Cortesogno L, Venturelli G (1978) Metamorphic evolution of the Ophiolite sequences and associated sediments in the Northern Apennines-Voltri Group, Italy. IUGS Sci Rep 38:253-360

Dal Piaz GV (1988) Revised setting of the Piedmont zone in the northern Aosta Valley, Western Alps. Ofioliti 13:157-162

Dal Piaz GV, Di Battistini G, Kienast JR, Venturelli G (1979) Manganiferous quartzitic schists of the Piemonte ophiolite nappe in the Valsesia-Valtournanche area (Italian western Alps). Memorie Sci Geol 32:1-24

Deer WA, Howie RA, Zussman J (eds) (1986) Rock-forming minerals. Vol. 1b: Disilicates and ring silicates. 2nd Ed. Longman, Harlow, UK

Della Ventura G, Mottana A, Parodi GC, Griffin WL (1996) FTIR spectroscopy in the OH-stretching region of monoclinic epidotes from Praborna (St. Marcel, Aosta valley, Italy). Eur J Mineral 8:655-665

Dollase WA (1968) Refinement and comparison of the structures of zoisite and clinozoisite. Amer Mineral 53: 1882-1898

Dollase WA (1969) Crystal structure and cation ordering of piemontite. Amer Mineral 54:710-717

Dollase WA (1971) Refinement of the crystal structures of epidote, allanite and hancockite. Amer Mineral 56: 447-464

Dollase W A (1973) Mössbauer spectra and iron distribution in the epidote-group minerals. Z Kristallogr 138: 41-63

Dzhaksybaev ES, Kaun AV, Kovrov LE (1991) [Lead-manganese ores from the Ushkatyn III deposit. Geologiya Rudnykh Mestorozhdenii 33:107-111]. (in Russian; English abstr.)

Enami M (1986) Ardennite in a quartz schist from the Asemi-gawa area in the Sanbagawa metamorphic terrain, central Shikoku, Japan. Mineral J 13:151-160

Enami M, Banno Y (2001) Partitioning of Sr between coexisting minerals of the hollandite- and piemontite -groups in a quartz-rich schist from the Sanbagawa metamorphic belt, Japan. Amer Mineral 86:205-214

Enami M, Liou JG, Mattinson CG (2004) Epidote minerals in high P/T metamorphic terranes: Subduction zone and high- to ultrahigh-pressure metamorphism. Rev Mineral Geochem 56:347-398

Enami M, Wallis S, Banno Y (1994) Paragenesis of sodic pyroxene-bearing quartz schists: implications for the P-T hystory of the Sambagawa belt. Contrib Mineral Petrol 116:182-198

Ernst WG (1964) Petrochemical study of coexisting minerals from low-grade schists, Eastern Japan. Geochim Cosmochim Acta 28:1631-1668

Ernst WG, Seki Y (1967) Petrologic comparison of Franciscan and Sanbagawa metamorphic terranes. Tectonophysics 4:463-478

Ernst WG, Seki Y, Onuki H, Gilbert MC (1970) Comparative study of low-grade metamorphism in the California Coast Ranges and the outer Metamorphic Belt of Japan. Geol Soc of America Memoir 124: 1-276

Exley RA (1980) Microprobe studies of REE-rich accessory minerals: implications for Skye granite petrogenesis ans REE mobility in hydrothermal systems. Earth Planet Sci Lett 48:97-110

Fermor LL (1909) The manganese ore deposits of India. Mem Geol Survey India 37:78-157

Ferraris G, Ivaldi G, Fuess H, Gregson D (1989) Manganese/iron distribution in a strontian piemontite by neutron diffraction. Z Kristallogr 187:145-151

Fleischer M (1985) A summary of the variations in relative abundances of the lanthanide and yttrium in allanites and epidotes. Bull Geol Soc Finl 57:151-155

Franceschelli M, Puxeddu M, Carcangiu G, Gattiglio M, Pannuti F (1996) Breccia-hosted manganese-rich minerals of Alpi Apuane, Italy: A marine, redox-generated deposit. Lithos 37:309-333

Frank E (1983) Alpine metamorphism of calcareous rocks along a cross-section in the Central Alps: occurrence and breakdown of muscovite, margarite and paragonite. Schweiz Mineral Petrogr Mitt 63:37-93

Franz G, Liebscher A (2004) Physical and chemical properties of the epidote minerals–an introduction. Rev Mineral Geochem 56:1-82

Frondel W (1964) Variations of some rare earths in allanite. Amer Mineral 49:1159-1177

Fukuoka M, Mondal A, Guha D, Chattopadhyay G (1990) Petrochemistry of piemontite -bearing assemblages in calc-silicate rocks from Sausar Group, India. J Geol Soc India 36:403-412

Gabe EJ, Portheine JC, Whitlow SH (1973) A reinvestigation of the epidote structure: Confirmation of the iron location. Amer Mineral 58:218-223

Gaudefroy C, Laurent Y, Permingeat F (1965) La piémontite du gîte de manganèse de Tachgagalt (Anti-Atlas) et sa signification génétique. Notes serv géol Maroc 24:99-102

Gelos EM, Spagnuolo JO, Lizasoin GO (1988) Mineralogia y caracterizacion granulometrica de sedimentos actuales de la plataforma Argentina. Rev Asoc Geol Argentina 43:3-79

Gieré R, Sorensen SS (2004) Allanite and other REE-rich epidote-group minerals. Rev Mineral Geochem 56: 431-494

Giuli G, Bonazzi P, Menchetti S (1999) Al-Fe disorder in synthetic epidotes: a single-crystal X-ray diffraction study. Amer Mineral 84:933-936

Grambling JA, Williams ML (1985) The effects of Fe^{3+} and Mn^{3+} on aluminium silicate phase relations in North.central New Mexico, U.S.A. J Petrol 26:324-354

Grapes RH, Hashimoto S (1978) Manganesiferous schists and their origin, Hidaka Mountains, Hokkaido, Japan. Contrib Mineral Petrol 68:23-35

Grapes RH, Hoskin PWO (2004) Epidote group minerals in low–medium pressure metamorphic terranes. Rev Mineral Geochem 56:301-345

Guild FN (1935) Piedmontite in Arizona. Amer Mineral 20:679-692

Gutzmer J, Beukes NJ (1996) Mineral paragenesis of the Kalahari manganese field, South Africa. Ore Geol Rev 11:405-428

Haüy R J (1822) Traité de Mineralogie. 2:575

Hirata D, Yamashita H, Imanaga I, Takahashi H, Kato A (1995) Manganoan grossular-piemontite association in a low grade metamorphic manganese ore from the Dainichi mine, Hadano City, Kanagawa Prefecture, Japan. Mineral J 17:211-218

Hiroi Y, Harada-Kondo H, Ogo Y (1992) Cuprian manganoan phlogopite in highly oxidized Mineoka siliceous schists from Kamogawa, Boso Peninsula, central Japan. Amer Mineral 77:1099-1106

Holdaway MJ (1966) Hydrothermal stability of clinozoisite plus quartz. Amer J Sci 264:643-667

Hutton CO (1938) On the nature of withamite from Glen Coe, Scotland. Mineral Mag 25:119-124

Hutton CO (1940) [Metamorphism in the Lake Wakatipu region, western Otago, New Zealand. Dept Sci Ind Res, New Zealand, Geol Mem 5] (abstr).

Ishibashi K (1969) [On the paragenesis of piemontite and hematite in the Sambagawa cristalline schist. Sci Fac Sci Rept Kyushu Univ, Geol 9:147-158.] (English abstract) Zentralblatt f Mineralogie 1971. I: 145

Ismagilov MI (1976) Pumpyellite and minerals of the epidote group in ores and wall-rock metasomatites of Baimak gold-pyrite deposits (Southern Urals). *In:* Vopr. Mineral. Geokhim Rud Gorn Porod Yuzhn. Pshenichnyi GN (eds) Akad Nauk SSSR, Bashkir Fil, Inst Geol, Ufa, USSR, p 17-23 (in Russian; English abstr.)

Ito T, Morimoto N, Sadanaga R (1954) On the structure of epidote. Acta Cryst 7:53-59

Izadyar J (2000) Chemical composition of piemontites and reaction relations of piemontite and spessartine in piemontite-quartz schists of central Shikoku, Sanbagawa metamorphic belt, Japan. Schweiz Mineral Petrogr Mitt 80:199-211

Izadyar J, Hirajima T, Nakamura D (2000) Talc-phengite-albite assemblage in piemontite -quartz schist of the Sanbagawa metamorphic belt, central Shikoku, Japan. Island Arc 9:145-158

Izadyar J, Tomita K, Shinjoe H (2003) Geochemistry and origin of piemontite-quartz schist in the Sanbagawa Metamorphic Belt, central Shikoku, Japan. J Asian Earth Sci 21:711-713

Jan MQ, Symes RF (1977) Piemontite schists from Upper Swat, north-west Pakistan. Mineral Mag 41:537-540

Jiménez-Millán J, Velilla N (1993) Compositional variation of piemontite s from different manganese-rich rock-types of the Iberian Massif (SW Spain). Eur J Mineral 5:961-970

Kato A, Matsubara S (1986) Strontian piemontite. 1986 Joint Annual Meeting of The Japanese Association of Mineralogy, Petrology and Economic Geology, Mineralogical Society of Japan, and Society of Resource Geology. 69. (In Japanese).

Kato A, Matsubara S, Tiba T (1982) A pale colored aegirine from the Kamisugai Mine, Ehime Prefecture, Japan. Bull Nat Sci Museum, Series C: Geology Paleontol 8:37-42

Kawachi Y, Grapes RH, Coombs DS, Dowse M (1983) Mineralogy and petrology of a piemontite -bearing schist, western Otago, New Zealand. J Metamorphic Geol 1:353-372

Keskinen M (1981) Petrochemical investigation of the Shadow Lake Piemontite Zone, eastern Sierra Nevada, California. Amer J Science 281:896-921

Keskinen M, Liou JG (1979) Synthesis and stability relations of Mn-Al piemontite, $Ca_2MnAl_2Si_3O_{12}(OH)$. Amer Mineral 64:317-328

Keskinen M, Liou JG (1987) Stability relations of manganese-iron-aluminum piemontite. J Metamorphic Geol 5: 495-507

Kozyreva IV, Shvetsova IV, Ketris MP (2001) Find of Mn-scorodite in schist of the circum-Polar Urals. Dokl Akademii Nauk 376:224-228

Kramm U (1979) Kanonaite-rich viridines from the Venn-Stavelot Massif, Belgian Ardennes. Contrib Mineral Petrol 69:387-395

Krizhevskikh Yu.G (1995) Jasper belt in the Urals. Izvestiya Vysshikh Uchebnykh Zavedenii, Gornyi Zhurnal 8:88-97 (in Russian; English abstr.)

Krogh EJ (1977) Origin and metamorphism of iron formations and associated rocks, Lofoten-Vesteralen, N Norway. I The Vestpolltind iron-manganese deposit. Lithos 10:243-255

Langer K, Abu-Eid RM (1977) Measurement of the polarized absorption spectra of synthetic transition metal-bearing silicate microcrystals in the spectral range 44000-4000 cm^{-1}. Phys Chem Min 1:273-299

Langer K, Abu-Eid RM, Anastasiou P (1976) Absorptionsspektren synthetischer Piemontite in den Bereichen 43000-11000 cm^{-1} (232.6–909.1 nm) und 4000–250 cm^{-1} (2.5–40 μm) Z Kristallogr 144:434-436

Langer K, Raith M (1974) Infrared spectra of Al-Fe(III)-epidotes and zoisites, $Ca_2(Al_{1-p}Fe^{3+}_p)Al_2O(OH)$ $[Si_2O_7][SiO_4]$. Amer Mineral 59:1249-1258

Langer K, Tillmanns M, Kersten M, Almen H, Arni RK (2002) The crystal chemistry of Mn^{3+} in the clino- and orthozoisite structure types, $Ca_2M^{3+}_3[OH|O|SiO_4|Si_2O_7]$: A structural and spectroscopic study of some natural piemontites and "thulites" and their synthetic equivalents. Z Kristallogr 217:563-580

Lausen C (1927) Piedmontite from the Sulphur Spring Valley, Arizona. Amer Mineral 12:283-287

Leblanc M, Lbouabi M (1988) Native silver mineralization along a rodingite tectonic contact between serpentinite and quartz diorite (Bou Azzer, Morocco). Econ Geol 83:1379-1391

Liebscher A (2004) Spectroscopy of epidote minerals. Rev Mineral Geochem. 56:125-170

Liou JG (1973) Synthesis and stability relations of epidote, $Ca_2Al_2FeSi_3O_{12}(OH)$. J Petrol 14:381-413

Litoshko DN, Nikitina VD (1984) Manganese-rich piemontite from metasomatites of the Polar Urals. Trudy Instituta Geologii, Rossiiskaya Akademiya Nauk, Ural'skoe Otdelenie, Komi Nauchnyi Tsentr 46:110-112

Liu H, Xue Y (1999) Sedimentology of Triassic Dounan-type manganese deposits, western margin, Yangtze Platform, China. Ore Geol Rev 15:165-176

Liu J, Wu Y, Guo L (1998) Eclogites and their country gneisses: studies on inclusions in the accessory minerals of country gneisses. Chinese Sci Bull 43:65-68

Lucchetti G, Cortesogno L, Palenzona A (1988) Low-temperature metamorphic mineral assemblages in manganese-iron ores from Cerchiara Mine (northern Apennine, Italy). N Jb Miner Mh 367-383

Lyashkevich ZM (1958). On piemontite from the Alai Range. Min Mag Lvov Geol Soc 12:323-331 (Mineral Abstracts, 15, 144)

Makanjuola AA, Howie RA (1972) Mineralogy of the glaucophane schists and associated rocks from Ile de Groix, Brittany, France. Contrib Mineral Petrol 35:83-118

Malmqvist D (1929) [Studien innerhalb der Epidotgruppe mit besonderer Rücksicht auf die manganhältigen Glieder. Bull Geol Inst 22:223-280]. *In:* Rock-Forming Minerals. Vol. 1B Disilicates and Ring Silicates. Deer WA, Howie RA, Zussman J (eds) Longman, Harlow, UK

Mandarino JA (1981) The Glastone-Dale relationship: Part IV. The compatibility concept and its application. Canad Mineral 19:441-450

Marmo V, Neuvonen KJ, Ojanpera P (1959) The piedmontites of Piedmont (Italy), Kajlidongri (India), and Marampa Sierra Leone). Bull Comm géol Finlande 184:11-20

Marthaler M, Stampfli GM (1989) Les schistes lustrés à ophiolites de la nappe du Tsaté: un ancien prisme d'accrétion issu de la marge active apulienne? Schweiz Mineral Petrogr Mitt 69:211-216

Martin S and Kienast JR (1987) The HP-LT manganiferous quartzites of Praborna, Piemonte ophiolite nappe, Italian western Alps. Schweiz Mineral Petrogr Mitt 67: 339-360

Masuda T, Shibutani T, Kuriyama M, Igarashi T (1990) Development of microboudinage: an estimate of changing differential stress with increasing strain. Tectonophysics 178:379-387

Masuda T, Shibutani T, Yamaguchi H (1995) Comparative rheological behaviour of albite and quartz in siliceous schists revealed by the microboudinage of piemontite. J Struct Geol 17:1523-1533

Mayo EB (1932) Two new occurrences of piedmontite in California. Amer Mineral 17:238-248

Meinhold KD, FrischT (1970) Manganese-silicate-bearing metamorphic rocks from central Tanzania. Schweiz Mineral Petrogr Mitt 50:493-507

Minakawa T, Momoi H (1987) Occurrences of ardennite and sursassite from the metamorphic manganese deposits in the Sanbagawa belt, Shikoku, Japan. Kobutsugaku Zasshi 18:87-98 (in Japanese, English abstr.)

Minagawa T (1992) Study on characteristic mineral assemblages and formation process of metamorphosed manganese ore deposits in the Sanbagawa belt. Mem.Fac.Sci. Ehime Univ. 1:1-74 (in Japanese, English abstr.)

Mitra FN (1964) Manganese minerals in a calc-alkaline pegmatite vein cutting across the manganese ore band, Sitasaongi Mine, Bhandara district, Maharastra. Indian Mineral 5:1-16

Morton RD, Carter NL (1963) Contributions to the mineralogy of Norway. On the occurrence of Mn-poor piemontite and withamite in Norway. Norsk Geol Tidsskr 43: 445-455 (English abstr.)

Mottana A (1986) Blueschist-facies metamorphism of manganiferous cherts: A review of the alpine occurrence. *In:* Blueschists and Eclogites. Evans, BW, Brown EH (eds) Mem Geol Soc America 164:267-300

Mottana A, Griffin WL (1982) The crystallochemistry of piemontite from the type-locality (St. Marcel, val d'Aosta, Italy) Reports 13 IMA Meeting:635-640

Nayak VK (1969) Piemontite from the manganese ore deposit of Kajlidongri mine, Jhabua district, Madhya Pradesh. Indian Mineral 10:174-180

Nayak VK Neuvonen KJ (1966) Some manganese minerals from India. Bull Comm Géol Finlande 33:27-37

Ödman OH (1950) [Manganese mineralization in the Ultevis district, Jokkmokk, north Sweden: Part 2. Mineralogical notes. Arsbok Sveriges Geol Undersok 44: n°2]. (English abstract) Mineralogical Abstracts 11:472-473

Ogo Y, Hiroi Y (1991) Origin of various mineral assemblages of the Mineoka Metamorphic rocks from Kamogawa, Boso Peninsula, central Japan. With special reference to the effect of high oxygen fugacity. Ganko 86:226-240 (in Japanese, English abstr.)

Peacor DR, Dunn PJ (1988) Dollaseite-(Ce) (magnesium orthite redefined): structure refinement and implications for F^- + M^{2+} substitutions in epidote-group minerals. Amer Mineral 73:838-842

Peng M, Zheng C (1984) Stability field of piemontite from Hainan Island, Guangdong Province (China). Dizhi Xuebao, 58:63-72 (in Chinese, English abstr.)

Perseil EA (1987) Particularités des piémontites de Saint-Marcel-Praborna (Italie); spectres I.R. Actes du 112ème Congrès National des Sociétés Savantes. Edition du CTHS, Paris

Perseil EA (1988) Presence of strontium in manganese oxides of the St. Marcel-Praborna-Val d'Aosta ore deposit, Italy. Mineralium Deposita 23:306-308

Perseil EA (1990) Sur la présence du strontium dans les minéralisations manganésifères de Falotta et de Parsettens (Grisons-Suisse) – Evolution des paragenèses. Schweiz Mineral Petrog Mitt 70:315-320

Perseil EA (1991) La presence de Sb-rutile dans les concentrations manganésifères de St. Marcel-Praborna (V. Aoste – Italie). Schweiz Mineral Petrog Mitt 71:341-347

Pletnev PA, Kulikova IM, Spiridonov EM (1999) High-aluminum and high-fluorine titanite in gondites and metavolcanites of prehnite-pumpellyite facies from Uchaly deposit, the Southern Urals. Zapiski Vserossiiskogo Mineralogicheskogo Obshchestva 128:69-71

Pouliot G, Trudel P, Valiquette G, Samson P (1984) Armenite - thulite - albite veins at Remigny, Quebec: the second occurrence of armenite. Canad Mineral 22:453-464

Reinecke T (1986a) Phase relationships of sursassite and other manganese-silicates in highly oxidized low-grade, high-pressure metamorphic rocks from Evvia and Andros Islands, Greece. Contrib Mineral Petrol 94:110-126

Reinecke T (1986b) Crystal chemistry and reaction relations of piemontite s and thulites from highly oxidized low grade metamorphic rocks at Vitali, Andros Island, Greece. Contrib Mineral Petrol 93:56-76

Reinecke T (1991) Very-high-pressure metamorphism and uplift of coesite-bearing metasediments from the Zermatt-Saas zone, Western Alps. Eur J Mineral 3:7-17

Reinecke T, Tillmans E, Bernhardt HJ (1991) Abswurmbachite, $Cu^{2+}Mn^{3+}_6$ $[O_8/SiO_4]$, a new mineral of the braunite group: natural occurrence, synthesis, and crystal structure. N Jb Miner Abh 163:117-143

Roy SR, Purkait PK (1968) Mineralogy and genesis of the metamorphosed manganese silicate rocks (gondite) of Gowari Wadhona, Madhya Pradesh, India. Contrib Mineral Petrol 20:86-114

Sakai C, Higashino T, Enami M (1984) REE-bearing epidote from Sanbagawa pelitic schist, central Shikoku, Japan. Geochem Journ 18:45-53

Sasaki N, Yano M, Matsuyama F (2002) Ardennite from the Tone mine, Nagasaki Prefecture, Japan. Chigaku Kenkyu 51:67-72 (in Japanese, English abstr.)

Shannon RD (1976) Revised effective ionic radii and systematic studies on interatomic distances in halides and chalcogenides. Acta Cryst A32:751-757

Short AM (1933) A chemical study of piedmontite from Shadow Lake, Madera County, California. Amer Mineral 18:493-500

Schreyer W, Abraham K (1977) Howieite and other high-pressure indicators from the contact aureole of the Brezovica, Yugoslavia, peridotite. N Jb Miner Abh 130:114-133

Schreyer W, Fransolet AM, Abraham K (1986) A miscibility gap in trioctahedral manganese-magnesium-iron chlorites: Evidence from the Lienne Valley manganese deposit, Ardennes, Belgium. Contrib Mineral Petrol 94:333-342

Simonson RR (1935) Piedmontite from Los Angeles County, California. Amer Mineral 20:737-738

Singharajwarapan S, Berry R (2000) Tectonic implications of the Nam Suture Zone and its relationship to the Sukhothai Fold belt, Nothern Thailand. J Asian Earth Sci 18:663-673

Smith D, Albee AL (1967) Petrology of a piemontite-bearing gneiss, San Gorgonio Pass, California. Contrib Mineral Petrol 16:189-203

Smith G, Halenius U, Langer K (1982) Low temperature spectral studies of Mn^{3+}-bearing andalusite and epidote type minerals in the range 30000-5000 cm^{-1}. Phys Chem Minerals 8:136-142

Somarin AK, Moayyed M (2002) Granite- and gabbrodiorite-associated skarn deposits of NW Iran. Ore Geology Rev 20:127-138

Spisiak J, Hovorka D, Rybka R Turan J (1989) Spessartine and piemontite in Lower Paleozoic metasediments of the Inner West Carpathians. Casopis pro Mineralogii a Geologii 34:17-30

Stensrud HL (1973) Does piemontite represent only greenschist facies metamorphism? Contrib Mineral Petrol 40:79-82

Strens RGJ (1964) Synthesis and properties of piemontite. Nature 201:175-176

Strens RGJ (1966) Properties of the Al-Fe-Mn epidotes. Mineral Mag 35:928-944

Tanaka K, Imai N, Nakamura T (1972) A high magnesian piemontite from the Nagatoro disctrict, Saitama Prefecture, Japan. J Jap Assoc Min Petr Econ Geol 67:117-127

Taylor FC, Baer AJ (1973) Piemontite-bearing explosion breccia in Archean rocks, Labrador, Newfoundland. Geol Surv Canad J Earth Sc 10:1397-1402

Togari K, Akasaka M (1987) Okhotskite, a new mineral, an Mn^{3+}-dominant member of the pumpellyite group, from the Kokuriki mine, Hokkaido, Japan. Mineral Mag 51:611-614

Togari K, Akasaka M, Sakakibara M, Watanabe T (1988) Mineralogy of manganesiferous iron ore deposits and chert from the Tokoro belt, Hokkaido. Mininig Geology Special Issue 12:115-126

Velilla N, Jiménez-Millán J (2003) Origin and metamorphic evolution of rocks with braunite and pyrophanite from the Iberian Massif (SW Spain). Mineral Petrol 78:73-91

Voznesenskii SD (1961) Piemontite schists from the left bank of the Khemchik River, Western Tuva. Zapiski Vsesoyuz. Mineral. Obshchestva 90:345-348 (English abstr.)

Wenk HR, Maurizio R (1978) Kutnahorite, a rare manganese mineral from Piz Cam (Bergell Alps). Schweiz Mineral Petrog Mitt 58:97-100

Wieser T (1973) Piemontite and associated minerals from Sudeten Mountains (Poland) and Euboea Island (Greece). Mineralogia Polonica 4:3-19.

Williams GH (1893) Piedmontite and scheelite from the ancient rhyolite of South Mountain, Pennsylvania. Amer J Science 46:50-57

Wood BJ, Strens RGJ (1972) Calculation of crystal field splitting in distorted coordination polyhedra: spectra and thermodynamic properties of minerals. Mineral Mag 38:909-917

Yoshimura T, Momoi H (1964) [Withamite from the Yamanaka mine, Hyogo Prefecture. Sci Rept Kyushu Univ, Geol 6:201-206]. (English abstract) Mineralogical Abstracts 17:299

Yudovich YaE, Kozyreva IV, Ketris MP, Shvetsova IV (2001) Geochemistry of rare earth elements in the zone of interformational contact in the Maldynyrd Range (Subpolar Urals). Geochem Internat 39:1-12

Yudovich YaE, Kozyreva IV, Shvetsova IV, Efanova LI, Filippov VN (2000) Manganiferous REE-bearing nodules in metamorphic schists from Polar Urals. Dokl Earth Sci 371:233-235

Zhou G, Liu YJ, Eide EA, Liou JG, Ernst WJ (1993) High-pressure/low-temperature metamorphism in northern Hubei Province, central China. J Metamorphic Geol 11:561-574

APPENDIX

Table A. Chemical analyses (oxides wt.%) of REE free piemontites from literature.

Ref. #	2	3	4	5	6	7	8	9	10	11
SiO_2	36.60	36.63	35.57	38.64	37.54	37.16	36.82	36.08	37.28	37.85
TiO_2	0.60	0.21	—	—	0.54	0.04	0.07	—	0.23	0.13
Al_2O_3	15.24	17.21	18.27	15.03	19.80	19.96	19.17	19.19	20.53	22.19
Fe_2O_3	7.04	6.85	7.06	8.38	10.46	6.47	8.03	3.87	10.81	12.58
Mn_2O_3	14.93	17.78	12.43	15.00	7.32	11.11	10.80	14.91	—	—
FeO	—	—	—	—	—	—	—	—	—	—
MnO	—	—	2.94	—	2.00	0.45	0.51	—	5.89	3.22
MgO	2.92	0.85	0.96	—	0.08	0.17	0.04	0.60	0.94	0.54
CaO	17.47	18.98	19.53	22.19	20.47	22.6	22.29	22.10	22.73	21.88
SrO	—	—	—	—	—	—	—	—	—	—
Na_2O	2.41	—	1.14	—	0.13	0.05	0.10	0.14	0.09	0.09
K_2O	0.95	—	0.87	—	0.01	—	—	—	0.11	0.10
H_2O	1.95	1.75	0.85	1.78	1.46	1.75	1.85	2.54	1.80	1.80
CuO	0.31	—	—	—	—	0.01	0.04	—	—	—
PbO	—	—	—	—	—	—	0.01	—	—	—
BaO	—	—	—	—	—	—	—	—	—	—
total	100.42	100.26	99.62	101.02	99.81	99.77	99.74	99.43	100.45	100.42

Ref. #	12	13	14	15	16	17	18	19	20	21
SiO_2	37.30	36.90	38.15	36.75	35.29	36.40	35.90	36.50	37.00	37.00
TiO_2	0.04	0.05	0.12	0.02	0.05	—	—	—	—	—
Al_2O_3	23.70	21.80	23.56	19.59	17.51	20.00	19.30	21.10	19.80	20.30
Fe_2O_3	12.20	12.80	8.70	8.17	6.06	4.10	7.10	5.40	6.20	7.10
Mn_2O_3	0.95	4.30	—	12.55	15.42	14.50	11.20	10.50	11.80	10.60
FeO	—	—	—	—	—	—	—	—	—	—
MnO	—	—	7.24	—	—	2.10	3.00	3.60	3.30	4.10
MgO	0.24	0.24	0.14	0.07	0.72	0.22	0.20	0.05	0.13	0.01
CaO	23.20	21.70	20.33	19.90	21.77	21.40	20.10	20.00	20.10	20.00
SrO	—	—	—	—	—	—	—	—	—	—
Na_2O	0.02	0.01	0.20	—	—	—	—	—	—	—
K_2O	—	—	0.13	0.13	0.52	—	—	—	—	—
H_2O	—	—	1.68	—	2.66	—	—	—	—	—
CuO	—	—	—	—	—	—	—	—	—	—
PbO	—	—	—	—	—	—	—	—	—	—
BaO	—	—	—	—	—	—	—	—	—	—
total	97.65	97.80	100.25	97.18	100.00	98.72	96.80	97.15	98.33	99.11

**Table A (continued). Chemical analyses (oxides wt.%)
of REE free piemontites from literature.**

Ref. #	22	23	24	25	26	27	28	29	30	31
SiO_2	35.90	37.50	36.60	37.20	37.50	38.20	36.60	37.00	37.00	36.80
TiO_2	—	—	0.03	0.03	—	—	—	—	0.05	—
Al_2O_3	19.20	22.20	19.90	23.30	23.10	24.20	20.60	20.20	19.70	19.80
Fe_2O_3	8.70	11.20	9.16	7.54	8.69	13.00	8.05	8.48	11.30	8.46
Mn_2O_3	9.70	3.50	11.70	6.50	5.24	0.91	11.20	11.30	11.50	11.90
FeO	—	—	—	—	—	—	—	—	—	—
MnO	3.40	0.54	—	—	—	—	—	—	—	—
MgO	0.08	0.03	—	0.06	0.04	—	0.07	—	—	—
CaO	19.80	22.40	18.80	22.50	23.00	22.80	20.70	20.50	17.90	19.30
SrO	—	—	—	—	—	—	—	—	—	—
Na_2O	0.03	0.28	—	0.04	—	0.03	—	—	—	—
K_2O	0.09	0.04	—	—	—	—	—	—	—	—
H_2O	—	—	—	—	—	—	—	—	—	—
CuO	—	—	—	—	—	—	—	—	—	—
PbO	—	—	—	—	—	—	—	—	—	—
BaO	—	—	—	—	—	—	—	—	—	—
total	96.90	97.69	96.19	97.17	97.57	99.14	97.22	97.48	97.45	96.26

Ref. #	32	33	34	35	36	37	38	39	40	41
SiO_2	36.60	36.80	36.90	36.80	36.70	36.70	36.58	36.97	37.43	37.29
TiO_2	—	0.03	—	0.03	0.03	—	—	—	—	—
Al_2O_3	21.20	21.30	20.70	20.90	20.90	20.70	21.75	21.25	23.41	22.41
Fe_2O_3	10.40	9.70	9.60	8.28	7.68	7.77	—	—	—	—
Mn_2O_3	7.30	7.80	8.16	10.70	11.10	11.40	—	—	—	—
FeO	—	—	—	—	—	—	3.40	5.81	8.94	9.33
MnO	—	—	—	—	—	—	10.20	10.15	4.43	4.65
MgO	0.10	0.07	0.06	0.27	0.23	0.42	0.06	0.09	0.05	0.12
CaO	20.10	20.60	20.40	19.40	19.70	19.00	22.02	21.70	21.59	21.39
SrO	—	—	—	—	—	—	—	—	—	—
Na_2O	0.04	—	0.04	—	0.07	0.06	0.98	—	—	—
K_2O	—	—	—	—	—	—	—	—	—	—
H_2O	—	—	—	—	—	—	—	—	—	—
CuO	—	—	—	—	—	—	—	—	—	—
PbO	—	—	—	—	—	—	—	—	—	—
BaO	—	—	—	—	—	—	—	—	—	—
total	95.74	96.30	95.86	96.38	96.41	96.05	94.99	95.97	95.85	95.19

Bonazzi & Menchetti

Table A (continued). Chemical analyses (oxides wt.%)
of REE free piemontites from literature.

Ref. #	42	44	45	46	47	48	49	50	51	52
SiO_2	37.43	37.40	35.9	36.57	37.56	36.66	36.69	35.25	35.47	36.82
TiO_2	0.10	0.03	0.24	0.10	0.02	0.06	0.06	—	—	—
Al_2O_3	21.27	22.85	19.97	21.17	21.04	19.85	19.33	17.95	16.71	19.81
Fe_2O_3	3.80	13.60	8.53	8.17	10.81	8.64	2.47	7.72	10.08	7.86
Mn_2O_3	11.80	1.11	9.94	8.40	5.70	8.76	18.94	14.61	12.93	10.64
FeO	—	—	—	—	—	—	—	—	—	—
MnO	—	1.22	2.42	3.16	1.82	3.55	—	—	—	—
MgO	—	0.02	0.05	0.03	0.01	0.03	—	—	—	—
CaO	24.75	22.69	21.23	20.68	21.21	19.83	21.44	22.26	22.79	22.64
SrO	—	—	—	—	—	—	—	—	—	—
Na_2O	—	0.05	0.02	0.05	0.03	0.01	—	—	—	—
K_2O	—	0.02	—	—	0.01	—	—	0.04	—	—
H_2O	0.92	—	—	—	—	—	—	—	—	—
CuO	—	—	—	—	—	—	—	—	—	—
PbO	—	—	—	—	—	—	—	—	—	—
BaO	—	—	—	—	—	—	—	—	—	—
total	100.07	98.99	98.3	98.33	98.21	97.39	98.93	97.83	97.98	97.77

Ref. #	53	54	55	56	57	58	59	60	61	62
SiO_2	36.44	36.95	37.93	36.93	37.01	37.16	37.72	37.54	38.5	38.80
TiO_2	0.06	—	—	—	—	—	—	—	0.19	0.14
Al_2O_3	18.42	23.65	24.77	20.65	20.71	22.21	24.23	22.23	26.2	23.80
Fe_2O_3	11.40	7.37	10.15	6.64	6.52	2.42	0.32	3.04	7.70	12.8
Mn_2O_3	9.63	6.29	3.35	9.36	8.73	13.91	12.74	13.51	1.86	0.21
FeO	—	—	—	—	—	—	—	—	—	—
MnO	—	—	—	3.31	3.45	—	—	—	—	—
MgO	0.05	—	—	—	—	0.10	—	—	0.10	0.10
CaO	21.66	22.58	22.94	19.47	18.33	20.99	22.39	20.60	23.60	23.40
SrO	—	—	—	0.20	0.52	—	—	—	—	—
Na_2O	0.06	—	—	—	—	—	—	—	—	—
K_2O	—	—	—	—	—	—	—	—	—	—
H_2O	—	—	—	—	—	—	—	—	—	—
CuO	—	—	—	—	—	—	—	—	—	—
PbO	—	—	—	—	—	—	—	—	—	—
BaO	—	—	—	—	—	—	—	—	—	—
total	97.72	96.84	99.14	96.56	95.27	96.79	97.40	96.92	98.15	99.25

**Table A (continued). Chemical analyses (oxides wt.%)
of REE free piemontites from literature.**

Ref. #	63	64	65	66	67	68	69	70	71	72
SiO_2	38.00	37.70	37.00	36.50	36.40	36.80	36.10	36.50	36.50	37.74
TiO_2	0.10	—	—	—	—	—	—	—	0.03	0.07
Al_2O_3	24.00	23.00	19.50	19.60	19.80	19.40	19.60	19.00	19.60	26.73
Fe_2O_3	7.70	3.70	8.86	7.15	4.94	6.07	8.82	9.34	8.50	7.66
Mn_2O_3	—	—	11.20	12.90	14.1	13.60	11.90	11.50	11.70	—
FeO	—	—	—	—	—	—	—	—	—	—
MnO	5.90	11.60	—	—	—	—	—	—	—	3.52
MgO	0.10	0.20	0.08	0.07	0.06	0.08	0.09	0.10	0.10	0.09
CaO	22.30	22.10	20.5	19.90	24.40	20.10	19.50	19.50	19.80	22.61
SrO	—	—	—	—	—	—	—	—	—	—
Na_2O	—	—	—	—	—	0.08	—	0.06	—	0.01
K_2O	—	—	—	—	—	—	—	—	—	—
H_2O	—	—	—	—	—	—	—	—	—	—
CuO	—	—	—	—	—	—	—	—	—	—
PbO	—	—	—	—	—	—	—	—	—	—
BaO	—	—	—	—	—	—	—	—	—	—
total	98.10	98.30	97.14	96.12	99.70	96.13	96.01	96.00	96.23	98.43

Ref. #	73	74	75	76	77	78	79	80	81	82
SiO_2	37.43	37.06	37.38	38.10	38.29	38.31	37.57	37.58	38.05	35.26
TiO_2	0.33	0.24	—	—	—	—	—	—	—	0.12
Al_2O_3	22.18	21.86	23.83	23.89	21.95	25.99	22.15	22.54	23.53	23.50
Fe_2O_3	2.57	2.21	11.08	12.97	12.9	6.72	8.19	13.36	12.49	4.65
Mn_2O_3	13.65	15.44	3.22	2.52	2.96	3.96	7.53	2.25	1.17	12.13
FeO	—	—	—	—	—	—	—	—	—	—
MnO	—	—	—	—	—	—	—	—	—	—
MgO	0.11	0.05	0.09	0.20	0.09	0.20	0.08	0.08	0.05	0.21
CaO	21.86	21.73	22.38	21.91	21.89	23.27	23.14	22.10	23.19	22.73
SrO	—	—	—	—	—	—	—	—	—	—
Na_2O	0.03	0.02	—	—	0.01	0.03	—	0.04	0.01	—
K_2O	—	—	0.05	0.03	0.04	—	—	0.05	0.04	—
H_2O	—	—	—	—	—	—	—	—	—	1.37
CuO	—	—	—	—	—	—	—	—	—	—
PbO	—	—	—	—	—	—	—	—	—	—
BaO	—	—	—	—	—	—	—	—	—	—
total	98.16	98.61	98.03	99.62	98.13	98.48	98.66	98.00	98.53	99.97

Bonazzi & Menchetti

**Table A (continued). Chemical analyses (oxides wt.%)
of REE free piemontites from literature.**

Ref. #	83	84	85	86	87	88	89	90	91	92
SiO_2	36.40	35.83	34.78	37.20	37.30	36.40	36.60	36.90	36.70	37.60
TiO_2	0.01	—	—	—	—	—	—	—	—	—
Al_2O_3	18.92	17.28	16.42	21.40	22.90	18.70	18.90	20.50	18.70	24.00
Fe_2O_3	5.56	0.59	1.59	0.60	11.40	7.20	7.90	10.90	7.20	1.80
Mn_2O_3	13.24	20.43	19.21	15.30	1.90	11.80	10.20	5.20	11.70	10.00
FeO	—	—	—	—	—	—	—	—	—	—
MnO	2.58	—	0.15	0.90	—	—	—	—	—	—
MgO	0.19	0.11	—	—	—	—	—	—	—	—
CaO	20.47	22.18	17.03	22.60	23.80	21.60	22.30	22.90	22.00	21.90
SrO	—	0.78	8.53	—	—	2.90	0.90	0.60	2.00	2.70
Na_2O	0.02	—	—	—	—	—	—	—	—	—
K_2O	—	—	—	—	—	—	—	—	—	—
H_2O	—	—	—	—	1.90	1.80	1.80	1.80	1.80	1.90
CuO	—	—	—	—	—	—	—	—	—	—
PbO	—	—	—	—	—	—	—	—	—	—
BaO	—	—	—	—	—	—	—	—	—	—
total	97.39	97.20	97.71	98.00	99.20	100.4	98.60	98.80	100.10	99.90

Ref. #	93	94	95	96	97	98	99	101	102	103
SiO_2	36.50	35.70	36.90	37.70	37.10	38.80	39.80	36.99	35.31	36.61
TiO_2	—	—	—	—	—	—	—	0.15	0.09	0.05
Al_2O_3	21.30	18.80	20.10	25.00	21.00	28.90	31.50	22.04	21.32	20.85
Fe_2O_3	1.00	7.80	11.20	0.20	0.90	0.10	0.20	0.22	4.38	10.75
Mn_2O_3	14.30	10.80	9.00	10.50	14.60	5.20	3.30	15.69	9.51	6.91
FeO	—	—	—	—	—	—	—	—	—	—
MnO	—	—	—	—	—	—	—	—	—	—
MgO	—	—	—	—	—	—	—	—	0.08	0.15
CaO	20.20	17.90	21.30	22.70	22.20	24.10	24.70	23.09	16.00	22.10
SrO	4.40	6.00	—	1.60	1.20	—	—	—	10.25	—
Na_2O	—	—	—	—	—	—	—	—	0.04	0.07
K_2O	—	—	—	—	—	—	—	0.04	—	0.02
H_2O	1.90	1.80	1.90	1.90	1.80	1.90	2.00	—	—	—
CuO	—	—	—	—	—	—	—	—	—	—
PbO	—	—	—	—	—	—	—	—	—	—
BaO	—	—	—	—	—	—	—	—	—	—
total	99.60	98.80	100.4	99.60	98.80	99.00	101.50	98.22	96.98	97.51

**Table A (continued). Chemical analyses (oxides wt.%)
of REE free piemontites from literature.**

Ref. #	104	105	106	107	108	109	110	111	112	113
SiO_2	37.86	36.85	37.35	37.25	35.52	36.91	38.25	43.51	36.93	34.27
TiO_2	0.09	0.29	0.05	0.06	0.42	0.17	0.09	0.05	0.03	—
Al_2O_3	19.18	20.04	18.25	17.58	15.37	15.77	23.24	18.55	25.06	17.56
Fe_2O_3	4.65	1.17	2.32	7.26	5.24	11.05	—	—	—	4.89
Mn_2O_3	14.48	17.1	17.51	13.10	17.50	12.48	—	—	—	12.93
FeO	—	—	—	—	—	—	13.47	2.26	4.87	—
MnO	—	—	—	—	—	—	0.38	11.67	5.74	2.87
MgO	0.19	0.22	0.34	0.20	0.80	0.07	0.14	0.27	0.15	—
CaO	22.30	22.64	22.00	22.07	20.89	22.12	22.03	19.27	23.16	11.69
SrO	—	—	—	—	—	—	—	—	—	13.45
Na_2O	0.07	—	—	0.03	0.25	—	—	—	—	—
K_2O	0.03	—	—	0.02	0.03	—	0.01	—	—	—
H_2O	—	—	—	—	—	—	—	—	—	1.72
CuO	—	—	—	—	—	—	—	—	—	—
PbO	—	—	—	—	—	—	—	—	—	—
BaO	—	—	—	—	—	—	—	—	—	—
total	98.85	98.31	97.82	97.57	96.02	98.57	97.61	95.58	95.94	99.38

Ref. #	114	115	116	117	118	119	120	121	122	123
SiO_2	36.00	34.40	35.54	35.43	35.58	35.57	36.40	36.70	36.79	36.94
TiO_2	—	—	—	—	—	—	—	—	—	—
Al_2O_3	19.49	18.00	18.85	18.94	19.95	19.83	20.00	20.20	18.63	18.29
Fe_2O_3	6.78	9.01	8.96	8.88	12.75	12.97	7.40	8.50	8.34	9.65
Mn_2O_3	10.70	9.27	8.08	8.86	4.17	4.17	11.40	11.00	10.60	10.42
FeO	—	—	—	—	—	—	—	—	—	—
MnO	—	—	—	—	—	—	—	—	—	—
MgO	—	—	—	—	—	—	0.66	0.06	—	—
CaO	19.54	19.31	19.14	18.32	18.13	17.77	19.50	20.80	22.85	22.15
SrO	3.62	3.30	4.01	4.87	5.64	6.19	—	—	—	—
Na_2O	—	—	—	—	—	—	—	—	—	—
K_2O	—	—	—	—	—	—	—	—	—	—
H_2O	3.44	3.33	3.38	3.41	3.42	3.40	—	—	—	—
CuO	—	—	—	—	—	—	—	—	—	—
PbO	—	2.34	1.05	1.11	—	—	—	—	—	—
BaO	—	—	—	—	—	—	—	—	—	—
total	99.57	98.96	99.01	99.82	99.64	99.90	95.36	97.26	97.21	97.45

Bonazzi & Menchetti

**Table A (continued). Chemical analyses (oxides wt.%)
of REE free piemontites from literature.**

Ref. #	124	125	126	127	128	129	130	131	132	133
SiO_2	37.06	37.34	36.93	36.39	37.01	36.75	36.73	36.50	36.88	37.13
TiO_2	—	—	—	—	—	—	—	—	—	—
Al_2O_3	20.89	21.00	20.65	19.64	19.94	19.21	18.65	17.77	18.73	21.87
Fe_2O_3	6.98	6.62	6.64	8.18	4.52	4.51	8.15	9.33	10.78	11.94
Mn_2O_3	9.07	9.26	9.43	9.90	12.78	14.03	11.02	11.17	8.78	2.74
FeO	—	—	—	—	—	—	—	—	—	—
MnO	1.16	1.09	3.25	—	—	—	1.01	1.70	0.57	2.17
MgO	—	—	—	—	—	—	—	—	—	—
CaO	21.41	21.27	19.47	21.47	22.98	22.52	21.52	21.13	22.26	21.53
SrO	0.30	0.25	0.20	0.93	0.33	0.71	0.18	0.17	0.23	0.20
Na_2O	—	—	—	—	—	—	—	—	—	—
K_2O	—	—	—	—	—	—	—	—	—	—
H_2O	—	—	—	—	—	—	—	—	—	—
CuO	—	—	—	—	—	—	—	—	—	—
PbO	—	—	—	—	—	—	—	—	—	—
BaO	—	—	—	—	—	—	—	—	—	—
total	96.87	96.83	96.57	96.51	97.56	97.73	97.26	97.77	98.23	97.58

Ref. #	134	135	136	152	153	154	155	156	157	158
SiO_2	37.16	37.15	36.54	36.60	31.10	36.70	30.00	31.10	32.10	37.40
TiO_2	—	—	—	0.02	0.48	—	0.27	0.53	0.23	—
Al_2O_3	21.92	21.83	20.67	19.4	8.92	19.10	6.25	8.95	11.90	19.40
Fe_2O_3	11.86	12.66	7.91	5.50	9.10	5.85	10.70	9.19	6.97	6.60
Mn_2O_3	2.85	2.39	8.44	12.60	17.5	12.80	18.70	17.40	16.90	11.80
FeO	—	—	—	—	—	—	—	—	—	—
MnO	2.54	1.90	3.41	—	—	—	—	—	—	—
MgO	—	—	—	0.04	0.02	0.06	0.01	0.01	0.02	0.09
CaO	20.18	21.07	19.59	22.20	10.2	22.3	10.10	10.30	11.00	22.80
SrO	0.64	0.37	0.77	0.97	8.59	1.00	9.98	8.68	13.10	0.48
Na_2O	—	—	—	0.01	0.03	—	0.01	—	0.02	0.01
K_2O	—	—	—	—	—	—	—	—	0.01	—
H_2O	—	—	—	—	—	—	—	—	—	—
CuO	—	—	—	—	—	0.02	—	—	—	—
PbO	—	—	0.06	—	5.44	—	7.55	5.61	2.79	—
BaO	—	—	—	0.06	6.44	—	3.66	6.71	2.71	0.01
total	97.15	97.37	97.39	97.40	97.82	97.83	97.23	98.48	97.75	98.59

**Table A (continued). Chemical analyses (oxides wt.%)
of REE free piemontites from literature.**

Ref. #	159	160	161	162	163	164	165	166	167	168
SiO_2	37.20	36.90	37.74	38.55	38.12	39.00	37.61	38.43	37.50	37.82
TiO_2	0.08	—	0.11	0.07	0.06	0.07	0.04	0.06	—	—
Al_2O_3	19.20	20.00	20.25	19.07	20.59	19.51	20.30	18.81	20.87	21.59
Fe_2O_3	7.02	10.40	2.90	9.78	3.82	9.34	6.11	9.10	11.12	10.61
Mn_2O_3	11.50	6.89	14.58	11.75	13.28	12.70	11.35	12.34	6.69	6.32
FeO	—	—	—	—	—	—	—	—	—	—
MnO	—	—	—	—	—	—	—	—	—	—
MgO	0.01	0.07	—	—	—	—	—	—	—	—
CaO	23.00	22.50	22.99	19.81	22.48	18.98	23.04	19.64	20.29	20.63
SrO	0.22	0.17	—	—	—	—	—	—	—	—
Na_2O	—	—	—	—	—	—	—	—	—	—
K_2O	—	—	—	—	—	—	—	—	—	—
H_2O	—	—	—	—	—	—	—	—	—	—
CuO	—	—	—	—	—	—	—	—	—	—
PbO	—	—	—	—	—	—	—	—	—	—
BaO	—	0.04	—	—	—	—	—	—	—	—
total	98.23	96.97	98.57	99.03	98.35	99.60	98.45	98.38	96.47	96.97

Ref. #	169	170	171	172	173	174	175	176	177	178
SiO_2	37.89	37.89	37.58	37.47	38.21	37.89	39.96	38.09	38.28	38.65
TiO_2	—	—	—	—	—	0.08	—	—	—	0.05
Al_2O_3	21.25	21.19	21.86	20.15	20.04	22.61	22.11	21.32	22.86	22.00
Fe_2O_3	8.89	9.31	4.60	7.17	7.59	10.88	8.49	6.52	10.34	9.63
Mn_2O_3	7.03	7.42	10.42	10.93	9.44	2.04	5.38	8.90	2.52	4.68
FeO	—	—	—	—	—	—	—	—	—	—
MnO	—	—	—	—	—	—	—	—	—	—
MgO	—	—	—	—	—	—	—	—	—	—
CaO	21.30	20.85	21.98	20.95	21.27	23.05	22.25	22.47	23.01	22.83
SrO	—	—	—	—	—	—	—	—	—	—
Na_2O	—	—	—	—	—	—	—	—	—	—
K_2O	—	—	—	—	—	—	—	—	—	—
H_2O	—	—	—	—	—	—	—	—	—	—
CuO	—	—	—	—	—	—	—	—	—	—
PbO	—	—	—	—	—	—	—	—	—	—
BaO	—	—	—	—	—	—	—	—	—	—
total	96.36	96.66	96.44	96.67	96.55	96.55	98.19	97.30	97.01	97.84

Bonazzi & Menchetti

Table A (continued). Chemical analyses (oxides wt.%)
of REE free piemontites from literature.

Ref. #	179	180	181	182	183	184	185	186	187	188
SiO_2	38.38	38.48	39.24	38.35	38.20	37.79	38.33	39.04	40.18	38.58
TiO_2	0.04	—	0.03	—	—	—	—	—	—	—
Al_2O_3	20.97	22.64	22.46	22.22	23.02	21.20	22.97	22.23	21.32	22.67
Fe_2O_3	7.52	10.77	10.57	11.72	12.41	10.77	11.76	12.31	10.63	10.54
Mn_2O_3	8.58	2.23	3.87	3.24	2.16	5.01	1.32	4.41	6.45	4.07
FeO	—	—	—	—	—	—	—	—	—	—
MnO	—	—	—	—	—	—	—	—	—	—
MgO	—	—	—	—	—	—	—	—	—	—
CaO	22.18	23.14	22.89	21.89	21.69	21.47	22.19	20.97	20.57	21.85
SrO	—	—	—	—	—	—	—	—	—	—
Na_2O	—	—	—	—	—	—	—	—	—	—
K_2O	—	—	—	—	—	—	—	—	—	—
H_2O	—	—	—	—	—	—	—	—	—	—
CuO	—	—	—	—	—	—	—	—	—	—
PbO	—	—	—	—	—	—	—	—	—	—
BaO	—	—	—	—	—	—	—	—	—	—
total	97.67	97.26	99.06	97.42	97.48	96.24	96.57	98.96	99.15	97.71

Ref. #	189	190	191	192	193	194	197	198	199	200
SiO_2	38.57	37.10	36.20	35.51	37.26	36.76	36.40	37.30	38.75	37.57
TiO_2	—	0.05	—	—	—	—	0.11	0.51	0.41	0.24
Al_2O_3	23.3	19.50	19.50	12.68	20.76	21.00	15.89	20.55	24.71	24.7
Fe_2O_3	12.07	2.20	5.70	10.88	11.28	4.56	11.06	13.50	10.77	11.31
Mn_2O_3	1.40	16.00	15.30	16.83	6.21	12.08	11.99	—	0.83	0.96
FeO	—	—	—	—	—	—	—	0.50	—	—
MnO	—	—	—	—	—	—	0.55	2.84	—	—
MgO	—	0.02	—	—	0.34	—	—	0.16	0.43	0.09
CaO	22.34	22.10	21.00	23.12	22.21	22.69	22.25	21.87	21.86	23.32
SrO	—	—	—	—	—	—	—	—	0.31	0.09
Na_2O	—	—	—	—	—	—	0.41	0.04	0.26	—
K_2O	—	—	—	—	—	—	0.04	—	0.11	—
H_2O	—	—	—	1.56	1.88	1.92	0.93	2.09	1.93	1.83
CuO	—	—	—	—	—	—	—	—	—	—
PbO	—	—	—	—	—	—	0.04	—	—	—
BaO	—	—	—	—	—	—	—	—	—	—
total	97.68	96.97	97.70	100.58	99.94	99.01	99.80	99.36	100.37	100.11

**Table A (continued). Chemical analyses (oxides wt.%)
of REE free piemontites from literature.**

Ref. #	201	202	203	204	205	206	207	208	209
SiO_2	38.42	36.90	35.65	36.29	35.46	35.84	35.87	35.83	36.08
TiO_2	—	0.05	—	—	—	—	—	—	0.19
Al_2O_3	20.53	20.30	18.47	19.20	16.13	16.47	18.00	17.28	20.86
Fe_2O_3	8.86	—	6.04	4.59	3.64	3.26	3.36	0.59	2.17
Mn_2O_3	5.31	—	13.16	14.29	18.31	18.55	16.8	20.43	13.53
FeO	—	4.36	—	—	—	—	—	—	—
MnO	3.60	12.65	—	—	—	—	—	—	—
MgO	0.36	0.10	0.24	0.10	—	—	—	0.11	0.10
CaO	20.81	22.80	19.09	21.36	18.45	18.76	19.93	22.18	19.89
SrO	—	—	5.32	1.89	5.93	5.86	4.26	0.78	4.98
Na_2O	0.07	—	—	—	—	—	—	—	—
K_2O	0.07	0.06	—	—	—	—	—	—	—
H_2O	1.80	—	—	—	—	—	—	—	—
CuO	—	—	—	—	—	—	—	—	—
PbO	—	—	—	—	—	—	—	—	—
BaO	—	—	—	—	0.13	—	—	—	—
total	99.89	97.22	97.97	97.72	98.05	98.74	98.22	97.20	97.80

Ref. #	210	211	212	213	214	215	216	217	218
SiO_2	36.20	36.71	36.55	37.97	38.94	39.27	37.93	37.39	38.02
TiO_2	0.14	—	0.01	0.36	—	—	—	—	0.24
Al_2O_3	19.19	20.68	29.77	22.27	19.98	22.40	26.38	17.70	22.72
Fe_2O_3	0.90	9.98	7.01	12.27	14.49	10.30	5.17	14.20	8.16
Mn_2O_3	18.50	7.21	—	—	2.16	—	3.90	4.09	—
FeO	—	—	0.36	0.24	—	—	0.26	—	0.18
MnO	—	—	1.08	1.90	—	3.92	—	—	5.13
MgO	—	—	0.06	0.69	0.74	0.14	0.36	0.63	0.57
CaO	20.29	20.15	21.54	22.60	21.33	21.87	23.15	21.91	22.95
SrO	3.52	3.71	—	—	—	—	—	—	—
Na_2O	—	—	0.41	0.09	0.36	—	0.89	0.43	0.09
K_2O	—	—	0.10	0.02	0.32	—	0.34	0.65	0.07
H_2O	—	—	2.51	1.74	1.89	2.38	2.08	2.60	1.72
CuO	—	—	—	—	—	—	—	—	—
PbO	—	—	—	—	—	—	—	—	—
BaO	—	—	—	—	—	—	—	—	—
total	98.74	98.44	99.40	100.15	100.21	100.41	100.46	99.60	99.85

Bonazzi & Menchetti

**Table A (continued). Chemical analyses (oxides wt.%)
of REE free piemontites from literature.**

Ref. #	219	220	221	222	223	224	225
SiO_2	36.19	36.82	36.56	36.55	33.79	33.47	33.22
TiO_2	0.13	0.61	—	0.31	—	—	—
Al_2O_3	18.62	20.65	20.79	12.43	16.49	16.48	17.51
Fe_2O_3	11.3	9.68	7.20	6.43	8.06	9.39	8.44
Mn_2O_3	8.98	9.99	12.77	22.00	10.98	10.52	10.22
FeO	—	—	—	—	—	—	—
MnO	0.28	—	—	—	—	—	—
MgO	0.17	0.04	3.70	—	—	—	—
CaO	22.34	18.96	17.36	16.10	12.18	10.94	10.85
SrO	—	1.23	—	—	16.79	16.99	17.51
Na_2O	—	—	—	2.59	—	—	—
K_2O	—	—	—	0.59	—	—	—
H_2O	2.2	2.06	2.04	3.02	—	—	—
CuO	—	—	—	—	—	—	—
PbO	—	—	—	—	—	—	—
BaO	0.01	—	—	—	0.60	0.73	0.57
total	100.27	100.04	100.42	100.02	98.89	98.52	98.32

References: 2, 3, 4, 5 Bilgrami (1956); 6, 7, 8 (includes SnO 0.01) Marmo et al. (1959); 9 Gaudefroy et al. (1965); 10 (includes P_2O_5 0.04), 11 (includes P_2O_5 0.04), 12, 13 Smith and Albee (1967); 14 Cooper (1971); 15 Jan and Symes (1977); 16 Battaglia et al. (1977); 17, 18, 19, 20, 21, 22, 23 Chopin (1978); 24, 25, 26, 27, 28, 29, 30, 31, 32, 33, 34, 35, 36, 37, 38, 39, 40, 41 Dal Piaz et el. (1979); 42 Guild (1935); 44, 45, 46, 47, 48 Kawachi et al. (1983); 49, 50, 51, 52, 53, 54, 55 Ashley (1984); 56, 57 Velilla and Jiménez—Millán (2003); 58, 59, 60 Abraham and Schreyer (1975); 61, 62 Taylor and Baer (1973); 63, 64 Krogh (1977); 65, 66, 67, 68, 69, 70, 71 Dal Piaz et al. (1979); 72, 73, 74 Grapes and Hashimoto (1978); 75, 76, 77, 78, 79, 80, 81 Keskinen (1981); 82 Short (1933); 83 Smith et al. (1982); 84, 85, 86 Mottana (1986); 87, 88, 89, 90, 91, 92, 93, 94, 95, 96, 97, 98, 99 Reinecke (1986b); 101 Lucchetti et al. (1988); 102, 103, 104, 105, 106, 107, 108, 109 Akasaka et al. (1988); 110, 111 Leblanc and Lbouabi (1988); 112 Basu and Mruma (1985); 113 Bonazzi et al. (1990); 114, 115, 116, 117, 118, 119 Perseil (1991); 120, 121 Reinecke (1991); 122, 123 Hiroi et al. (1992); 124, 125, 126, 127, 128, 129, 130, 131, 132, 133, 134, 135 Jiménez—Millán and Velilla (1993); 136 Coombs et al. (1993); 152, 153, 154, 155, 156, 157, 158, 159, 160 Enami and Banno (2001); 161, 162, 163, 164, 165, 166, 167, 168, 169, 170, 171, 172, 173, 174, 175, 176, 177, 178, 179, 180, 181, 182, 183, 184, 185, 186, 187, 188, 189 Izadyar (2000); 190, 191 Reinecke et al. (1991); 192, 193, 194 Hirata et al. (1995); 197 (includes P_2O_5 0.13) Nayak and Neuvonen (1966); 198 Ernst et al. (1970); 199, 200 Hutton (1938); 201 (includes P_2O_5 0.06) Ernst (1964); 202 Franceschelli et al. (1996); 203, 204, 205, 206, 207, 208, 209, 210, 211 Della Ventura et al. (1996); 212 Yoshimura and Momoi (1964); 213, 218 Ishibashi (1969); 214, 217 Wieser (1973); 215 (includes P_2O_5 0.13) Banno (1964); 216 Lyashkevich (1958); 219 (includes F 0.05) Ödman (1950); 220 Hutton (1940); 221 Tanaka et al. (1972); 222 Malmqvist (1929); 223, 224, 225 Kato and Matsubara (1986).

Table B. Chemical analyses (oxides wt.%) of
REE bearing piemontite from literature.

Ref. #	1	43	100	137	138	139	140	141	142	143
SiO_2	37.37	35.6	34.61	31.81	32.06	31.73	32.29	30.95	30.77	31.75
TiO_2	—	0.10	—	0.03	—	0.06	0.04	0.02	0.04	0.03
Al_2O_3	22.07	19.27	20.54	14.34	14.63	14.29	14.48	13.21	13.41	14.58
Fe_2O_3	4.78	4.92	3.71	7.52	7.66	7.55	7.73	7.48	7.62	7.27
Mn_2O_3	8.15	10.08	17.33	13.93	13.25	13.68	13.91	12.88	13.27	13.87
FeO	—	—	—	—	—	—	—	—	—	—
MnO	2.29	—	—	—	—	—	—	—	—	—
MgO	0.30	1.48	—	0.56	0.44	0.52	0.45	0.51	0.54	0.49
CaO	18.83	19.48	12.90	12.08	12.80	11.88	12.43	10.99	11.16	12.18
SrO	—	—	—	—	—	—	—	—	—	—
Na_2O	0.27	—	—	0.19	0.18	0.17	0.13	0.12	0.13	0.24
K_2O	0.81	—	—	0.02	—	0.02	—	0.01	—	0.02
H_2O	2.48	—	—	—	—	—	—	—	—	—
La_2O_3	—	5.00	—	3.88	2.64	3.87	3.61	4.36	4.55	3.26
Ce_2O_3	2.41	—	4.09	3.11	2.63	1.96	1.35	1.59	1.20	2.46
Pr_2O_3	—	—	—	—	—	—	—	—	—	—
Nd_2O_3	—	—	—	1.57	1.43	1.26	1.11	1.10	1.07	1.51
Gd_2O_3	—	—	—	—	—	—	—	—	—	—
Sm_2O_3	—	—	—	—	—	—	—	—	—	—
ThO_2	—	—	—	—	—	—	—	—	—	—
CuO	0.11	—	—	—	—	—	—	—	—	—
PbO	0.14	—	—	6.08	6.27	6.88	6.77	10.35	9.86	5.78
ZnO	—	—	—	0.74	0.65	0.68	0.60	0.65	0.69	0.75
BaO	—	—	—	—	—	—	—	—	—	—
F	—	—	—	—	—	—	—	—	—	—
total	100.00	95.93	93.18	95.86	94.64	94.55	94.9	94.22	94.31	94.19

References: 1 Hillebrand in Williams (1893); 43 Kramm (1979); 100 Schreyer et al. (1986); 137, 138, 139, 140, 141, 142, 143 Bermanec et al. (1994)

**Table B (continued). Chemical analyses (oxides wt.%) of
REE bearing piemontite from literature.**

Ref. #	144	145	146	147	148	149	150	151	195	196
SiO_2	32.52	31.54	31.97	30.52	34.06	35	35.36	33.85	31.33	30.41
TiO_2	—	0.05	0.04	0.04	—	—	—	—	—	—
Al_2O_3	14.78	14.96	14.48	13.7	17.02	18.5	18.49	16.86	15.11	8.54
Fe_2O_3	7.53	7.14	8.19	7.86	5.93	7.02	6.92	6.32	5.52	1.17
Mn_2O_3	12.65	13.98	13.95	12.98	14.36	13.54	13.62	15.18	—	—
FeO	—	—	—	—	—	—	—	—	—	—
MnO	—	—	—	—	—	—	—	—	11.35	28.29
MgO	0.43	0.56	0.48	0.6	0.63	0.18	0.26	0.49	1.16	—
CaO	12.67	13.02	12.83	11.32	16.29	18.64	18.48	15.97	9.40	5.81
SrO	—	—	—	—	0.48	0.62	0.68	0.69	3.49	0.66
Na_2O	0.17	0.24	0.18	0.21	—	—	—	—	—	—
K_2O	0.02	—	—	—	—	—	—	—	—	—
H_2O	—	—	—	—	—	—	—	—	—	—
La_2O_3	2.2	2.68	3.62	5.09	4.39	0.97	1.77	3.73	2.95	7.22
Ce_2O_3	3.06	3.40	1.47	1.82	1.29	0.97	0.59	1.33	6.43	6.67
Pr_2O_3	—	—	—	—	0.58	0.19	0.36	0.59	0.91	1.34
Nd_2O_3	1.58	1.77	1.00	0.98	1.69	0.63	1.32	1.98	2.84	4.72
Gd_2O_3	—	—	—	—	0.11	0.09	0.1	0.13	0.45	0.31
Sm_2O_3	—	—	—	—	—	—	—	—	0.21	0.03
ThO_2	—	—	—	—	0.15	—	—	—	0.94	0.03
CuO	—	—	—	—	—	—	—	—	1.81	0.16
PbO	6.37	5.57	6.27	10.28	—	—	—	—	—	—
ZnO	0.70	0.73	0.62	0.68	—	—	—	—	—	—
BaO	—	—	—	—	—	—	—	—	—	—
F	—	—	—	—	—	—	—	—	0.11	0.10
total	94.68	95.64	95.10	96.08	96.98	96.35	97.95	97.12	94.01	95.47

References: 144, 145, 146, 147 Bermanec et al. (1994); 148, 149, 150, 151 Bonazzi et al. (1992); 195, 196 Bonazzi et al. (1996).